

Seeing Without Rods or Cones: Contributions of Intrinsically-Photosensitive Retinal Ganglion
Cells to the Image-Forming Visual System

Stewart Madon

Lakehead University, Thunder Bay

Supervisor: Dr. Michael Wesner, Psychology Department, Lakehead University

Second Reader: Dr. Ron Davis, Psychology Department, Lakehead University

Internal-External Reviewer: Dr. Philip Hicks, Lakehead University

Internal-Internal Reviewer: Dr. Robert Omeljaniuk, Lakehead University

External Reviewer: Dr. Paul DeMarco, University of Louisville

Dissertation submitted as partial fulfillment of the requirements of a Doctorate of Philosophy in
Clinical Psychology.

Table of Contents

Acknowledgements.....	4
Abstract.....	5
Introduction.....	7
IpRGC Physiology.....	8
Melanopsin.....	8
G-Protein-Coupled Transduction Cascade.....	10
Chromophore Bistability.....	11
Photoisomerisation Properties and Retinal Distribution.....	13
IpRGC Morphology and Retinal Connectivity.....	15
Amacrine Cell Inputs to ipRGCs.....	23
Excitatory Inputs to ipRGCs.....	25
Inhibitory Inputs to ipRGCs.....	25
Molecular Markers of ipRGC Subtypes.....	26
Central Projections of ipRGCs.....	28
Summary of IpRGC Physiology.....	29
Non-Image-Forming (NIF) Functionality of ipRGCs.....	32
Circadian Photoentrainment.....	33
Sleep Regulation.....	41
IpRGCs and the Pineal Organ.....	42
Pupillary Light Reflex.....	42
Summary of Non-Image-Forming Functionality of ipRGCs.....	45
Contributions of ipRGCs to Image-Forming Pathways.....	46
Potential Evidence for Modulatory Effects on Image Formation.....	49
Summary of Contributions of ipRGCs to Image-Forming Pathways.....	51
S-Cones.....	52
S-Cone Physiology.....	52
S-ON vs. S-OFF.....	53
Koniocellular Pathway.....	55
Overall Summary and Proposed Model.....	56
Methods.....	72
Participants.....	72
Stimuli and Apparatus.....	72
Visual Function Screening.....	72
Psychophysical experiments.....	74
Apparatus.....	74
Adapting Field Calibration.....	74
Photopic Sawtooth Stimulus Design.....	75
Contrast Sensitivity Stimulus Design.....	77
Procedure.....	78

Recruitment of participants.....	78
Experimental Session.....	78
Experiment 1 (Photopic Sawtooth Brightness Sensitivity).....	80
Experiment 2 (Periodic Contrast Sensitivity).....	82
Results.....	83
Analytic Strategy.....	83
Parametric Assumptions.....	83
Short-Wavelength Automated Perimetry.....	83
Photopic Sawtooth Brightness Sensitivity.....	84
Brightness Sensitivity.....	86
δ (SWLS(OFF)/ SWLS(ON) Asymmetry).....	86
X ($\delta_{\text{condition}}/ \delta_{\text{control}}$).....	87
<i>A Priori</i> Hypotheses.....	87
Contrast Sensitivity Task.....	87
Short-Wavelength Automated Perimetry (SWAP).....	88
Correlation between S-Cone function and Task Performance.....	88
Photopic Sawtooth Brightness Sensitivity.....	88
Brightness Sensitivity.....	88
δ (SWLS(OFF)/ SWLS(ON) Asymmetry).....	90
X ($\delta_{\text{condition}}/ \delta_{\text{control}}$).....	90
<i>A Priori</i> Hypotheses.....	91
Contrast Sensitivity Task.....	91
Discussion.....	94
S-Cone Sensitivity and ipRGC Function.....	94
IpRGC Involvement in Brightness Perception.....	95
IpRGC Involvement in Contrast Sensitivity.....	100
Implications of Data in the Proposed Model.....	103
Limitations.....	106
Future Directions.....	108
Conclusion.....	111
References.....	112
Tables.....	132
Figures.....	142
Appendices.....	149

Acknowledgements

I would like to begin by dedicating this dissertation to the three most important people in my life; my amazing wife Erin, and my two wonderful sons, Felix and Theodore. Without their love, support, sacrifice, and understanding, none of what I have accomplished these past years would have been possible.

I would also like to thank my supervisor, Dr. Michael Wesner, for his tireless dedication and (seemingly) infinite patience. To use his words – “this stuff is not trivial!” – and thus many late nights, whiteboard debate sessions, and revisions were needed to bring this study to fruition.

Finally, I would like to thank the graduate students (past and present) at the Sensory Neuroscience and Perception Lab (Meghan, Frank, Emily, and Sarah), my research assistants (Alyssa and Brandon), and my review committee.

Abstract

It was long thought that rods and cones were the only components of the mammalian retina capable of conveying light information to the brain. Recently, a novel class of transduction-capable retinal ganglion cells containing the photopigment melanopsin were discovered in the mammalian retina identified as an “intrinsically photosensitive retinal ganglion cell” or ipRGC. Most of the functionality associated with ipRGCs has been linked to nonperceptual, non-cortical visual operations such as circadian (day-night) phase modulation and pupillary constriction. More recently, however, two subpopulations of ipRGCs have been identified called M1 and M2 cells, with the latter showing “blue-yellow” chromatic opponency that possibly links to brightness or colour pattern vision – properties associated with the retinogeniculostriate, or image-forming visual system. The present study expands on the current understanding of these putative image-forming non-traditional photoreceptor systems. To this end, I developed two stimulus paradigms that target short-wavelength-sensitive cones (S-cones) to tease out the unique contributions of ipRGCs that have neural associations with S-cone visual functioning. In the first paradigm, I measured detection thresholds using short-wavelength selective stimuli that are temporally presented with either an onset or offset “sawtooth” profile to ascertain ipRGC input to the S-OFF, “brightness” pathways. The results revealed differences in the asymmetry between S-ON and S-OFF pathways dependent upon adapting field conditions that were expected to influence ipRGCs over other photoreceptors. In the second experiment, I used a modification of an S-cone contrast sensitivity task employing homochromatic “blue” sine-grating gabors of varying spatial frequencies to directly test ipRGC involvement in spatial pattern vision. The results from the second experiment showed a slight advantage to the perception of low spatial frequency gabors superimposed on chromatic adapting fields that were

expected to influence ipRGCs more than the others. Preliminary evidence supporting a spatial tuning property of ipRGCs was also found. Overall, these findings suggest that ipRGCs have measurable influences on conscious, image-forming perceptions, and shed further light on the microcircuitry of the retinogeniculate pathway.

Seeing Without Rods or Cones: Contributions of Intrinsically-Photosensitive Retinal Ganglion Cells to the Image-Forming Visual System in Humans

It was long thought that rods and cones were the only components of the mammalian retina capable of conveying light information to the brain (Bailes & Lucas, 2010). These specialized sensory cells contain photopigments whose configuration allows for absorption properties that are selective to different wavelengths of light. It is the absorption properties of these pigments that define them as cyanolabe (contained in short-wavelength-sensitive or S-cones; peak absorption at 420 nm), chlorolabe (contained in middle-wavelength-sensitive or M-cones; peak absorption at 534 nm), erythrolabe (contained in long-wavelength-sensitive or L-cones; peak absorption at 564 nm), and rhodopsin (contained in rods; peak absorption at 498 nm). Recently, however, a novel type of photopigment (melanopsin) was discovered in ganglion cells that are now termed “intrinsically photosensitive retinal ganglion cells” (ipRGCs; Provencio, 1998). Once thought to be mere signal accumulators and neural relays for the more prevalent rods and cones in the retina, these ipRGCs are now known to have a broad range of anatomical projections, from the hypothalamus and suprachiasmatic nucleus (SCN), to the olivary pretectal nuclei and lateral geniculate nucleus of thalamus (Pickard & Sollars, 2010). These projections have been extensively studied and are known to be part of non-image forming pathways that are primarily responsible for vegetative circadian functioning (e.g., photoentrainment, circadian phase setting) and pupillary light reflexes. Recently, a few studies have also implicated ipRGCs involvement with the communication of image-forming visual information (e.g., Brown et al., 2010; Dacey, et al., 2005; Ecker, et al., 2010; Zaidi, et al., 2007), and that the interplay between these newly-discovered cells, the circadian system and the classic rod/cone system is far more complex than was originally believed. The present study elucidates

the link between these novel photoreceptors and the image-forming visual system by exploring the contributions of ipRGCs to the visual system's involvement with brightness perception and pattern vision. The following will include a review of the current literature on ipRGCs, including their functional physiology and photopigmentation, their place in the receptor mosaic of the retina, projections to the brain, and recent discoveries about their potential role in image-forming visual perception. This review of the literature will be followed by a brief review of short-wavelength sensitive cone (S-cone) communication, as well as a proposed model for the integration of some of the classic photoreceptor signalling and ipRGC function. It is important to note that many of the studies cited herein use the terms "melanopsin-expressing", "melanopsin-containing" and "intrinsically-photosensitive" interchangeably; therefore, to simplify, the present author will refer to all retinal ganglion cells (RGCs) containing the melanopsin chromophore as "intrinsically-photosensitive" (i.e., ipRGCs).

IpRGC Physiology

Melanopsin

In the 1920s, Keeler and colleagues discovered a strain of mice with an autosomal recessive mutation that lacked rods, cones, external nuclear layers and external molecular layers (Keeler, 1924). Despite their lack of rods and cones, the mutant mice maintained their pupillary light reflex (PLR), even in the absence of response from electroretinograms (Keeler, 1927; Keeler, Sutcliffe, & Chaffee, 1928). The authors surmised that the maintenance of PLR must have been due to an as-yet-undiscovered photoreceptive channel in the retina.

Following this discovery, other research groups noted that *rd/rd cl* mutant mice lacking rods and cones could still photoentrain to light stimulation (Ebihara & Tsuji, 1980; Foster et al., 1991). Foster et al. noted that light-evoked responses were still present in *rd/rd cl* mice, and that

this was either due to a novel, and as yet undiscovered photoreceptor in the murine retina, or that the mutation had spared a small number of cones that still transmitted light information to the brain. Later, Freedman et al. (1999) studied *rd/rd cl* mice and found that these mice retained their ability to photoentrain. Two studies by Lucas and colleagues (Lucas et al., 1999; Lucas, Douglas & Foster, 2001) also showed that other notable non-image-forming (NIF) visual functions, namely the PLR and suppression of melatonin in response to light, were maintained in *rd/rd cl* mice. Further, Lucas et al. (2001) also measured the action spectrum of the *rd/rd cl* mouse's PLR, and found that it peaked near 480 nm, which was a significant deviation from the predicted maximum based on murine cone opsins.

Provencio et al. (1998) took the first step toward the discovery of ipRGCs with their discovery of melanopsin, a previously unknown photopigment of the opsin family found in the dermal melanophores of the African clawed frog (*Xenopus laevis*). Two years later, Provencio, Rodriguez, Jiang, et al. (2000) isolated the very same photopigment in retinal ganglion cells (or RGCs) in both primates and rodents, thus suggesting that these cells were directly photosensitive and not reliant on rod/cone input to convey light information. Heterologous expression studies have subsequently introduced melanopsin into *Xenopus* oocytes (Panda et al., 2005; Qiu et al., 2005) and mouse neuroblastoma (Melyan et al., 2005). These studies found that not only did these cells gain intrinsic photosensitivity from the addition of melanopsin, but that they also shared similar response kinetics, demonstrated sustained membrane depolarization, and had similar spectral sensitivity (peak at ~480 nm). Further, the intrinsic photosensitivity of the cells was greatly attenuated by either the intracellular introduction of competitive Gq-protein-subunit blockers or the extracellular application of phospholipase C antagonists, suggesting the involvement of G-protein-phospholipase C transduction cascade.

The melanopsin pigment also appears to be homogeneous across species. For example, Smith et al. (2003) confirmed the existence of melanopsin in the macaque retina. The authors noted that this pigment was effectively analogous to the novel opsin found in mice and other lower animals. They also found that it had a peak spectral sensitivity of ~483 nm, supporting similar findings in studies that used other species (e.g., Dacey et al., 2005); see also reviews by Bailes and Lucas (2010), Pickard and Sollars (2010) and Schmidt, Chen & Hattar (2011).

Finally, melanopsin is different from other retinal photopigments not only because of its spectral sensitivity properties, but also because of its lower membrane density. A study of transgenic mice revealed that membrane melanopsin protein density is 10^4 times less than that of pigment protein densities found in rods and cones (Do et al., 2009), leading to poor photon catch rates, and thus phototransduction in only relatively bright light.

G-protein-coupled transduction cascade. Melanopsin appears to be part of a G-protein coupled receptor that is homologous to the rhabdomeric photopigments found in invertebrates (Do & Yau, 2010; Hankins et al., 2008). The photopigment consists of two halves: the protein half (the opsin), and the chromophore, 11-*cis*-retinal half. When subjected to short- or middle-wavelength light, 11-*cis*-retinal isomerizes to all-*trans*-retinal, resulting in a configurational change of the opsin that instigates the bioelectric signal.

Graham et al. (2008) sought to identify the phototransduction cascade within ipRGCs. Using broad-spectrum light from a tungsten-halogen lamp (4×10^{12} - 1×10^{14} photons/cm²/sec), the authors illuminated mounted retinas of Sprague-Dawley rats. Then, using single-cell recordings and microscopy, the authors determined the exact phototransduction cascade: Once melanopsin absorbs a photon and changes configuration, it activates the membrane bound G_{q11}-protein, which in turn triggers the enzyme phospholipase C. Once activated, phospholipase C catabolises

the membrane lipid phosphatidylinositol 3,4-bisphosphate (PIP₂) which leads to the opening of cationic channels and cellular depolarization. Graham et al. concluded that this cascade was typical of a rhabdomeric phototransducer, thought to be found only in invertebrates prior to this discovery, thus establishing melanopsin as an evolutionarily “older” photopigment.

Chromophore bistability. Melanopsin differs from classic rod/cone photopigments in that it does not require an external enzyme to convert them back to 11-*cis*-retinal; rather, they seem to be regenerated within the ipRGCs. One hypothesis, proposed by a number of researchers (Fu et al., 2005; Mure et al., 2007; Mure et al., 2009), is that melanopsin is a bistable chromophore, and that while short- to middle-wavelength light causes isomerization, long wavelength light (~ 620 nm peak) can actually regenerate the chromophore. This was established using indirect *in vivo* recordings of single suprachiasmatic nucleus (SCN) cells in mice. Prior exposure to long-wavelength light increased the activity of SCN neurons and increased the amplitude of the pupillary light reflex in response to 480 nm light, while prior exposure to short-wavelength light decreased subsequent SCN activity and reduced the amplitude of the pupillary light reflex, supporting the notion of melanopsin’s bistability. These early studies, however, failed to take into account a potential bidirectional relationship between the ipRGCs and other photoreceptors such as the rods, and therefore the researchers may have drawn premature conclusions about the chromophores’ self-sustaining bistability. For example, Walker, Brown, Cronin and Robinson (2008) reported that their *in vitro* studies of ipRGCs found no bistability, suggesting that an interaction or secondary retinal signalling process, or a light-independent regenerative pathway, or all three, may be necessary to regenerate melanopsin photopigments. Indeed, Mawad and Van Gelder (2008) performed *in vitro* recordings of mice retinas subjected to either 480 or 620 nm narrowband light, and found no potentiating effect of

the long wavelength light exposure, and suggested that a second-order pathway was involved in the recycling of the melanopsin chromophore. Do et al. (2009) found that subsequent to long-term high-intensity light exposure, significant attenuation of photoresponses was still possible in ipRGCs, demonstrating that melanopsin's regeneration mechanism may have temporal limits in addition to other requirements. Schmidt, Chen and Hattar (2011) noted that only 11-*cis*-retinal was isolated in dark-adapted vertebrate ipRGCs. This finding runs counter to the idea that melanopsin is a truly bistable photopigment, since one would expect a mix of 11-*cis*-retinal and all-*trans*-retinal in the absence of long-wavelength pigment regeneration (Walker et al., 2008). Studies on mutant mice lacking the retinal pigment epithelial enzyme, isomerase which is responsible for converting standard photopigments from their all-*trans* state to their 11-*cis* state (*RPE65*^{-/-}), have shown that these mice have no cone function (which is to be expected) and weak rod function (Fu et al., 2005; Tu et al., 2005). These studies have also shown that ipRGC function related to circadian phase shifting is severely compromised in *RPE65*^{-/-} mice. A study by Doyle et al. (2006) further modified the *RPE65*^{-/-} strain and ablated their remaining rods. This new strain, *RPE65*^{-/-} *rdta* showed enhanced circadian phase shift responses to light, and posited that this was due to an increased availability of chromophore to ipRGCs in the absence of rods. It can thus be inferred that a secondary chromophore regeneration pathway exists outside the light-driven one that is responsible for the maintenance of adequate chromophore concentration in the absence of light, and that this system favours rod and cone chromophore concentration, perhaps only contributing to melanopsin regeneration in the presence of adequate rod and cone chromophore concentrations.

Given the above information, Schmidt, Chen and Hattar (2011) suggested a model for melanopsin regeneration in vertebrate ipRGCs. The authors posit that the since the retinal

pigment epithelium is relatively removed from the ganglion cell layer of the retina, an intermediary cells, such as the Müller glial cells, may “recycle” and produce a converted by-product of all-*trans*-retinal. In this model, the all-*trans*-retinal is converted to its alcohol form in the ipRGC or the Müller cell, is then converted to the alcohol form of 11-*cis*-retinal, and finally transported back to the ipRGC where it is reconverted to 11-*cis*-retinal in a process similar to that found in cones. This process is thought to occur in parallel with the long-wavelength-light-activated process which converts all-*trans*-retinal to 11-*cis*-retinal within the ipRGC itself. Zhu et al. (2007) also hypothesized that the secondary phases of melanopsin were photosensitive in their own right, and that they may respond to different wavelengths.

Photoisomerisation Properties and Retinal Distribution

IpRGCs make up a relatively small proportion of the cells in the murine, primate and human retina (Dacey et al., 2005). Estimates currently place the ipRGC population at between 0.2% and 1-5% of the total ganglion cell population in the human and mouse retina, respectively.

After Provencio et al.'s (1998) discovery of melanopsin, Berson, Dunn and Takao (2002) successfully labelled a melanopsin containing ganglion cell projecting to the SCN. The authors established the basic properties of these cells using whole-cell recordings of the ipRGCs from mounted rat retinas subjected to varying wavelengths (440-600 nm) at different intensities (10^{13} - 10^{16} photons/cm²/sec). Their findings were numerous and substantial: (a) the peak sensitivity was discovered to be 484 nm; (b) the threshold irradiance for *in vitro* electrophysiological response with narrowband 500-nm light presentation was found to be 5×10^{11} photons/cm²/sec, which corresponds to an *in vivo* corneal irradiance of $\sim 2 \times 10^{13}$ photons/cm²/sec; (c) they found the saturation point of the cells, as defined by a plateau in firing frequency, to be approximately 3 log-units above the cells' calculated threshold ($\sim 2 \times 10^{16}$ photons/cm²/sec); and (d) they noted that

the intrinsic response kinetics of the cells were quite sluggish compared to rods and cones, requiring several hundred to a thousand milliseconds depending on stimulus intensity to reach a full depolarized state, and several minutes to repolarise after stimulus offset. It is to be noted that these findings only related to *intrinsic* properties of the ipRGCs, and that other studies have found that when integrated with other retinal elements, the ipRGC-response kinetics normalize in a fashion similar to other ganglion cells (a fuller description is outlined later).

Do *et al.* (2009) found that though ipRGCs (and their inherent melanopsin) have a relatively poor photon capture rate at scotopic and low-photopic light levels compared to rods and cones, they do have a highly efficient signalling property once photon capture occurs. According to Do and colleagues, it is possible that ipRGCs can convey sustain responses based on a single absorbed photon, and that they can signal that photon's presence to the brain.

A study by Warren, Allen, Brown and Robinson (2003) used patch-clamp recordings to measure the firing pattern of SCN-projecting ipRGCs exposed to 25 s broad spectrum (visually "white") light at various intensities (2.6×10^{-6} to 5.8×10^{-5} W/cm²). No subtype of ipRGC was specified, however. Given the preponderance of M1 cells that project to the SCN, it can be assumed that the findings of this study are more characteristic of M1 than M2 cells. They found that ipRGCs in general fire sporadically, though with increasing spike frequency corresponding to increasing intensities of light. The authors also noted that even at the highest intensity exposure, the ipRGCs only showed peak depolarization after ~5.3 s, revealing a more sluggish response property compared to rods or cones.

Hankins and Lucas (2002) sought to elucidate the properties of a "novel, vitamin-A based opsin" believed to be melanopsin in retina. Three participants were exposed to a ganzfeld-dome consisting of a 512 nm, rod-saturating background with 15-120 minute presentations of 420-

441-, 471-, 495-, 531-, 551-, and 576-nm stimuli. Electroretinographic measurements (ERGs) were taken during the presentations. Placing particular emphasis on implicit ERG cone b-wave time (a purported measure of second-order retinal processing), the authors found that with the application of light pulses of varying durations (15-120 minutes) while modulating the irradiances to deliver approximately equal quantities of photons to the retina across all the wavelengths, there were wavelength-dependent reductions in nocturnal cone b-wave time, with the 471-nm stimulus eliciting the greatest overall b-wave time reduction. Hankins and Lucas concluded that ipRGCs function well as temporal integrators for circadian stimuli, and that the novel, vitamin-A based opsin had a peak sensitivity of 483-nm, consistent with the sensitivity of melanopsin.

In sum, ipRGCs are sparsely distributed and account for between 0.2% (in primates) and 1-5% (in mice) of the total volume of RGCs in the retina. Their peak sensitivity, defined by the melanopsin photopigment, is between 480-484 nm. They are capable of sustained activity in the form of spike trains after a single photon capture, and have an approximate radiometric operating range between 10^{11} and 10^{16} photons/cm²/sec.

IpRGC Morphology and Retinal Connectivity

Although they are often referred to as a single subtype of ganglion cell, researchers generally do not consider ipRGCs to be a homogeneous group of cells. Recent studies in mice have found at least five distinct subtypes of the cells within the inner plexiform layer (IPL) of the murine retina, with increasing similarities to those found in primate and human retinas (Sand, Schimdt & Hattar, 2012; Schmidt, Chen & Hattar, 2011; Schmidt, Do, Dacey, Lucas, Hattar & Matynia, 2011). These classifications are based on a combination of features such as the depth and location of the dendritic arborisation in the IPL (ON versus OFF layers), the extent of the

dendritic field (narrow versus broad), and the density of the dendritic branching (bushy versus sparse).

In the mammalian retina, light increments and light decrements are processed by two different channels: bipolar cells in the ON channel depolarize in response to light and stratify in the inner part of the IPL (“ON sublamina”), while bipolar cells in the OFF channel are excited when light is turned down and occupy the outer IPL (“OFF sublamina”; Famiglietti and Kolb, 1976). This functional distinction suggests that ipRGCs cannot be classified by morphology alone; retinal projections and connectivity form an integral part of their function as well.

The general morphological characteristics of ipRGCs include a small- to medium-sized soma coupled with a very large, sparse dendritic field. Soma sizes range from 13-22 μm in mice and primates, but dendritic field size differ substantially between species; 200-300 μm in mice, 500-600 μm in marmosets, and 400-1200 μm in macaques (Sand et al., 2012). Further, the dendritic fields associated with ipRGCs in primates tend to conform to the parafoveal region of the retina, contrary to those in cats, which tend to be more randomly situated throughout the retinal photoreceptor mosaic. Some researchers have posited that this eccentric arrangement outside of the foveal pit may have evolved to prevent interference with the high-acuity vision associated with the central visual field in higher-ordered mammals (Schmidt, Do, Dacey, et al., 2011). Curiously, this parafoveal arrangement correlates with the anatomical location of S-cones in the primate retina, and may be indicative of a link between these two cell types (Calkins, 2001).

The following is a review of known ipRGC subtypes and their morphological characteristics, purported connections in the retina, and cortical projections. The descriptions

herein will be summarized in Table 1, which expands on a table originally provided by Schmidt, Chen and Hattar (2011).

Provencio, Rollag and Castrucci (2002) were the first to employ immunocytochemical staining in the form of a melanopsin anti-serum to ascertain the extent of retinal projections of ipRGCs. The authors used a broad staining technique and noted that melanopsin projecting dendrites could be found in both the inner and outer lamina of the IPL.

A later study by Hattar, Liao, Takao, Berson and Yau (2002) used 24 adult male and female B6/129 mice (*Opn4^{tau-lacZ}*) reporter mice, genetically modified to replace the melanopsin gene *opn4* with *tau-lacZ*, which provides a marker enzyme binding site for a subsequently injected tracer. They found that most of the melanopsin containing projection in retina were found in the outer (OFF) sublamina of the IPL. It is to be noted that this may have been due to the relatively increased availability of melanopsin M1 ipRGC subtype in mice compared to other, non-M1 subtypes (see below for details).

A study by Sekaran et al. (2003) examined the irradiance-coding properties of ipRGCs in rodless-coneless mouse retinas. FURA-2 fluorescent calcium imaging was combined with 470 nm light stimulation, resulting in three separate patterns of light activation, namely sustained, transient, and repetitive activation, suggestive of three separate ipRGC subtypes.

Tu et al. (2005) used multi-electrode arrays on ex-vivo intact murine retinas to ascertain the developmental course of ipRGC function, as well as functional differences in firing patterns in response to light stimulation. Tu and colleagues noted three subtypes of ipRGCs in postnatal mice: a) Subtype I displayed a long latency of onset, high photosensitivity, and fast termination of activity at “lights-off”, b) Subtype II displayed long latency to activity onset in subsaturation light conditions and slow activity termination at “lights-off”, and c) Subtype III were found to

have short latency to activity onset and highly sustained activity following lights-off. In adult mice, however, Tu and colleagues noted only two prominent subtypes of ipRGCs, whose firing patterns were consistent with subtypes II and III in the postnatal mouse retinas, with no comparable firing patterns to those found in postnatal subtype I. The absence of the subtype I firing pattern in adult mice, combined with the 4-fold decrease in the number of ipRGCs at adulthood compared to birth, suggests that postnatal type I cells may serve some early developmental role that is subsumed by traditional photoreceptors as the mouse ages. This mirrors findings from Ruggiero et al. (2009) suggesting that traditional photoreceptors play a role in the apoptotic “pruning” of ipRGCs in adult retinas. The implications of these findings in primate and human populations are unknown at this time, though Schmidt, Chen and Hattar (2011) posit that they may have a function in human neonatal light avoidance.

A study by Dacey et al. (2005) used *in vitro* recording of affixed macaque and human retinal cells and found a subset of “giant” melanopsin-expressing ganglion cells that receive strong rod and cone input (see above). They showed that these ipRGCs display a rare S-OFF, (L+M)-ON overlapping colour opponent receptive field, and that rod and (L+M)-cone activity is combined within the ganglion cells to signal irradiance (or brightness) to the LGN and beyond.

Dacey, Peterson, Liao and Yau (2006) combined confocal microscopy and immunocytochemistry on mounted human and macaque retinas to elucidate morphological and connective differences between subpopulations of ipRGCs in primates. Their results confirmed that two distinct subpopulations do, in fact, exist in humans, referred to in Dacey et al. as “outer” and “inner” cells. The authors also found that these subpopulations had distinct functional connections within the retina: the outer cells synapsed extensively with dopaminergic amacrine cells, whereas the inner cells synapsed primarily with the DB6 cone bipolar, which has been

shown to exhibit yellow-ON response properties. Given the location of these cells, and their functional connections, it was assumed that the “outer” cells to be of the M1 subtype, and the “inner” cells to be of the M2 subtype. With respect to M2, despite the fact that mice have “M2” ipRGCs in sublamina B which is known to be part of the bipolar to ganglion cell ON synapses, I argue that Dacey et al.’s primate “inner” M2 cells with their DB6 cone bipolar connections are still behaving as an ON type for “yellow” (L+M) chromatic processing, but as discussed later, chromatic opponency demands an additional “blue” (S) OFF arrangement for these cells. This is why, later, M2 is discussed as having S-OFF properties despite its sublamina B morphological location.

Schmidt, Taniguchi and Kofuji (2008) used *Enhanced Green Fluorescent Protein* (EGFP)-labelled newborn mouse pups to investigate the developmental propagation of ipRGC postnatally. The authors found three distinct subtypes of ipRGC in the mouse retina; M1, M2, and M3. The M1 subtype was found to project to the outer (OFF) sublamina of the IPL, the M2 subtype projected to the M2 (ON) sublamina of the IPL, and the M3 subtype was bistratified, with projections to both sublaminae. The authors also used electrophysiological recordings of the pups’ retinal response to 5 s light pulses (full-spectrum or 480 nm narrow-band) at postnatal days 0 to 24 and at adulthood. They found that during the period in which mice have their eyes closed (postnatal 0 to 7 days) their ERG response to the stimuli was more sluggish and lower in amplitude than during the postnatal period after they opened their eyes. Once the pups’ eyes were open, the ERG responses were comparable to those of other ganglion cells, supporting the idea that these ipRGCs can function as “regular” ganglion cells in the transmission of rod and/or cone signals. They also found that, due to the input of M cones, the actual peak sensitivity of these cells in mice and rats could be closer to 490-510 nm at photopic levels, depending on

species. It is unclear how this cone input could relate to human ipRGC peak sensitivity; however the overlapping involvement of M-cones in rodents should not be underestimated as a possible indicator of cone-ipRGC interaction in humans.

Schmidt and Kofuji (2009) sought to elucidate the functional and morphological differences between M1 and M2 cells in mice. They used intracellular recordings to determine cellular activation to a 30 s light pulse on a group of mice. Following this, the animals were killed and their retinas stained to determine morphology. The authors found that M1 and M2 cells differed not only in terms of morphology, but also in terms of light response and membrane characteristics. Morphologically, as stated above, the M1 cells seem to be contained exclusively within sublamina A (the OFF sublayer) and M2 cells to sublamina B (the ON sublayer). Further, they noted that M2 cells had a much larger, more complex dendritic field than M1. In terms of light response characteristics, Schmidt and Kofuji noted that compared to M2 cells, M1 cells show a significantly larger depolarization in response to light, have a larger light evoked current, and have a faster response decay rate at stimulus offset. M2 cells show a smaller, but more sustained current in response to light. Finally, with regard to membrane characteristics, M1 cells showed a higher input resistance, a more depolarized resting membrane potential, and a lower maximal firing frequency (~80 Hz), whereas M2 cells had a lower input resistance, a more hyperpolarized resting membrane potential and a higher maximal firing frequency (~240 Hz). Thus, M2 cells may be better suited for communication with traditional, rod and cone driven photoreceptor pathways. M1 cells, on the other hand, may be better suited for communicating sustained photoresponses independent of rods and cones.

Using immunofluorescent labelling, Berson, Castrucci and Provencio (2010) were able to identify two distinct types of “M” cell in the retina of C57BL/6J mice with M1 cells again being

located in the outer sublamina of the inner plexiform layer (IPL) and M2 cells being located in the inner sublamina of the IPL. The authors hypothesize that these two types of cells could be differentially sensitive to light, or be functionally different (i.e., have different projection pathways). A review by Bailes and Lucas (2010) expanded on this categorization and noted that “M1” ipRGCs are found in sublamina A of the human IPL, which is closest to the rods/cones and thought to contain ganglion cells that synapse with OFF bipolar cells (i.e., responsive to light decrements). “M2” ipRGCs, on the other hand, are found in sublamina B of the IPL, which is known for ganglion cell synapses with ON bipolar cells (i.e., responsive to light increments; Bailes & Lucas, 2010). As stated above, the third subset of the newly discovered murine ipRGCs has been identified as “M3” ipRGCs and they appear to be bistratified with dendritic arborisation in both sublaminae. There are also morphological differences between the subtypes: M2 cells have larger soma, larger dendritic fields, and greater dendritic length than M1 cells. M3 cells have demonstrated overlapping arborisation, suggestive of overlapping receptive fields. It is to be noted that the M1 and M2 classifications of ipRGCs have recently been adopted in human nomenclature as well (Bailes & Lucas, 2010), whereas M3 cells are still thought to be found only in mice.

Neumann, Haverkamp and Auferkorte (2011) performed a wide anatomical screen for glycine and GABA receptors in ipRGCs. Using immunocytochemical staining on the retinas of two adult macaque monkeys, they found that M1 cells expressed $\alpha 2$ glycine receptors and $\alpha 3$ GABA_A receptors, whereas M2 cells showed very weak expression of all inhibitory receptors included in the test. Curiously, the authors concluded that all ipRGC cells received inhibitory ON inputs and, as such, further experimentation is required to ascertain the seemingly

contradictory role of inhibitory ON inputs to the sustained firing pattern of these specialized cells.

A recent study by Ecker et al. (2010) identified two additional subtypes of ipRGCs, previously not discovered due to their very low melanopsin content. The authors combined two strains of mice – a reporter line and a driver line – and EGFP, and revealed approximately three times the number of melanopsin containing cells in the mouse retina than were previously thought to exist. The additional ipRGCs discovered, the M4 and M5 subtypes were both shown to have dendritic projection in the inner (ON) sublamina of the IPL. The M4 subtype has a relatively large dendritic net, whereas the M5 subtype's net is smaller. Further, the M4 subtype closely resembles traditional ON-RGA1 ganglion cells.

A recent review by Schmidt, Chen and Hattar (2011) summarized the connectivity of all currently known ipRGC subtypes. The authors stated that regardless of IPL stratification patterns, all ipRGCs received input from ON-bipolar cells, and that a weak OFF input to the M1 ipRGC subtype was only notable under pharmacological blockade of dopaminergic amacrine cells (see below). The seemingly contradictory “ON” connectivity of the M1 subtype, despite its outer IPL stratification, is due to cone bipolar cells making ectopic ribbon synapses with M1 dendrites while crossing the outer IPL.

A review by Do and Yau (2010) also noted that the synaptic input to M2 ipRGCs in primates is approximately twice that of M1 cells, leading the authors to postulate that synaptic contact may be a compensation mechanism for the M2 cells' lower intrinsic photosensitivity. They also noted that ipRGCs receive synaptic input from a variety of cone bipolar cells, including DB1, DB6 and giant bistratified subtypes.

Perez-Leon, Warren, Allen, Robinson and Brown (2006) used a combination of synaptic blockers (e.g., tetrodotoxin, bicuculline, strychnine) injected locally into a population of Sprague-Dawley rats to study the unique contribution of rod and cone photoreceptors on circadian photoentrainment. Using whole-cell patch-clamp recordings, the authors found two simultaneously generated synaptic events: a large amplitude slow-decay event, and a smaller amplitude fast decay event. These two events showed a similar pattern to those found in Schmidt et al.'s (2008) mouse study, and suggest that though the intrinsic light response of these cells is sluggish, their ability to function as a “typical” interconnected ganglion cell also exists. Thus, SCN-projecting ipRGCs can respond to light both via an intrinsic, melanopsin-based signalling cascade and via a traditional synaptic pathway driven by rods and cones, or both.

There are also some developmental differences between ipRGC subtypes. McNeill et al. (2011) found that ipRGCs typically develop between embryonic days 11-15 in mice. Further, they noted that a subset of ipRGCs develops after the primary group, suggesting a potential difference in functionality; e.g., the group of ipRGCs that co-develops with traditional RGCs may share some of their functions regarding pattern vision, whereas latter developing ipRGCs may be strictly segregated to non-image-forming functions. Finally, the authors noted that the SCN connections from ipRGCs are developmentally distinct from their connections to the LGN, providing further evidence of the functional and developmental differences between ipRGC subtypes.

Amacrine cell inputs to ipRGCs. As stated above, various ipRGC subtypes are found within the sublaminae of the IPL that have afferent and efferent connections to multiple retinal cell types. They share a remarkable amount of connections with traditional retinal cells, most

notably to amacrine cells (Bailes & Lucas, 2010; Pickard & Sollars, 2010). These amacrine cells are thought to reconfigure retinal functioning according to prevailing luminance levels.

A study by Viney et al. (2007) employed two-photon microscopy, immunofluorescent viral labeling (using a retrograde-only pseudorabies virus) and electrophysiological recording to map local ipRGC circuitry in the mouse retina and cortex. The authors communicated two major findings with respect to retinal circuitry. First, they found that type 2 (M2) ipRGCs receive monostratified, inhibitory input from amacrine cells in the inner plexiform layer in response to light stimulation. They also found that type 1 (M1) ipRGCs receive interplexiform (inner and outer plexiform) synaptic input from dopaminergic amacrine cells. The authors concluded that ipRGC function or gene expression is directly influenced by dopaminergic inputs.

Paul, Saafir and Tosini (2009) noted that M1 cells are the only cells to make intra-retinal connection with dopaminergic amacrine cells, and thus may have a modulating role on receptive field size and other retinal characteristics. Zhang et al. (2008) also studied the reciprocal communication of ipRGCs with other cells in the retina. Using a population of transgenic mice, they isolated and stained the afferent and efferent connections from the ipRGCs after exposure to bright light. The authors found that the dopaminergic cells forming synapses with M1 ipRGCs were driven by ON-pathway activity despite the fact they have anatomical synapses found in the OFF layer of the IPL. They also found that ipRGCs showed continuous signs of communication with “sustained” dopaminergic amacrine cells, which in turn formed direct synapses with cone bipolar and horizontal cells. This upstream communication could be responsible for the reconfiguration noted in the reviews above, and could potentially impact the contrast sensitivity of pattern systems to different periodic spatial frequencies (e.g., Wesner & Tan, 2006) or to contrast gain systems (Witkovsky, 2004).

A review by Do and Yau (2010) also reported that presynaptic contact between M1 ipRGCs and dopaminergic amacrine cells. They state that dopamine appears to increase melanopsin production in ipRGCs via D2 receptor action.

Excitatory inputs to ipRGCs. Do and Yau (2010) reported that ipRGCs receive excitatory synaptic input in dark-adapted conditions, which is analogous to the spontaneous dark currents present in traditional (non-photosensitive) retinal ganglion cells (RGCs). The review noted that the synaptic input to ipRGCs is much more sensitive than its intrinsic photosensitivity. The authors also noted that the firing pattern of the ipRGCs was long and sustained, contrasting greatly with the transient excitatory nature of traditional RGCs. The authors also reported that murine ipRGCs receive a minor OFF-pathway input under heavy pharmacological blockade, and posited that it may have some function in registering light offset. Finally, the authors noted that primate ipRGCs received rod-driven excitation via type-II amacrine cells, allowing for functioning at relatively low luminance levels. Further, they reiterated the S-OFF-pathway input that appears to be unique to ipRGCs in primates.

Inhibitory inputs to ipRGCs. In addition to the excitatory inputs in darkness, Do and Yau (2010) reported that ipRGCs receive inhibitory inputs via GABA_A-receptors in both dark-adapted retinas and retinas exposed to light. In the dark, inhibitory currents are smaller than those typical of standard RGCs, but are sufficient to block spontaneous firing ipRGCs. Exposure to light also produces a varying inhibitory signaling in ipRGC, which may indicate the presence of a positive feedback system between amacrine cells and ipRGCs. The authors also noted that the source of inhibitory inputs, in both darkness and light conditions, varies depending on ipRGC subtype; M1 ipRGCs are thought to receive inhibitory synapses from dopaminergic amacrine

cells that co-release GABA, whereas M2 ipRGCs inhibition likely originates in the monostratified amacrine cells of the inner plexiform layer, mentioned above.

Do and Yau posited that the function of these inhibitory signals is to improve ipRGC synaptic response across a range of light levels. In darkness, the inhibition may prevent random signalling to circadian centres of the brain. When exposed to light, a feedback inhibitory system may function as a gain mechanism, making ipRGC responses more transient at low light intensities, and reducing “depolarization block” at higher light intensity to extend the cells’ functional range.

Molecular Markers of ipRGC Subtypes

Pires et al. (2009) used immunocytochemical staining and genetic sequencing on wild type and *Opn4*^{-/-} mice to examine two variants of the melanopsin isoform. The authors found that the M1 and M3 subtypes of ipRGC in mice contained both a long (Opn4L) and short (Opn4S) isoform of melanopsin, whereas the M2 subtype only contained the Opn4L isoform. Further, the authors noted that the Opn4S isoform is approximately 40 times more abundant than Opn4L. There did not appear to be any functional or spectral sensitivity differences between the proteins coded by either isoform, however the authors speculated that the functional differences observed between M1 and M2 ipRGCs may be linked to the amount of isoforms each cell type contains. Specifically, the relatively greater inherent photosensitivity of M1 compared to M2 cells may be due to the increased availability of melanopsin as expressed by the greater amount of Opn4S isoform in these cells. Similarly, the lower expressed concentration of melanopsin in the M2 cells may produce less long-term photoisomerized depolarization effects, thus allowing for greater influential input from the traditional photoreceptors.

A study by Jain, Ravindran and Dhingra (2012) sought to examine the heterogeneity of the Brn3b transcription factor across ipRGC subtypes. The Brn3b transcription factor has been associated with RGC differentiation and survival; specifically, cells that contain the Brn3b transcription factor (Brn3b+ cells) may be more susceptible to early damage and pruning than cells that do not contain this transcription factor (Brn3b- cells). Using double immunofluorescent staining techniques on mouse retinas, the authors found that only non-M1 ipRGCs expressed Brn3b (were Brn3b+). Another related study by Chen, Badea and Hattar (2011) found that blocking the expression of Br3nb impairs PLR in genetically modified mice, but leaves circadian photoentrainment – measured by wheel running activity – intact. They concluded that only M1 (Brn3b-) ipRGCs project specifically to the SCN, which suggests that distinct molecular ipRGC subtypes may be functionally specific. This finding was supported by Nadal-Nicolas and colleagues (2012), who used fluorogold tracing on pigmented and albino rats to identify the distribution of Brn3a, Brn3b, and Brn3c RGCs in the retina. The authors found that all RGCs express at least one of the three Brn3 subtypes, and that many of them express two, or all three. That said, only Brn3b was reliably identifiable in ipRGCs, and then only in approximately 10-14% of them. They noted that this proportion of Brn3b+ ipRGCs in rats was significantly less than that found in mice, whose total proportion of Brn3b+ cells is closer to 65%, and suggests that the expression of the Brn3b transcription factor may be species-specific. Overall, the above studies suggest a species-specific differential expression of the Brn3b transcription factor in ipRGC. The implications of this differential expression are discussed in the summary below.

Central Projections of ipRGCs

Hattar, Liao, Takao, Berson and Yau (2002), and Hattar et al. (2006) provided an extensive overview of the central projections of ipRGCs and their targets in the mouse brain. The results showed a uniformity of ipRGC distribution in the retina that shed new light on their projections to the mouse cortex, which are more widespread than previously thought. The authors confirmed that a sizable proportion of ipRGCs project to the core of the SCN which is known to relay light information necessary for photoentrainment. They also confirmed projections to the intergeniculate leaflet (IGL), the olivary pretectal nucleus (OPN), the ventral lateral geniculate nucleus (vLGN), and the preoptic area. Interestingly, they found additional projections to the lateral nucleus, peri-supraoptic nucleus, and subparaventricular nucleus of the hypothalamus, the medial amygdala, the margin of the lateral habenula, posterior limitans nucleus, superior colliculus, the periaqueductal grey, and the dorsal lateral geniculate nucleus (dLGN). The last connection could provide some basis for the communication of image-forming signals to the perceptual visual cortex vis-à-vis the ipRGCs, as the dLGN has long been established as part of the retinogeniculostriate, visual image-forming pathway in mammals.

Once out of the retina, the projections from the ipRGCs are relatively interspersed among projections from other fibres along the optic nerve until they reach the optic chiasm, at which point they are situated primarily (and overwhelmingly) in the dorsal periphery of the tract (Hattar et al., 2006). Hattar et al. also showed that beyond the hypothalamus, virtually all projections were contralateral to their ocular point of origin.

Reviews by Schmidt, Chen and Hattar (2011) and Schmidt, Do, Dacey et al. (2011) expanded on Hattar et al.'s (2006) review and enumerated the specific cortical projections of M1 and non-M1 ipRGC subtypes. M1 ipRGCs are now known to project to the SCN and the shell of

the OPN. These nuclei are responsible for circadian photoentrainment and the pupillary light reflex (PLR), respectively. Other brain regions thought to be involved in circadian behaviours were also identified as receiving input from M1 cells, namely the IGL and vLGN. By contrast, non-M1 cells (primarily M2 cells) project to the dLGN, which as stated above, play an important role in the relay of visual information to the cortex. Further, non-M1 projections to the periaqueductal gray and the amygdala could signal involvement in photophobia, anxiety, fear, and other functions. With respect to primates, Paul, Saafir and Tosini (2009) reviewed M1 and M2 cell projections and noted that M1 cells project primarily to the SCN (approximately 80% of fibres), whereas in M2 cells approximately 45% of fibres project to the olivary pretectal nucleus (OPN).

Summary of IpRGC Physiology.

IpRGCs are a sparsely-distributed ganglion cell population within the vertebrate retina. Their intrinsic photosensitivity is caused by the presence of melanopsin, a vitamin-A-based opsin with a peak spectral sensitivity of ~480 nm. Melanopsin, typically found in rhabdomeric photoreceptors in invertebrates, communicates by activating the membrane-bound G_{q11} -protein, which in turn triggers phospholipase C that opens membrane-bound cationic channels and causes depolarization. IpRGCs have been shown to have sluggish intrinsic photosensitivity, which has been attributed to the low photopigment density in the pigment and their role as temporal integrators for the circadian system. As such, the irradiance necessary for saturation of these cells is quite high (on the order of 2×10^{16} photons/cm²/s), but they have been shown to respond to much lower irradiance levels ($\sim 1 \times 10^{11}$ photons/cm²/s). Further, many of the studies summarized herein describe the “intrinsic” properties of ipRGCs. These intrinsic properties refer to the unique contribution of the melanopsin phototransduction cascade to functioning both

within ipRGC cells themselves and to visual functioning as a whole. It is to be noted that the “intrinsic” properties of ipRGCs refer to the molecular kinetics of the melanopsin photopigment only, and that connections to traditional photoreceptors also exist as is the case with other retinal ganglion cells.

Two primary types of ipRGC exist in the primate (including human) retina, classified as M1 and M2 cells, though up to five subtypes have been identified in mice. For the purpose of this study, attention will be given to the M1 and M2 subtypes, as they currently have the most literature supporting their existence and functioning in primates and humans.

M1 cells are primarily located in the outer (OFF) sublamina of the inner plexiform layer, though they still receive ON-pathway input from cone bipolar cells. They contain both the long and short isoforms of melanopsin. They also have a subpopulation that does not express the Brn3b transcription factor. They contain the largest concentration of melanopsin of any of the ipRGC subtypes, and have the least complex dendritic arborisation. They show the largest depolarisations and larger current transmission in response to light stimulation as well as faster response decay than M2 cells. They are more cone-input-resistant ($\sim 710 \text{ M}\Omega$), have a greater depolarized resting membrane potential, and are capable of maximal firing rates of $\sim 80 \text{ Hz}$, indicating that they likely rely more on their intrinsic photosensitivity than cone inputs to convey light information to the brain. These cells form both pre- and post-synaptic connection to dopaminergic amacrine cells in the IPL. This complex feedback loop, in which M1 ipRGCs provide excitatory input to sustained-DA-amacrine cells, and receive feedback from these same cells, may be involved in either the regulation of ipRGC responses to increasing light input, modulation of cone firing rates, modulation of receptive field size, or combinations of the three. M1 cells project approximately 80% of their efferent axons to the SCN which hypothetically

makes them the primary class of M cells responsible cells for photoentrainment; whereas the bulk of the remainder of these cells project to the OPN shell, and are likely responsible for the maintenance of the PLR during prolonged light exposure. The photoentrainment hypothesis putatively supports the notion that a cell whose primary function is to communicate longer-duration light information to the SCN does not require a very high maximal firing frequency. Further, such a cell would benefit from a more depolarized resting state, given that such a property would prevent it from responding to shorter/dimmer light stimuli during sleep hours. Further, the M1 ipRGCs typically does not express the Brn3b transcription factor; this differential expression could be a guard against early developmental pruning, and might be responsible for allowing the maintenance of photoentrainment responses in the event of retinal malformation.

M2 cells are primarily located in the ON sublamina of the IPL. These cells contain only the long isoform of melanopsin (Opn4L). Again, as stated earlier, the functional distinction between the two isoforms has yet to be established although there has been some suggestion that the lower overall concentration of the Opn4L isoform is responsible for the lower melanopsin concentration, and thus the lower intrinsic photosensitivity in these M2 cells. M2 cells also express the Brn3b transcription factor. Although the effects of this expression are not known, it is believed to be involved in retinal neurogenesis and differentiation, and is found in other RGCs. This similarity between M2 and traditional RGCs may be indicative of similar neural development, and may explain why M2 ipRGCs are more apt to receive rod and cone input than their M1 counterparts. M2 cells also have a more complex dendritic arborisation than M1 cells. They show lower amplitude spiking and more sustained firing than that of the M1 cells, and they have a slower post-stimulus-offset decay function. Their membranes are less cone-input

resistant, their resting membrane potential is more hyperpolarized, and they have a higher maximum firing rate (~240 Hz). Though this slower decay and faster firing rate may seem counterintuitive, it is to be noted that these figures are reflective of the intrinsic properties of these cells, and that ipRGCs, including M2 cells, may show different properties when included in the retinal circuit. This indicates that M2 cells function more like traditional RGCs, in that they rely more heavily on cone input to convey light information to the brain. M2 cells also synapse with monostriated amacrine cells and type-II (rod) amacrine cells, both of whose function seems to be to extend the M2 cells' dynamic temporal and irradiance coding properties. These characteristics could make these cells ideal for the transmission of cone-bipolar signals, because they would not be as readily depolarized by their intrinsic phototransduction cascade as M1 cells, and also possess a maximal firing rate more conducive to the temporal resolution required of visual pathways. They seem to receive input primarily from DB6 cone-bipolar ["yellow" or (L+M)-ON], and project primarily to the OPN core, the dLGN and the superior colliculus; that said, the most interesting of these with respect to the present study is in the dLGN, due to its involvement in image-forming visual communication to be discussed later.

Non-Image-Forming (NIF) Functionality of ipRGCs

The modulatory effect of ipRGCs on the circadian system of both nocturnal and diurnal animals has been extensively researched, though the interplay of rods and cones with this non-image-forming (NIF) pathway has only recently become apparent. The primary functions of the NIF pathway are circadian phase setting (and by extension photoentrainment, sleep regulation, and melatonin suppression) and pupillary light reflex. The following is a review of the role of ipRGCs, rods and cones in the regulation of NIF functions in non-human animals and humans.

Circadian Photoentrainment

Hattar et al. (2003) used genetically modified mice to determine the influence of rods, cones and ipRGCs on circadian and vegetative functioning. They bred mice with no rods or cones (melanopsin-only; MO), mice with no ipRGCs (melanopsin knock-out; MKO), and mice lacking any photoreceptor (triple knock-out; TKO), and compared their behaviour to those of “wild-type” (WT) mice. In their first experiment, they exposed the mice to varied circadian cycles, modifying their light:dark cycles from 12h:12h to 16h:8h to 3.5h:3.5h using an 800 lux “daytime” light. They found that phase-delay and phase resetting (measured by free wheel-running behaviour) were both impaired in MKO and eliminated in TKO mice, but that MO mice were able to properly photoentrain despite the absence of “classical” photoreceptors. In the second part of the experiment, they used a 15-min, near monochromatic light pulse at 420, 460, 471, 506, 540, 560 or 580 nm (10^9 - 10^{14} photons/cm²/sec; irradiance corrected for lens transmission) to determine the effects of acute light exposure on phase shift. They found that the optimal wavelength of light for photoentrainment matched that for optimal pupillary constriction (i.e., 481 nm) in mice with the intact melanopsin gene, further supporting the notion that these cells drive both the pupil reflex and circadian photoentrainment. In their third experiment, the same mice were exposed to a 60 s flash of 360 to 660 nm light (in 10-nm steps) delivered at 86-140 μ W/cm². Maximum sensitivity, defined by pupillary constriction, was shown to be at 480 nm. They found that MO and MKO mice showed impaired pupillary constriction and TKO mice showed no pupillary constriction at all; though MO mice showed a slower onset to stimulus presentation compared to the other groups, and MKO mice had difficulty sustaining the response to stimulus presentation compared to the other groups. The authors concluded that both classic

and novel photoreceptors were required for normal pupillary constriction, though only ipRGCs are required for circadian photoentrainment.

Because of the significant spectral sensitivity overlap between mouse M-cone opsin and melanopsin, Lall et al. (2010) used cloned mice in which the murine M-cone opsin was replaced with a human L-cone opsin to determine the distinct contributions of rods, cones and ipRGCs to irradiance encoding in the circadian system. They accomplished this by measuring pupillary light reflex and circadian photoentrainment (measured by wheel running activity) to broad spectrum, 498-nm, or 644-nm light. They found that M-cones contributed to the pupillary light reflex, but only in terms of response speed, and that cones alone were unable to maintain full pupillary constriction after they adapted. Contributions of S-cones were ignored because their peak sensitivity in mice is 360 nm which is well outside the operating range of mouse ipRGCs. Just as the cones were unable to sustain tonic pupillary responses, so too did the authors find that the cones could not contribute to sustained circadian photoentrainment due to their faster light adaptation periods. The above two findings are well in line with findings from other studies (e.g., Hattar et al., 2003). Finally, and surprisingly, Lall and colleagues found that at scotopic light levels, rods can influence ipRGC behaviour and thus circadian phase (but not pupillary response). The authors noted that the accepted pathway for rod signal transfer under photopic conditions is through gap junctions to the cones, and then relayed through the cone bipolar cells to the RGCs. Since it was shown that rods were able to effect change on ipRGCs without cone contribution, the authors proposed that the rods were either forming synapses to a population of ON-cone bipolar cells, or that the rod bipolars were forming synapses directly to the ipRGCs themselves.

A study by Ruggiero, Allen, Brown and Robinson (2009) genetically modified knock-out mice to examine the developmental course of retinas in mice lacking outer photoreceptors. They found that the absence of rods and cones in developing mice does not inhibit the development of ipRGCs; in fact, the contrary is true. Using an immunocytochemical staining technique, they found that mice raised without classical photoreceptors actually had retinas that contained *more* ipRGCs than normal or wild-type mice. The authors concluded that: a) rods and cones are not necessary for the development of ipRGCs, and b) the classical photoreceptors may actually contribute to “pruning” ipRGCs as mice mature. This finding suggests that ipRGCs may have more of a role in the early stages of retinal development and circadian photoentrainment, and that some functions related to photoreception may be performed by rods and cones as the retina matures. In a later study, Ruggiero, Allen, Brown and Robinson (2010) took their previous findings a step further and examined how the lack of functional rods and cones would affect higher-order circadian systems (i.e., SCN functionality). Using the same population of knock-out mice, they measured the number of SCN cells expressing vasoactive intestinal peptide (VIP) and vasopressin (VP), two neuropeptides with important roles in circadian rhythmicity. Their findings showed that the increase in retinal ipRGC populations demonstrated in their previous study (i.e., Ruggiero, et al., 2009) directly correlated with an increase in VIP- and VP-positive cells in the SCN. They concluded that the presence of rods and cones contributed to the normal maturation of the circadian system by reducing overabundant ipRGCs.

Altimus et al. (2008) found that rods, cones and melanopsin (via ipRGCs) were all required for photoentrainment in mice. They used a combination of electroencephalographic and electromyographic recordings on a group of mutant mice lacking either ipRGCs, phototransduction pathways of rods and cones, or the melanopsin protein, and exposed them to

light and dark pulses at various stages of the sleep-wake cycle. They found that the presence of melanopsin containing ipRGCs and rods/cones were enough to induce sleep and/or wakefulness in response to light/dark pulses respectively, but that the combination of both systems was required to sustain the response during the entire test period. Mice with no ipRGCs did not respond to light pulses at all, indicating that these cells are crucial in the relay of light/dark information to the circadian centres of the brain. The authors construed that in order for photoentrainment to be optimal, mice must have both traditional photoreceptor and ipRGC (melanopsin) mechanisms available during changes in ambient light.

Rovsing, Rath, Lund-Andersen, Klein and Moller (2010) examined the effects of circadian modulation on mice with and without rod or cone photoreceptors, but with intact ipRGCs. They monitored the wheel running activity and temperature of the mice over forty days, and found that though mice lacking outer photoreceptors still displayed photoentrainment behaviours and diurnal temperature variation, their cycle was less robust than that of wild-type mice. The authors concluded that rods and cones may be necessary for more accurate photoentrainment. There are some caveats to these findings, however, in that the authors acknowledged that the knockout mice used in the study could have had an underdeveloped SCN as a result of being born with no rods or cones (see Ruggiero, Allen, Brown, & Robinson, 2010). Further, the present author was unable to find within the publication a measurement of the light source used to photoentrain the mice. Since it has been established that the ipRGCs' intrinsic light response requires relatively high irradiances to achieve peak functionality, it is possible that the light used by Rovsing and colleagues was simply insufficient for maximal entrainment efficiency.

In a study by Boudard et al. (2009), 16 young adult male Long Evans rats were injected with a solution of *N*-methyl-*N*-nitrosourea, a compound that causes acute retinal degeneration including the destruction of virtually all rods/cones and approximately 37% of ipRGCs. After a 12:12 day/night photoentrainment period, the treated rats were able to entrain properly with bright light exposures (~300 lux), but showed significant impairment with a lower light intensity (15 lux) and no ability to photoentrain at all with the lowest intensity light exposure (1 lux). This study provides further evidence that though responsive, ipRGCs are far less sensitive to light than traditional photoreceptors, and thus rods/cones may be needed to photoentrain at lower than normal luminances. In line with this idea, a recent study by Dollet, Albrecht, Cooper and Dkhissi-Benyahya (2010) showed that the mice lacking the M-cones had a reduction in phase-shift associated behaviours in response to middle- (480 nm) and long- (530 nm) wavelength pulsing light stimulation. The authors concluded that cones could provide a strong initial phasic input to the ipRGCs (and thus the SCN), and may in fact “prime” ipRGC responses to shorter-duration light exposures.

With humans, Gooley et al. (2010) explored the contributions of cones to the circadian system. Individuals were exposed to 6.5 hours of either 555 nm or 460 nm light at the onset of nocturnal melatonin secretion. The stimulus intensities were varied in logsteps from 0.4 to 375 lux. Their results showed that 555 nm light was effective in delaying melatonin onset acutely, but over time, the light suppression diminished rapidly compared to the 460-nm light exposure. Further, Gooley et al. showed that 555 nm light was more effective in acutely suppressing melatonin at lower irradiance levels than the 460 nm light. They concluded that rods and cones together contribute to circadian photoreception at lower irradiances, but that these effects cannot be maintained for longer-term phase-setting unless the ipRGCs are involved.

Rea, Figueiro, Bullough and Bierman (2005) wrote a review detailing one current model of phototransduction by rods, cones and ipRGCs in the human NIF circadian system. In addition to providing support for some of the currently held connectivity models described herein, the authors elucidated the mechanism by which all three photoreceptors communicate with the SCN. When considering rod contributions to the circadian system, the authors stated that low (scotopic) light levels do not provide robust, measurable circadian responses, and that rods, on their own, cannot be considered direct circadian phototransducers. Rea et al. however, postulated that rods may play an indirect role in the entrainment of the circadian system via type-II amacrine cell connections to ipRGCs. Effectively, the rods in this model would act as “gatekeepers”, hyperpolarizing the ipRGCs via AII amacrine cells until such time that the rods are saturated or that the excitation effect of light directly on the ipRGCs was large enough to send a signal to the SCN, or both.

Further, Rea and colleagues proposed a spectral opponency component to their model that runs counter to that proposed by Dacey et al. (2005) in which, in addition to shunting rod inhibition, the ipRGCs receive afferent signals from the classic S-ON, (L+M)-OFF cone-bipolar cells. Further discussion of possible S-cone opponency is detailed in the image-forming pathway section below, however it is possible that given Rea et al.’s focus on the circadian system, their conclusions *may* be focused on M1 ipRGCs, whereas Dacey and colleagues *may* be referring to the M2 subtype. "*May*", because these subtypes were not mentioned in the aforementioned papers.

Figueiro, Bullough, Parsons and Rea (2004) found preliminary evidence for spectral opponency in the circadian system. They measured nocturnal melatonin suppression in a group of four male human participants to either a “blue” LED (peak at ~480 nm) or broad-spectrum

mercury-vapour (multiple peaks at ~436, 550, and 580 nm) light sources. The luminance provided by the sources was matched to 460 nm luminance at the cornea. The results of this study showed that the LED light source was more effective at suppressing melatonin concentration levels than the polychromatic source, and, given the roughly equivalent power spectra at shorter wavelengths, the authors concluded that a spectral opponency may exist in the circadian photoreceptor system.

Later, Figueiro, Bierman and Rea (2008) sought to further elucidate the potential spectral opponency first suggested by Figueiro, Bullough, Parsons and Rea (2004) and Rea, Bullough and Bierman (2005). They measured light-induced melatonin suppression in a group of 10 humans with combinations of monochromatic light delivered to both eyes. In one condition, one unit of blue ($\lambda_{\max}=450$ nm; 0.077 W/m²) light was delivered to the right eye, and one unit of green ($\lambda_{\max}=525$ nm; 0.211 W/m²) was delivered to the left eye (units of light were matched for their ability to suppress melatonin during a 45-minute exposure). In the second condition, the blue and green lights were delivered to the opposite eyes, and in the final condition, each eye was exposed to a half unit of both wavelengths mixed. The authors found that though there was no difference between the first two conditions (they both suppressed melatonin equally well), the third condition showed a significant decrease in suppression leading the authors to posit a novel spectral opponency response by the non-image forming circadian pathway.

Weng, Wong and Berson (2009) attempted to determine whether ipRGCs themselves were subject to circadian regulation via a light-dependent feedback system or through retinal circadian oscillators (i.e., “clock cells”). A group of Sprague-Dawley rats were initially photoentrained to a 12h:12h light:dark cycle, and their retinas harvested for testing at different circadian times conforming to early morning (within the first hour of the light cycle), midday

(between the sixth and seventh hour of the light cycle), early night (between the twelfth and thirteenth hour of the light cycle), and midnight (between the sixth and seventh hour of the dark cycle). Recording was accomplished using mounted retina on a multielectrode array. Their finding showed a modest increase in response gain in the “early night” phase when cells were exposed to intense light. The authors concluded that ipRGCs lack cell-autonomous circadian modulation and that the phase-dependent alterations in the efficacy of retinohypothalamic tract transmission may be governed by a more global feedback system originating from the SCN itself.

A study by Thompson et al. (2010) examined the influence of image-forming and non-image-forming visual systems on a series of behavioural tasks in mice. Rodless-coneless mice (*rd/rd cl*) were compared to coneless mice (*Rpe -/-*) and wild-type mice on three tasks. The first was a light aversion task in which time spent in the “light” portion of a chamber was calculated for all three mouse types. The authors found that the wild-type mice avoided the “light” chamber more than the other two types and that no significant difference between the *rd/rd cl* and *Rpe -/-* types were noted. The second and third tasks involved positive and negative masking, respectively. Positive masking was defined as the introduction of a “dark pulse” at Zeitgeber Time 6 (ZT6; 6 hours after “lights on”), a period during which the mice would normally be asleep. In response to this “dark pulse”, an increase in wheel-running behaviour was expected. The authors found that *rd/rd cl* mice did not show this increase in wheel running, and that it was limited in *Rpe -/-* mice when compared to wild-type mice. In the negative masking task, a light pulse was introduced at ZT16, a period during which the mice would normally be active and a suppression of wheel running behaviour was expected. The authors found that *rd/rd cl* mice did reduce their wheel running, however *Rpe -/-* mice did not. They also noted that the reduction in

wheel-running in *rd/rd cl* was not linearly dependent to irradiance; rather, it appeared that a minimum “threshold” irradiance was required to trigger a reduction in wheel running, suggesting a less temporally-sensitive radiance detector such as ipRGC. Overall, the authors noted that ipRGC activity is sufficient to motivate certain circadian behaviours, but that they are less sensitive and have lower temporal resolution than rods and cones.

Sleep regulation. Altimus et al.’s (2008) EEG/EMG study described above also noted that ipRGCs were important for sleep regulation in rodents. The authors found that *Opn4*^{-/-} mice could not photoentrain to sleep-wake cycles like their wild-type counterparts.

Another study by Lupi, Oster, Thompson and Foster (2008) used wild-type, *rd/rd cl*, *Opn4*^{-/-}, and *Opn4* littermate controls (*Opn4*^{+/-}) to assess the contribution of ipRGCs to sleep induction in response to light. The authors found that photic sleep induction, even in extremely bright light, was preserved in all but the *Opn4*^{-/-} mice, supporting the position that ipRGCs, and not rods or cones, are crucial for sleep regulation. The authors further noted that sleep induction in response to light stimulation is rooted in the ventrolateral preoptic nucleus (VLPO), demonstrated by the finding that *c-fos* expression in the VLPO was unaffected in *rd/rd cl* or wild-type mice, but was significantly impaired in *Opn4*^{-/-} mice. This finding also supports the functional connection of ipRGCs to the VLPO, and speaks to its broad connectivity in the brain.

Tsai et al. (2009) compared sleep patterns and electrocorticogram recordings in wild-type and *Opn4*^{-/-} mice. Using a 1h:1h light-dark cycle, the authors were able to determine that the deficits in sleep regulation in *Opn4*^{-/-} mice were limited to the transition from dark to light, and not vice-versa, implicating ipRGCs in the detection of photic stimulation and not “dark currents” that are characteristic of photoreceptor depolarizations in the absence of light. They also found that *Opn4*^{-/-} mice slept significantly less than wild-type mice during a 12h light period. They

concluded that ipRGCs compensate for the transience of traditional photodetectors (e.g., rods and cones) during the day, and that ipRGCs also regulate sleep homeostasis.

IpRGCs and the pineal organ. Gooley et al.'s (2010) findings regarding wavelength-dependent melatonin suppression suggest a link between ipRGCs and the pineal organ. Other findings regarding the increased circadian sensitivity to short-wavelength light in humans support this link (Brainard et al., 2008; Thapan, Arendt, & Skene, 2001). As stated above, it has been established that ipRGCs, particularly the M1 subtype, have substantial projections to the SCN, which in turn regulates the production of melatonin in the pineal organ via a multisynaptic connection (Vigh et al, 2002). It has also been shown that the pineal organ is subject to central neuroendocrine feedback (Reuss, 2010), and that the pineal organ photoreceptors or photoreceptor-like cells may provide feedback to the retina and regulate circadian visual sensitivity (Li et al, 2012). The role of ipRGCs in this feedback system is as yet unknown; however it seems likely that they would provide indirect signalling via the SCN. It is also unclear at this time whether ipRGCs would receive neuromodulatory feedback from melatonin.

Pupillary Light Reflex

McNeill et al. (2011) noted that M1 ipRGC axons synapsing with the OPN shell during development co-occurred with the development of the PLR. Non-M1 synapses to the OPN core, which appear earlier in development, do not appear to have any effect on the PLR. This suggests that though both major subtypes of ipRGC synapse with the OPN during development, only the M1 subtype is linked to the PLR, and that non-M1 synapses to the OPN core may serve another purpose.

Guler et al. (2008) used melanopsin knockout mice to assess rod and cone contributions to circadian phase setting and pupillary light reflex. Their findings support the idea that intact

ipRGCs are required for adequate pupillary constriction at both lower ($1.8 \mu\text{W}/\text{cm}^2$ for 30s) and higher pupil irradiances ($3.0 \text{ mW}/\text{cm}^2$ for 30s). Studying wavelength selectivity on pupillary reflex, Gamlin, et al. (2007) investigated both human and macaque primates positioned in a Maxwellian-view optical system capable of delivering varying wavelengths from 430 to 613 nm in one eye, and the consensual constriction in the non-stimulated eye was measured. Macaques were injected with a combination of CNQX and L-AP4 to block ON and OFF retinal channels and isolate ipRGC activity. Their results showed that the pupil response kinetics of macaques under pharmacological blockade very closely approximated the sluggish and sustained response pattern of ipRGCs. In humans, they found that consensual pupil response was sustained during post-light offset when using a 493 nm light source compared to a 613 nm light source, which is putatively invisible to ipRGCs. Thus, although classical photoreceptors were responsible for the initial response to the stimulus, the post-stimulus maintenance of constriction was due to slower-acting ipRGCs. These results also indicate that ipRGC contributions to the PLR are bilateral, and likely controlled by feedback from the OPN shell.

Another study by McDougal and Gamlin (2010) sought to further detail the interaction between rods, cones and ipRGCs in terms of pupillary constriction. After topically instilling the anticholinergic, tropicamine to dilate the pupils (i.e., a parasympatholytic response), human subjects were presented with light stimuli ranging from 450 to 650 nm presented from 4 to 110 s in duration. They found that ipRGCs contributed to half the maximal pupillary constriction at low photopic irradiance. They also found that rods were greatly involved in this process at light levels below the threshold for ipRGC activity. Finally, they noted that though cones are initially involved in constriction, they “adapted out” very quickly, leaving the ipRGCs to sustain the reflex over longer periods (at photopic light levels), analogous to the findings of Lall et al.

(2010). This model was supported by Tsujimura, et al. (2010) who used a silent substitution method (defined below) on human participants to isolate the wavelength-based functioning of the ipRGCs, and their contribution to the pupillary light reflex. They found that ipRGCs contributed three times more to pupillary constriction than L- or M-cones; it is to be noted that the authors assumed negligible S-cone input to the irradiance detection system in the retina. Kimura and Young (2010) also explored the contribution of M- and L-cones to pupillary constriction. The authors varied the light projected onto the retina by irradiance and chromaticity, specifically isolating the contributions of M-cones, L-cones, rods and ipRGCs. Their findings indicate that pupillary constriction may involve a chromatic opponency channel as well as an irradiance coding channel. Indeed, the authors stated that sustained pupillary response is at least partially mediated by an L- and M-cone opponent interaction.

As stated above, Tsujimura et al. (2010) used a silent substitution stimulation technique on six human observers to ascertain the contribution of ipRGCs to the PLR. The silent substitution technique involved modulating either the relative ipRGC excitation (around 480 nm), the relative luminance, or both (ipRGC excitation + luminance) of a test probe with respect to an averaged “control” condition. The authors recorded pupil diameter change using an infrared camera while varying the relative contributions of (L+M) luminance and an ipRGC-specific wavelength to a steady-state light source. They found that ipRGC contribution to the PLR was approximately three times that of (L+M) luminance channels.

In a similar attempt to understand the contributions of ipRGCs, Fukuda, Tsujimura, Higuchi, Yasukouchi and Morita (2010) used human ERG measurements of retinal excitation to determine the unique contribution of ipRGCs on the circadian system. They used the ERG in combination with a silent substitution technique developed by Tsujimura *et al.* (2010) with

human participants, in which the luminance contrast (ranging from 10 to 50%) of a 3-s temporal sinusoidal wave, flickered at a frequency ranging from 0.5 to 30 Hz and modulated through a background kept at a constant luminance, was further varied along one of three “excitation” axes based on a) ipRGC excitation estimated from the pigment template nomogram provided by Dacey et al. (2005) with peak sensitivity at 482 nm, b) (L+M) cone excitation assuming negligible involvement of S-cones towards luminance processing, and c) radiant energy, defined as the combination of ipRGC sensitivity and L+M luminance channels. Fukuda et al. found that contrary to the predicted sluggish behaviour observed in past studies, the ipRGCs responded well to stimuli flickered up to 12.5 Hz and also responded to contrasts in a linear fashion. They concluded that their silent substitution approach was successful in behaviourally isolating ipRGC functionality from rods and cones.

Summary of Non-Image-Forming Functionality of ipRGCs

Although there is some debate as to the exact role rods, cones and ipRGCs play in the regulation of NIF visual function, a few tentative conclusions can be drawn.

First, it appears that in terms of pupillary light constriction, all three photoreceptor classes are required to maintain the full range of functionality across varying light levels. The above literature suggests that rods could offer some limited functionality at scotopic light levels (below the threshold for cone vision). It also suggests that cones may provide the initial, “fast” input for constriction at low and mid photopic levels, before the ipRGCs are fully depolarized. Once depolarized, the ipRGCs are then capable of maintaining the constriction over longer periods of time. This is a useful trait because the cones tend to “adapt out” quickly at higher photopic luminance levels.

As for circadian photoentrainment, the picture is less clear. Some authors argue that ipRGCs alone are required for the maintenance of circadian rhythms, while others purport that cones (and indeed even rods) are needed to fully (and reliably) photoentrain. It seems that the interplay between the classic and non-classic photoreceptors relies on the level of ambient luminance and time of exposure to a particular light source. The argument goes as follows: at light levels below the threshold of ipRGC activity, the classic photoreceptors are more sensitive and are thus able to transmit circadian information in a limited fashion in the absence of an intrinsic ipRGC response. Once ambient light levels are sufficient (or are present for a sufficient amount of time), the temporally-integrating ipRGCs provide a more robust, sustained signal to the SCN. Questions still remain, however, as to the exact connectivity and spectral opponent characteristics of these cell subtypes. For example, Rea and colleagues (2005) have identified a “cross-point” in the spectral sensitivity of the circadian system around 500 nm, that corresponds to the integration of rod, cone and melanopsin signals and that could only be possible with the addition of a fifth photoreceptor, namely ipRGC. The authors hypothesize that at photopic light levels, SCN circadian responses to wavelengths at or above 500 nm are entirely driven by ipRGC’s intrinsic photosensitivity, whereas those below 500 nm are driven by a combination of S-ON (via S-cone bipolar) and the loss of shunting rod inhibition as described above.

Contributions of ipRGCs to Image-Forming Pathways

In addition to the above studies supporting the notion that ipRGCs can function as “normal” ganglion cells in addition to their intrinsic photosensitivity, a few studies have recently posited that ipRGCs can also communicate directly with the image-forming visual system.

A study by Dacey et al. (2005) was the first to purport that ipRGCs could contribute to conscious visual perception. The authors used *in vitro* recordings of affixed macaque and human

retinal cells and found a subset of “giant” melanopsin-expressing (i.e., photosensitive) ganglion cells that receive strong rod and cone input. They showed that these ipRGCs display a rare S-OFF, (L+M)-ON colour opponent receptive field, and that rod and (L+M)-cone activity is combined within the ganglion cells to signal irradiance levels to the LGN and beyond.

In a case study, Zaidi et al. (2007) discovered that humans lacking any functional rods or cones could reliably detect the presence of light in a narrow spectrum. A female subject with autosomal-dominant rod-cone dystrophy was presented with a two-interval forced-choice task in which she was required to identify the interval that contained a light stimulus. She was accurate in detecting light stimuli at 481 nm, but failed at longer or shorter wavelengths, leading the authors to conclude that ipRGC input to the LGN did support image-forming or conscious light perception.

Another recent study by Ecker et al. (2010) demonstrated the input of ipRGCs to the visual system in mice. Using three groups of mice (WT; wild or control, MO, and TKO) they found that MO mice were capable of discriminating between two equiluminant fields, one a homogenous “grey” and the other containing a spatial-frequency varying sine-wave grating. The sensitivity of the MO mice was greatly reduced compared to the WT mice (0.16 cycles per degree [c/deg] vs. 0.55 c/deg, respectively), but the responses were still measurable, leading the authors to conclude that the ipRGC had some input into the image forming spatial pathways of the brain beyond simple light/dark or brightness information. It remains to be determined whether these results can be generalized to primate/human populations, owing to the differences in processing specificity in the mouse visual system.

There also exists evidence that ipRGCs can function as a circadian modulator of classical vision systems. A study by Barnard, Hattar, Hankins and Lucas (2006) used ERG on MKO and

wild-type mice to determine the diurnal variations in amplitude and speed of cone responses. They found that though these diurnal variations existed in wild-type mice (responses were both larger and faster during the day than at night), they were absent in knockout mice, leading the authors to conclude that ipRGCs modulate (and likely optimize) cone responses according to the time of day, leading to changes in conscious visual perception dependent on circadian phase.

Also using MKO mice, Guler et al. (2008) verified the contribution of ipRGCs on pattern vision using ERG, optokinetic nystagmus response, visual acuity and the ability of the animals to detect visual cues. Though no deficiencies were found in ERG patterns, nystagmus responses, or in the animals' ability to find a marked platform in a water maze using a cue, there was a slight deficiency noted in acuity which the authors attributed to an enlarged pupil diameter. The authors conclude that ipRGCs only contribute in a modulatory fashion to image-forming visual pathways. Nonetheless, these minute drops in acuity could also be explained by ipRGC dysfunction, as ipRGCs do not, in theory, contribute greatly to image formation (cf. Ecker *et al.*, 2010, above).

A recent study by Brown et al. (2010) revealed direct input to the visual cortex from ipRGCs. Using a combination of immunostaining and in-vivo cortical recording in *Opn4Cre/+* genetically modified mice, the authors were able to determine that under steady illumination, ipRGCs set the tonic firing rate for approximately 40% of all light-sensitive cells in the dLGN. They further noted that *Opn-/-* mice showed LGN saturation at around the photometric threshold for ipRGC activation. Brown and colleagues thus concluded that an irradiance-dependent “switch” from rod/cone to melanopsin-based irradiance coding exists at the dorsal LGN. This switch is similar to other melanopsin-based functions such as the PLR that require sustained input from ipRGCs to maintain their activity state beyond the limited temporal encoding capacity

of rods and cones. The authors posit that ipRGCs' sustained firing compensates for a fundamental limitation of cones to encode irradiance across the photopic visual range. They further posit that this may be explained by the saturation in the "steady-state" level of cone hyperpolarization under extended illumination, and that under those conditions, photoreceptor adaption and bleaching desensitization would allow cones to track higher frequency modulations in light intensity without necessarily encoding long-term changes in background illumination. In essence, the ipRGCs in the retinal circuit may be seen as setting the "baseline" perceptual luminance level from which the cones then track faster and more transient light-level changes.

Potential Evidence for Modulatory Effects on Image Formation

A study by Szabo et al. (2004) used a contrast sensitivity task involving static and temporally-modulated luminance sine-wave gratings to determine the effects of bright light therapy on participants with Seasonal Affective Disorder (SAD) and on healthy controls. Their results showed that SAD participants had higher contrast sensitivity after bright light therapy than controls for spatial frequencies up to 5.7 cycles/degree. This finding could suggest a hypersensitivity in the ipRGCs of persons suffering from SAD producing increased melanopsin-dependent dopamine release from dopaminergic amacrine cells. This could translate into greater gap junction decoupling of the horizontal cells, thereby reducing receptive field size and increasing sensitivity to higher spatial frequencies (Witkovsky, 2004). This was partially replicated (and expanded) by Wesner and Tan (2006) who used spatial or phase-modulated gabors to assess the contrast sensitivity of SAD, non-seasonally depressed, and control participants. They found that starting at 6 cycles/degree, SAD and depressed participants had significantly increased sensitivity to static gabors compared to controls. The SAD group also showed higher sensitivity to 4 c/deg, 2 cycles/s (Hz) stimuli. Given the evidence for the

interaction of ipRGCs with horizontal cells (via feedback from dopaminergic amacrine cells), it is possible that an increased sensitivity of ipRGCs, caused by a disruption in 5-HT, could cause increased decoupling of horizontal cells, with the net effect of an increase in higher-frequency contrast sensitivity.

A study by Bubl et al. (2010) used pattern electroretinograms to assess contrast gain in Major Depressive Disorder (MDD). The authors studied 40 people with diagnosed MDD and 40 age- and sex-matched controls using a contrast reversing, 0.8° checkerboard pattern. They found that regardless of medication level, participants with MDD showed significantly “flatter” contrast gain curve compared to controls, indicating that control participants had higher overall sensitivity gains as contrast was increased. Further, they noted that scores on the Beck Depression Inventory (BDI-II; Psychological Corporation, San Antonio, TX) directly and strongly inversely correlated with contrast gain. The authors concluded that reduced contrast gain could be a bio-marker for depression that is independent of linguistic biases.

A study by Ichinose and Lukasiewicz (2007) used electrophysiological recordings of prepared, ex-vivo tiger salamander retinas to ascertain the influence of bipolar cell sodium channels and dopaminergic amacrine cells on retinal gain changes. They found that voltage-gated sodium channels amplified light-evoked synaptic responses in cone pathways. They also found that under dim light, dopaminergic amacrine cells inhibited the sodium channels, minimizing signal saturation in the cone pathway. Given the established link between dopaminergic amacrine cells and ipRGCs, as well the ipRGCs’ intrinsic light sensitivity, it is possible that ipRGCs may also contribute to gain operations in the retina, either directly or as part of this dopamine-driven circuit.

Vugler et al. (2007) compared the retinas of wild-type and dystrophic rats with human retinas to ascertain the influence of dopaminergic neurons on ipRGCs. The authors used a triple-immunolabeling procedure that provided unidirectional signal tracing, and noted that ipRGCs are influenced by dopamine synapses. They also noted that the architecture was comparable between murine and human, leading to a further argument that dopamine may be able to influence circadian targets in the cortex of humans.

Summary of Contributions of ipRGCs to Image-Forming Pathways

Given the relative scarcity of studies that have examined the role of ipRGCs on image-forming vision, it should come as no surprise that definitive convergences in literature are, as yet, absent. What can be said about ipRGCs contributions to image-formation follows.

IpRGCs seem to show a novel chromatic opponency (Dacey et al., 2005). Though lacking a center-surround arrangement, the S-OFF, (L+M)-ON receptive field displayed by at least a subpopulation of these cells is of interest, as it could potentially affect higher-order chromatic-based pattern vision in humans. Also, ipRGCs appear to be capable of independent contributions to pattern vision (Ecker et al., 2010). Although this study's population was mice (and thus perhaps not generalizable to humans), it does provide support for the notion that some fibres from ipRGCs do synapse with the visual cortex. IpRGCs can also independently communicate perceived "brightness" information in humans (Zaidi et al., 2007). Though this conclusion is based on a case study and further replication is warranted, the ability of a person to "perceive" a relatively narrow wavelength of light, at the exclusion of all others without classic photoreceptors, lends some weight to this argument. Finally, the potential modulatory effect of ipRGCs on higher-order vision (i.e., contrast sensitivity) is also a potential avenue of exploration, and could provide a way to differentiate the two subpopulations of these cells.

S-Cones

The presence of a novel, S-OFF pathway emanating from the M2 subtype of ipRGCs in primates offers a potentially unique target in assessing their functionality in humans. The following is a brief review of the anatomical and functional characteristics of S-cones, and the koniocellular pathway.

S-Cone Physiology

Short-wavelength-sensitive cones (S-cones) are a subpopulation of traditional photoreceptors that express the photopigment *cyanolabe*, and differ greatly from middle-wavelength (M-) and long-wavelength (L-) sensitive cones (Calkins, 2001). S-cones' inner segments are long and wider than those in M- and L-cones, and their axon terminal is smaller and more deeply located in the synaptic layer of the retina (Calkins, 2001). The s-opsin is relatively homologous in primate species, with 92% concordance across humans, Old World primates and New World primates, with peak spectral sensitivity being maintained between 419-433 nm (Calkins, 2001). S-cones are also genetically distinct from other cone types; it is autosomal as opposed to the X-chromosome-linked properties of L- and M- cones. Further, S-cones only account for approximately 5-10% of the total cone population (depending on species), and they form a semi-regular mosaic in the retina, compared to the random placement of M- and L-cones. They are also absent from the very center of the foveal pit, concentrating instead in a region approximately 0.3-0.4° away from the center of the fovea (e.g., in the foveola; Calkins, 2001). The neurogenesis of S-cones during development also appears to be distinct from that of M- and L-cones; the migration of S-cones does not seem to follow the same centrally-flowing pattern as other photoreceptors, and its distribution seems to be more "regular" than the random allocation of M- and L-cones during development.

S-ON vs. S-OFF

The present study's design and hypotheses are based on the theory that light increments and decrements are processed by separate, parallel pathways beginning at the retina and projecting to the cortex. These two pathways are aptly named ON (responsive to light increments) and OFF (responsive to light decrements; Bowen, Pokorny & Smith, 1989; Celesia & DeMarco, 1994; Roveri, DeMarco & Celesia, 1997; DeMarco, Hughes & Purkiss, 2000). It is worth noting at this point that the baseline asymmetry between ON and OFF pathways differs when comparing luminance-based and S-cone specific systems. Specifically, it has been shown that luminance-based retinal systems tend to be more sensitive to decrements in light, and thus have an OFF bias (Bowen, Pokorny & Smith, 1989). That said, there is some debate about the baseline asymmetry of chromatic and S-cone specific systems. Demarco, Smith and Pokorny (1994) noted that there are no substantial sensitivity differences between ON and OFF pathways in the chromatic system. On the other hand, Racheva and Vassilev (2008) found a sensitivity advantage for light decrements (putatively involving the OFF pathway) for S-cone specific pathways. Further, Calkins and Sterling (2007) recently found morphological evidence suggesting that S-cones may communicate via DB2 and DB3 bipolar cells, typically associated with luminance signal communication in primates.

As for the S-cone properties specifically, Dacey (1996) reviewed the structure and function of a small S-ON/(L+M)-OFF bistratified ganglion cell. Rather than having a standard centre-surround receptive field, these ganglion cells have coextensive and overlapping ON and OFF regions, with the opponent signal being generated by excitatory input to either the inner or outer IPL.

Tailby, Solomon and Lennie (2008) performed single-unit LGN recordings in the presence of drifting sinusoidal gratings on 13 *Macaca fascicularis* primates to ascertain the functional asymmetries of S-ON and S-OFF pathways. The authors noted that at the level of the LGN, there was no difference in the actual number of S-ON and S-OFF cells, however they found substantial functional differences between the S-ON and S-OFF pathways. First, the chromatic preference of the S-ON cells seemed to align with the “S” colour axis (the axis in CIE colour space along which only S-cone excitation varies, and (L+M)-cone excitation remains constant), as was expected. Curiously, the S-OFF cells chromatic preference lay somewhere between the S-axis and the (L+M)-axis (the axis in CIE colour space along which only (L+M)-cone excitation varies, and S-cone excitation remains constant, indicating a poor response from (L+M), but also potentially involving other retinal elements (e.g., ipRGCs). Second, Tailby and colleagues noted that S-OFF cells had lower contrast sensitivity and greater susceptibility to habituation compared to S-ON cells. They posited that this may have been due to summation of signals in ganglion cells, amacrine cell habituation, or bipolar cell habituation. Third, the receptive field size of S-OFF cells was substantially larger than that of S-ON cells, and had lower sensitivity to low spatial frequencies. S-OFF sometimes showed higher spatial resolution when presented with achromatic gratings than S-cone specific gratings, whereas the spatial resolution of S-ON cells was consistent over all visible wavelength gratings. This suggests that S-OFF cells may be more influenced by L- and M-cone outputs. Fourth, the S-OFF cells seem to sum S-cone inputs over a much larger retinal area than S-ON cells. Fifth, the authors noted that, with respect to psychophysical characteristics, the S-OFF system (responsive to S-cone decrements) has an overall lower sensitivity and more linear contrast response than the S-ON system, and the two systems are thought to differ in terms of (L+M) contributions as well. The lower sensitivity of

individual S-OFF components does not appear to translate to a lower systemic sensitivity, however; Demarco, Smith and Pokorny (1994) established that there are no significant differences in the detection of ON and OFF signals by the S-cone system overall. Finally, that the S-OFF cells respond to (L+M)-cone excitation potentially implicates a modulatory photoreceptor system like ipRGC, especially given the M2 subtype's putative, coextensive S-OFF/(L+M)-ON receptive field.

Szmajda, Buzas, FitzGibbon and Martin (2006) used intracellular recordings and post-mortem pathway reconstruction to further analyze the differences between the S-ON and S-OFF pathways in S-cone rich adult marmosets. The authors reported that at least two classes of S-OFF ganglion cells exist in primates; ipRGCs and a smaller, non-photosensitive ganglion cell that shows a similar sparseness and sluggish response to ipRGC (Dacey, Peterson, Robinson & Gamlin, 2003). With respect to the communication of colour information, Szmajda et al. noted that the response characteristics and size of S-OFF cells recorded were a closer match to the non-photosensitive subtype. However, the authors did state that no clear segregation of temporal or chromatic properties was noted between the large and small cells, implying a potential functional redundancy between S-OFF ganglion cells, in that they both communicate S-OFF information. Not addressed by Szmajda et al. was the notion that the S-OFF properties of ipRGC may in fact be used to increase the chromatic range of the cells in signalling brightness changes, and may not communicate chromatic information like traditional, chromatically-opponent RGCs.

Koniocellular Pathway

Since it was first noticed as a group of “extremely small and lightly-stained somata outside the M and P layers of the LGN”, research into the koniocellular (KC) pathway has been

extensive and ongoing (Hendry & Reid, 2000). The following is a very brief summary of the relevant data on the KC-pathway, as it pertains to the current study.

Hendry and Reid (2000) described the KC-pathway organization as a homologous group of layers within the LGN of primates and prosimians that are “sandwiched” between the better-known magnocellular (M) and parvocellular (P) layers. Developmentally, koniocellular cells (K-cells) appears to organize first in the LGN, preceding M and P cells by 3-5 days. They are also apparently unaffected by the lack of early pattern vision, and display no reduction in size as a consequence. This was observed in studies in which one eye of a newborn primate was patched, suggesting that either no functional input is required for the normal development of these K-cells, or that a redundant, binocular developmental pathway independent of pattern-vision input is responsible (for review, see Hendry & Reid, 2000). In their review, Hendry and Reid also identified six K-cell layers in the simian LGN: K1, K4, and K6 receive input from contralateral retinas, and K2, K3, and K5 receive ipsilateral input. Further, they noted that three pairs of K-cell layers exist; the dorsal pair relays low-acuity visual information to V1, the middle pair relays S-cone information to cytochrome oxidase blobs in V1, and the ventral pair seems to project to the superior colliculus. Interestingly, the projections to the superior colliculus seem to be shared by known projections of ipRGCs (see above), potentially implicating these ganglion cells as contributors to the KC pathway in primates.

Overall Summary and Proposed Model

The above literature review shows that although much has been learned about the structure, function, and projections of ipRGCs in the past decade, much is still up for debate. Up to five subtypes of ipRGC have been identified in mice, though the functionality of all but the first two discovered subtypes is not fully known. Recent research has mapped the general

projection and function of the M1 and M2 subtypes of ipRGC, and thus these will be the focus of the model proposed herein. Though many of the above articles examined the intrinsic photoreception properties of these cells, they also support the notion that ipRGCs *can* function as “normal” RGCs as well, with the ability to relay more traditional rod and cone photoisomerized signals to the brain in addition to any intrinsic light-evoked signals.

Ontogenetically, M1 ipRGCs seem to develop after their M2 counterparts in mammals. They appear to form a complex feedback system with dopaminergic amacrine cells in the retina, which may be responsible for visual field modification to prevailing light conditions, or be a system designed to increase the operating range of the ipRGCs ensuring that they are not saturated at lower light levels. M1 cells are also far more sensitive to intrinsic light input, while being more resistant to input from other retinal elements, such as rods or cones. It is unclear whether they receive strictly S-ON input, as their dendritic arbour potentially synapses with multiple cone bipolar subtypes. It is also unclear whether they receive rod input, as the connection to type-II amacrine cells, and those cells’ putative rod inputs, are only speculative at this point. M1 ipRGCs appear to be composed of two subtypes, Brn3b⁺ and Brn3b⁻, which may follow differential developmental pathways, and are known to excite different areas of the brain (the shell of the OPN and the SCN, respectively). Functionally, M1 cells appear to be responsible for the NIF functions attributed to ipRGCs; namely circadian photoentrainment, PLR, and sleep regulation. This functional distinction is logical based on the morphological characteristics of the M1 cell, as its low threshold to activation by intrinsic light response makes it an ideal general ambient light photodetector.

M2 cells, on the other hand, seem to co-develop with more traditional RGCs, and share many of their characteristics. They are less intrinsically-sensitive to light, but more sensitive to

rod and cone input. Their retinal connections seem to include synapses from monostratified and type-II amacrine cells, which are purported to “gain” the M2 ipRGC’s response to light to extend its functionality in varying luminance conditions. The M2 subtype is alleged to have a co-extensive S-OFF/(L+M)-ON receptive field with respect to cone inputs, and projects primarily to the dLGN, the superior colliculus, and the OPN core. Though the function of this last connection is unclear at this time, the two former connections are thought to be involved in the communication of conscious visual information, such as luminance levels, to V1.

The mechanism by which ipRGCs, specifically the M2 subtype, communicate light information to the cerebral cortex is not clearly understood. Dacey et al. (2005) found evidence that a subtype of ipRGCs (M2) in macaques showed S-OFF response characteristics and that the ipRGCs synapsed with cells that projected to the dLGN. Brown et al. (2010) hypothesized that ipRGCs may contribute to luminance detection in mice. Ecker et al. (2010) also found that ipRGCs could contribute to the perception of coarse contrast gratings in the absence of other photoreceptors in mice. Szmajda et al.’s (2006) findings indicated that melanopsin containing ganglion cells contributed a negligible amount of conscious visual information to the S-OFF visual stream in marmosets, however more recent articles have submitted some findings that may challenge this. For example, Cheong et al. (2011) found slow intrinsic rhythms in the KC-pathway that corresponded to the sleep-wake cycles in marmosets, perhaps indicating that M1 ipRGCs use a portion of the koniocellular pathway to deliver their information to brain. Percival, Martin and Grunert (2011) noted that two different ganglion cell subtypes fed into the KC-pathway; one of which was a large, sparsely distributed cell with afferent connections from DB6 cone bipolar cells, mirroring findings from Dacey et al. (2006), and suggesting that ipRGCs may in fact use the KC pathway to communicate to the visual cortex.

In line with the above information, the present study proposes the following model of intra-retinal and cortical connectivity for ipRGCs. It appears that M1 ipRGCs provide the bulk of the functional input for NIF visual function. Their response characteristics with respect to chromatic opponency are unknown at this time, though they could show behaviour such as that described in Rea et al. (2005) in which rods provide an inhibitory function via activation of AII amacrine cells, hyperpolarizing the ipRGC until such time as the cone input, via S-ON, (L+M)-OFF cone bipolar cells provide enough net-depolarization to overcome the inhibition, or the rods “bleach” out, eliminating their hyperpolarizing influence, or both. Similarly, the S-cone bipolar cells might be communicating their signals via an excitatory synapse with the M1-type ipRGC in the ON sublayer of the IPL. Thus, it follows that the hyperpolarizing (L+M)-OFF signal, rather than being directly tied to the ipRGC, may be indirectly influencing ipRGC via amacrine cell activation. This means that the hyperpolarizing (L+M) signal would instead decouple the AII-rod inhibitory influence via an A18 amacrine cell and thus “inhibit the inhibitor”, resulting in a net positive current to the ipRGC via its intrinsic photosensitivity. Though this action pathway may seem inefficient, given its lack of direct activation by the longer wavelengths in the spectrum, it is to be noted that M1 cells are more sensitive than M2 cells to light due to their greater depolarized resting potential and higher melanopsin content. Further, M1 cells have a lower maximum firing rate, seemingly making them ideal as circadian communicators, which putatively requires a sustained firing rate over time. Once sufficiently depolarized, light signals are sent via the retinohypothalamic tract to the SCN, and feedback signals are sent upstream via sustained (as opposed to transient) dopaminergic amacrine cells to the horizontal cells, allowing for direct action on receptive field size. Finally, M1 cells may also communicate some low-level

visual information via the KC-pathway, and may be responsible for the “sub-beta” activity present in that channel during waking hours.

It is proposed that M2 cells, with their lower input resistance to rod and cone signals, lower intrinsic photosensitivity, and higher maximal firing rate, could be the ipRGC gateway to the conscious visual system. I concur with Dacey et al. (2005; 2006) that these cells form connections with DB6 cone bipolar cells and exhibit a co-extensive S-OFF/(L+M)-ON receptive field. Intraretinally, the M2 connection to type-II amacrine may allow for limited luminance coding at scotopic light levels via excitatory input from rods. Further, their synapses with monostratified inhibitory amacrine cells may offer a feedback system capable of “gaining down” the ipRGC’s firing rate in the presence of high photopic light levels, allowing them to continue to code for excitatory input from both their intrinsic light response and extrinsic cone responses. I also propose that M2 ipRGCs are an integral component of KC-pathway inputs, since the literature indicates that the projections of ipRGCs mirror those of KC-pathway studies.

One of the primary differences between these two populations seems to be their apparent chromatic opponency properties. Since the present study aims to tease out the visual contributions of ipRGCs, the selection of an appropriate stimulus to probe these systems is paramount. S-cones have a sparser distribution in the retina and have a much smaller impact on luminance detection, if any (e.g., Eisner & MacLeod, 1980). Thus, it seems almost fortuitous that one of the two tritan metamers (wavelength pairs in which the ratio of L-cone and M-cone activation remains unchanged while S-cone activity varies; Shevell, 1992) falls just off the peak sensitivity of ipRGCs (i.e., ~480 nm) at 490 nm. This coincidence was capitalized on, along with using other narrow-band-wavelength adapting fields, to tease out the involvement of the ipRGCs from the overwhelming influence of rods and cones in most image forming functions

(see below). In the present study, I exploited the unique properties of the S-cone pathway, together with a hybrid stimulus delivery system comprised of an optical bench (capable of projecting narrowband adaptation fields) and a stimulus delivery computer (capable of presenting specialized stimuli and recording responses) to accomplish this goal. It is to be noted that the combination of “traditional” (i.e., rod- and cone-based) and “non-traditional” (i.e., melanopsin-based) visual pathways poses a unique challenge in terms of experimental design. For example, though adapting fields typically eliminate the contributions of rods or particular cone types via “bleaching”, the intrinsic response of ipRGCs is such that an adapting field may actually promote continuous firing. As such, I needed to consider this continuous firing property to selective spectral wavelengths in differentiating the potential perceptual effects of ipRGCs from those of traditional light adapted rods and cones.

To examine the full range of vision-forming functionality of ipRGCs, I used four distinct levels of analysis comprising three separate stimulus designs. Because the most behaviourally relevant pathway to explore will involve S-cones, I began by assessing retinal S-cone response properties throughout all visual field positions using short-wavelength automated perimetry (SWAP). The data collected from this procedure were used to corroborate S-cone photoreceptor specific functionality from the overall functioning of the S-cone pathways, including those pathways tied to ipRGCs.

Following the S-cone SWAP assessment, I assessed ipRGC contributions to brightness perception. It is to be noted at this point that due to the sluggish response properties of ipRGCs, and the potential inputs from the four traditional photoreceptors, it is not possible to psychophysically assess the visual functioning of ipRGCs directly. Rather, I employed a combination of adapting fields to “select out” the input from the various cone types, and

examined the net difference in functioning produced by adapting fields that favour ipRGC activity. To this end, I used a “sawtooth” chromatic-luminance sensitivity task (see methods) to probe the contributions of ipRGCs associated with spatiotemporal short-wavelength luminance detection. In earlier works, the properties of these sawtooth temporal envelopes were considered superior to aperiodic pulses of light to activate incremental “ON” and decremental “OFF” visual mechanisms (Bowen, Pokorny, & Smith, 1989; Bowen, Pokorny, Smith, & Fowler, 1992; Purkiss & Demarco, 2002). Originally, based on spatiotemporal sawtooth adaptation paradigms, it was generally believed that a sawtooth with a ramping of intensity either upwards from an average luminance followed by an abrupt transient downwards or a ramping of intensity downwards followed by an upwards transient produced raised thresholds for incremental or decremental tests, respectively. Thus, the abrupt transient portion of the waveform defined the mechanism being isolated (i.e., a step “up” would target the ON pathway, and a step “down” would target the OFF pathway). These findings supported the dual-pathway model of exclusive ON and OFF mechanisms, at least for photopic vision. However, recent studies have shown that factors such as the polarity of the ramp (Racheva & Vassilev, 2008), as well as the presence of an equiluminant pedestal surrounding the test probe (Purkiss & DeMarco, 2002), can create a situation in which the “ramp” portion of the sawtooth defines the mechanism isolated, be it ON or OFF.

In the present study, sawtooth temporal envelopes were defined by aperiodic polarity as either decremental (ramp-down) or incremental (ramp-up) from average light intensity. Decremental (ramp-down) sawtooth envelopes produce stimuli that decrease gradually in luminance relative to mean-luminance pedestal-backgrounds, then “step” back to mean luminance after a pre-determined period of time – in this study, this time window was set to 500

ms. Incremental (ramp-up) sawtooth envelopes produce stimuli with gradual increases in luminance relative to a mean luminance background, with a “step” down in luminance. Though the “ramp-first” waveform configuration is at odds with some previous work, several factors unique to this study necessitated this configuration. First, the use of superimposed, narrowband adapting fields required that the stimuli be aperiodic in nature, to ensure that participants did not “adapt” to the stimulus presentation. This included the lack of any “background” in the stimuli; rather, I used a mean-luminance “pedestal” which appeared at the onset of every trial, and disappeared after response. The temporary nature of the pedestal was to ensure that participants preferentially adapted to the narrowband adapting field rather than the stimulus pedestals, in an attempt to mitigate any confounds related to this potential second “adaptation”. The aperiodic nature of the stimuli also was necessary because of the spatial 2AFC presentation paradigm. The design could not rely on an adaptation paradigm in which a sawtooth waveform is cycled through mean luminance prior to the presentation of the test stimulus. With this in mind, there were also concerns with the “appearance” and “disappearance” of the pedestal producing secondary ON and OFF “pulse harmonics”, confounding the polarity effects. To ensure that the actual ON and OFF probes were not confounded by this pulse, the “ramp” was present first, and its onset was delayed by 250 ms post-pedestal onset. Further, the use of a 500 ms presentation, equivalent to a 2 Hz periodic stimulus, in combination with a mean-luminance surround to the test stimulus, was found by Purkiss and Demarco (2002) to shift the sensitivity of the visual system from the transient “pulse” to the “ramp” portion of the waveform. Racheva and Vassilev (2008) also noted that with 500 ms stimuli, the “polarity” of the stimulus change drive ON and OFF systems with sawtooth waveforms, regardless of whether the “ramp” or “pulse” is presented first. Racheva and Vassilev did note that “ramp-first” stimuli are less salient than their

“pulse-first” counterparts, but that this sensitivity difference was consistent regardless of polarity. Thus, with regard to the current study, it was deemed advantageous to sacrifice potential increased sensitivity to ensure the separation of the pedestal onset and the stimulus onset; see methods for details concerning envelope harmonics and the use of mean-luminance background “pedestals”.

Prior to Dacey et al. (2005), no ganglion cells were reported to have S-OFF receptive fields. It was thus inferred that combinations of various wavelength-selective adapting fields with an incremental or decremental chromatic-luminance “blue” stimulus that preferentially activates S-cones, would adequately probe possible ipRGC perceptual contributions. Although S-cones traditionally do not directly contribute to luminance sensitivity (Boynton, 1979; Eisner & MacLeod, 1980), a “blue” computer screen (CRT) stimulus of moderate bandwidth presented with a temporal sawtooth should preferentially activate the S-OFF receptive field of the ipRGCs, particularly when used in combination with tritan metameric narrow-band adapting fields. S-cones, with their potential connectivity to ipRGCs, may be teased out by observing psychophysically-derived sensitivity asymmetries between incremental (ramp-up) and decremental (ramp-down) sawtooth “blue” stimuli. To this end, participants engaged in a two-alternative forced choice task in which incremental or decremental “blue” ($\lambda_d = 452$ nm) circular, 1.5°-dia. probes that are spatially superimposed onto 3° temporally aperiodic “blue” pedestals were simultaneously presented within a narrowband, optically-delivered 440-, 490-, 650-nm, 20° adapting field, or darkness (i.e., no adapting field). The intensities of the narrow-band fields were specifically chosen to isolate ipRGC functioning from the more sensitive rod- and cone-mediated systems, with a particular focus at the near-peak ipRGC spectral sensitivity wavelength of 490 nm. As such, two 490-nm adapting field conditions were used along with the 440 nm,

650 nm and dark conditions: one that was radiometrically calibrated to produce equal S-cone excitation with the 440-nm field (called the 490r field), and the other that was photometrically, luminance-matched to ensure equal (L+M) cone excitation with the 440-nm field (called the 490p field). In addition, the 650-nm field condition was luminance-matched to the 440 nm field, and the no-field (dark) condition was used as a control. Given the possible S-OFF/(L+M)-ON opponency properties of the M2 ipRGCs, it was hypothesized that their contribution to the short-wavelength-weighted brightness detection task will be enhanced in the 490r condition (the radiometrically-matched 490 nm adapting field), and thus the sensitivity asymmetry between S-cone-weighted decremental and incremental stimuli (i.e., S-OFF: S-ON) will be greater when compared to the “no-field” and photometrically-matched conditions. It is worth restating at this point that luminance-based and S-cone specific systems potentially have different initial OFF:ON response asymmetries; luminance-based systems are more sensitive to light decrements (OFF stimuli), whereas some debate still exists as to whether the S-cone chromatic system has a bias to ON or OFF temporal properties. Thus, in addition to using a stimulus that is more biased to the S-cone pathway, this experiment was also designed to control for both recognized achromatic luminance asymmetry as well as the individual contributions of both S-cone and (L+M)-cone circuits to task performance. The following equations detail the hypotheses related to the five adapting field conditions and their interactions with ipRGCs and traditional photoreceptors.

It is assumed that a base sensitivity asymmetry (δ) can be described as the ratio of the short-wavelength light sensitivity (SWL_S) of OFF-specific "blue" CRT stimuli to ON-specific "blue" CRT stimuli in each of the control (dark) plus four narrow-band adapting field conditions, such that:

$$(1) \quad \delta_{\text{control}} = \text{SWL}_S(\text{OFF})_{\text{control}} / \text{SWL}_S(\text{ON})_{\text{control}}$$

$$(2) \quad \delta_{440} = \text{SWL}_S(\text{OFF})_{440} / \text{SWL}_S(\text{ON})_{440}$$

$$(3) \quad \delta_{490r} = \text{SWL}_S(\text{OFF})_{490r} / \text{SWL}_S(\text{ON})_{490r}$$

$$(4) \quad \delta_{490p} = \text{SWL}_S(\text{OFF})_{490p} / \text{SWL}_S(\text{ON})_{490p}$$

$$(5) \quad \delta_{650} = \text{SWL}_S(\text{OFF})_{650} / \text{SWL}_S(\text{ON})_{650}$$

where the subscripts control is the “no-field” condition, 440 is the 440 nm condition, 490r is the 490-nm adapting field radiometrically matched to the 440 field with respect to S-cone excitation, 490p is the 490-nm adapting field photometrically (luminance) matched to the 440 nm field with respect to (L+M) excitation, and 650 is the 650 nm adapting field condition.

Given the possible S-OFF, (L+M)-ON opponency properties of the M2 ipRGCs, it was hypothesized that their contribution to the short-wavelength weighted brightness detection task will be enhanced in the 490r condition, and thus the sensitivity asymmetry between short-wavelength weighted decremental and incremental stimuli [i.e., $\text{SWL}_S(\text{OFF}) : \text{SWL}_S(\text{ON})$] will be increased compared to the “no-field” control condition. It is worth reiterating at this point that unlike traditional photoreceptors, ipRGCs steadily depolarize in the presence of chromatically-relevant light, and thus produce enhanced signaling. Thus, it was expected 490r adapting field, due to its intensity and appropriate spectral tuning, to be more effective at steadily depolarizing M2 cells, which may act on the S-OFF microcircuit pathway. Because previous studies have shown mean luminance asymmetry in favour of decrements, I examined whether a monotonic relationship existed between the asymmetries produced by the 490p and 490r conditions (compared to the control condition) to address this potential luminance decrement bias. Further, since the stimuli were composed of short-wavelength light, as opposed to

broadband or middle-wavelength light (e.g., Purkiss & DeMarco, 2002; Bowen, Pokorny, Smith, & Fowler, 1992), the mean-luminance asymmetry increase might not apply to this paradigm.

Similarly, given the evidence that melanopsin is bistable *in vivo*, it is proposed that the use of a long-wavelength (650 nm) adapting field will serve to bias S-ON over S-OFF sensitivity and therefore show increased ratio asymmetry compared to the “no field” condition by means of rejuvenating the melanopsin.

To circumvent the potential confounds offered by four dimensional axes defined by the three photopic cones and the ipRGCs (with a possible fifth dimension if rods are considered to have photopic involvement), the 440 and 490p adapting field conditions were added to the design. Because 440 nm and 490 nm are tritan metamers (i.e., the ratio of M- and L-cone activation is the same under 440 nm and 490 nm light, with only S-cone activation changing; Smith & Pokorny, 1996) both of these wavelengths can be used to help isolate the contributions of S-cones without substantially involving the (L+M) luminance channel. Further, by adding a 490r condition, in which the 490 nm field is radiometrically increased to match the S-cone excitation produced by the 440 nm field (i.e., factoring in the spectral sensitivity functions of S cones; Stockman, Macleod & Johnson, 1993), I argue that by examining both these S- and (L+M)-cone output conditions, it is possible to isolate ipRGC contributions. Given that ipRGCs will be maximally excited by the 490r condition, it is proposed that the $SWL_S(OFF) : SWL_S(ON)$ asymmetry discussed above should be greatest with the 490r adapting condition. If it can be assumed that they have a peak “intrinsic” (read: melanopsin-based) sensitivity near 490 nm (480-484 nm), and that this narrowband wavelength promotes the depolarization of the ipRGCs, this should culminate in an enhanced S-OFF cone signal. A similar, though not as prominent, asymmetry shift was predicted with the 490p condition, as the direction of change would be

preserved, but the radiance of the adapting field would be less intense. That said, if a mean-luminance increase compared to the control condition is the only factor driving the $SWL_S(\text{OFF}) : SWL_S(\text{ON})$ asymmetry shift, one would expect to see a monotonic change in the asymmetry ratio between the control condition, the 490p condition and the 490r condition, with increased sensitivity to “OFF” signals (decrements) as mean luminance increases. Finally, a decrease in the asymmetry ratio in the 440 nm condition was predicted due to its lessened involvement with ipRGCs, as well as the selective “bleaching” effect on S-cones. In order to accurately assess shifts in sensitivity on an individual basis, the “no-field” sensitivity ratio was used as a baseline for comparison, and the final analyses compared the *change* in asymmetry within each condition using adapting-field ratios to the baseline such that:

$$(6) \quad X_{440} = \delta_{440} / \delta_{\text{control}}$$

$$(7) \quad X_{490p} = \delta_{490p} / \delta_{\text{control}}$$

$$(8) \quad X_{490r} = \delta_{490r} / \delta_{\text{control}}$$

where the ratio X is defined as the relative magnitude of $SWL_S(\text{OFF}):SWL_S(\text{ON})$ asymmetry produced by the adapting field with respect to the individual’s baseline control asymmetry (i.e., δ_{control}).

Finally, the 490p and 490r conditions were compared, controlling for the 440 nm condition. Since the 490p and 440 nm conditions were photometrically equivalent, (L+M) activity was equal for both conditions, and thus the quotient of these terms would leave S-cone and ipRGC activity as the cause of any shifts in asymmetry. Similarly, because the 490r and 440 nm were radiometrically equivalent in terms of S-cone activity, the quotient of the terms from these two conditions would leave (L+M) and ipRGC as the causes of any shifts in asymmetry. Since ipRGC depolarizes in response to chromatically-relevant light, and will be most influenced

by the 490r condition, I expect the greatest contribution of ipRGC in this condition. In keeping with the above, the following is a formulaic summary of my hypotheses:

$$(9) \quad H_0 : [X_{490r} / X_{440}] = [X_{490p} / X_{440}]$$

$$(10) \quad H_1 : [X_{490r} / X_{440}] > [X_{490p} / X_{440}]$$

$$(11) \quad H_2 : [X_{490r} / X_{440}] < [X_{490p} / X_{440}]$$

where H_0 assumes no contribution of ipRGCs to conscious visual perception (at least via S-cone asymmetries), H_1 assumes an increased asymmetry based on increased excitatory ipRGC activity contributing to an enhanced S-OFF signal, and H_2 assumes other excitatory activity contributing to a relatively enhanced S-ON signal.

In line with the above, I also predicted an asymmetry shift with the 650-nm condition compared to the control owing to the potential blockade effect instigated by ipRGC chromophore regeneration such that:

$$(12) \quad H_0 : \delta_{\text{control}} = \delta_{650}$$

$$(13) \quad H_1 : \delta_{\text{control}} > \delta_{650}$$

Following the brightness experiment, the potential contributions of ipRGCs to pattern vision were examined. The present study used an S-cone-weighted spatial contrast sensitivity paradigm combined with the aforementioned narrowband adapting fields to factor out the functional inputs of ipRGCs from those of rods and cones. Participants performed a two-alternative forced-choice contrast sensitivity task in which they determined whether a homochromatic, sinusoidal “blue” (peak)-to-dark (trough) gabor was present in one of two spatially-distinct pedestals positioned on either side of a blue crosshair, with the whole experiment being presented on a black background to minimize competition with the optically-defined adapting fields. This approach differs from previous studies, which used “blue” gratings

modulating through a “yellow” background (Humanski & Wilson, 1993; Swanson, 1996); however, this departure from past protocols was necessary to ensure minimal interference with the adapting fields. The relative Michelson periodic contrast of the gabors was varied along three spatial frequencies (0.5, 1, and 2 cycles/degree visual angle) selected for their agreement with optimal S-cone spatial resolutions and visibility through a narrowband adapting field (Humanski & Wilson, 1993; Swanson, 1996). If ipRGCs are involved explicitly with pattern vision, and communicate this information via the magno-type KC pathway, the following results are expected; effects on contrast sensitivity should be most pronounced at lower spatial frequencies. This may manifest statistically as an interaction between the effects of spatial frequency and adapting field. One would expect that the control condition will have the highest sensitivity of any of the conditions due to lack of interference from an adapting field. It was also expected that sensitivity in the 440 nm condition will be slightly more attenuated than in the 490p condition, given that 440-nm light is more likely to decrease sensitivity to an S-cone weighted stimulus. It was further expected that contrast sensitivity will be most attenuated by the intense 490r condition compared to the 440-, dim 490p condition, and control (dark) condition, given that the 490r condition has a higher luminance than any other condition. The 650-nm adapting field should increase the regeneration of melanopsin in the ipRGCs, and thus decrease contrast sensitivity compared to the control condition via the “blockade” mentioned above. All of this assumes, of course, that ipRGCs are involved with S-cone spatial operations via M2 cell connections. In this second experiment, any modulatory effects that the dopaminergic feedback system may have through its links with the ipRGCs were also examined. Since M1 cells are the only ipRGC subtype to provide feedback to the dopaminergic amacrine cells of the retina, they are a likely candidate for this reciprocating mechanism and are

potentially able to modulate receptive field size which translates into changes in peak spatial frequency sensitivity in behaviourally-defined contrast sensitivity functions (CSFs). It was hypothesized that narrowband, 490 nm light will provide the highest increase in contrast sensitivity at the highest S-cone limited spatial frequencies, followed by the 440 nm field, since the 490 nm light closely approximates the optimal spectral tuning for ipRGCs, and the 440 nm light should contribute to the S-ON excitatory bipolar connections to the ipRGCs (according to Rea et al., 2005). Finally, in order to differentiate any overlapping effects of retinal sensitization, via excitatory activity of M2 ipRGCs, and increased contrast sensitivity due to DA-based retinal gain from M1 ipRGC input, changes at multiple frequencies were observed. Since increased DA amacrine activity due to increases in ipRGC activity should cause decoupling of horizontal and bipolar cells, and thus putatively decrease receptive field size (increasing high-frequency sensitivity), it is proposed that any sensitivity increases at higher frequencies that are not matched at lower frequencies (i.e., sensitivity divergence) suggests an ipRGC-driven, DA-based retinal gain.

Methods

Participants

Forty-five participants (21 male, 24 female; mean age=21.05 years, SD=5.44) were recruited from undergraduate psychology courses at Lakehead University. All participants were briefed as to the intent of the study, and informed consent was obtained during data collection and prior to beginning the study. All ethical guidelines from the *Tri-Council Policy Statement: Ethical Conduct for Research Involving Humans* (2005) were followed. Participants lacking normal or corrected-to-normal vision, participants with seasonal or major depressive disorders, Parkinson's disease or currently taking any medication were excluded from the study due to potentially uncontrolled confounds in retinal functioning. No anomalous results were found in any of the visual screening tasks, and thus no participant data were excluded after the collection was complete. Participants were given extra course credit and a \$5 coffee gift card as an incentive for their participation. See Appendices A and B for copies of the Consent Form and Screening Questionnaire, respectively.

Stimuli and Apparatus

Visual function screening. Participant's near visual acuity was assessed using the Freiberg visual acuity task (FrACT; Bach, 1996). The FrACT was delivered on a 30 cm CRT monitor. The monitor was placed 75 cm from the participants' pupil entrances, making a display diagonal subtense of 22.6 degrees. This distance was maintained for all vision tasks throughout this study by means of a height-adjustable chinrest and headrest. Participants were required to choose, on the number pad of a standard keyboard, the location of a gap in a Landolt 'C' presented onscreen in varying sizes. A total of eight possible gap locations were presented, and the test was adaptive to the responses of the user. Near acuity of 0.3 logMAR was required for continued testing.

S-cone visual field screenings were accomplished using an automated perimeter (Model no. AP200BY, Opto-Global, Adelaide, South Australia). A patch was placed over the participant's left eye and dark-adapted for 7 min followed by a three-minute light-adapt to a "yellow" (~580 nm; 100 cd/m²) background. Note that the perimeter was designed for monocular visual field assessment and only the right eye was tested. A full visual field threshold screening strategy was used to ascertain retinal S-cone sensitivity. This strategy consists of 164 "blue" (435 nm wavelength) test points (Goldmann size V, 9.03 mm diameter) superimposed and arranged from 0 to 50 degrees (perimetric angles) relative to a centered "red" (650 nm) fixation point. The stimulus dots appeared randomly at each of the 164 positions 3 times. Background luminance was constant at 100 cd/m² and the blue stimulus dots ranged in intensity from 0.0065 to 65 apostolibs (asb) presented in 0.1 log-unit adaptive steps. Participants clicked the response button when they perceived a blue dot anywhere in the test area. The exposure times used by the perimeter are also adaptive, with typical exposure time ranging from 500 to 1100 ms. Reaction time windows were fixed at 800 ms, requiring a response to be given within 800 ms of stimulus delivery to be accepted.

Finally, normal colour vision was assessed using the Farnsworth D-15 colour test (Farnsworth, 1947). In this test, participants are required to arrange 15 isoluminant colour chips in "colour order", (i.e., the logical order in which the colours progress starting from visual "blue"). The test was conducted in a dark room lit by a D-15 calibrated lamp as the only light source. The order in which the colour chips were arranged was plotted on a polar template, and colour-blindness or abnormal colour vision was determined by examining specific placement disorder identified as axes on the polar plot (see Appendix C).

Psychophysical experiments.

Apparatus. All stimuli were projected on a Viewsonic G225f monitor with a total viewing space of $30.2^\circ \times 22.1^\circ$. Stimulus generation was accomplished using VisionWorks software (Vision Research Graphics). Adaptation fields for all of the experiments were generated by an optical bench system using a Xenon arc lamp (Newport Corp.) as the light source. Interference filters (Andover Corp., Delta Photonics) were used to produce the 440-, 490-, and 650-nm narrowband adapting fields (half-bandwidth of 11nm), and neutral interference filters and a hot-mirror were used to prevent any ultraviolet and infrared light from reaching the eye. Once passed through these first filters, the light was focused on onto a variable neutral density “wedge” filter (maximum attenuation 3.0-log unit) affixed to a 250 step-motor; this filter was used to control the luminance of each adapting field. The light field was then passed through a holographic diffusion filter to eliminate any filament images. Finally, the light was magnified via a Newtonian view Fresnel lens and reflected towards the eye using a thin, beam-splitting pellicle (40% transmittance/40% reflection/20% absorption). The use of the pellicle granted two advantages: a) it allowed the participant to perform the task while still under the influence of the adaptation field (ensuring that the photoreceptors targeted by the field are adapted over the course the experiment), and b) the pellicle was composed of a specialized plastic that hold no internal reflection, eliminating potential confounds due to reflection artifacts. A full, detailed schematic of the optical/CRT apparatus is shown in Appendix D.

Adapting field calibration. Given the potentially small contributions of ipRGCs to the visual perceptual system, it was expected that mere photometric luminance matching of the various light fields would not be sufficient to ensure equal L-, M-, and S-cone, and ipRGC excitation with the adapting fields. As such, four 20° adapting fields and one “no-field” control

were used. These fields are hereafter referred to as: 440 nm, 490p (490 nm dim field photometrically matched to (L+M)-cone output at 440 nm), 490r (490 nm bright field radiometrically matched to S-cone output at 440 nm), 650 nm, and control. This was done in accordance to Smith's and Pokorny's (1996) use of cone chromaticity space and based on current knowledge of ipRGC spectral efficiency functions (Dacey et al., 2005). The adapting fields were also calibrated to macular, lens and optic medium density at chosen wavelength. Since absorption properties of the macula are virtually identical at 440 and 490 nm, the differential absorption properties of the lens for short-wavelength light posed a unique challenge in ensuring equal luminance and radiance at the cornea for all age groups used. The calibrations were based on the age-sensitive formula of Pokorny, Smith and Lutze (1987):

$$(14) \quad T_L = T_{L1} [1 + 0.02(A-32)] + T_{L2}$$

where T_L is the total optical density of the lens and ocular medium, T_{L1} is proportion of optical density affected by aging after age 20 years, T_{L2} is the proportion that is stable after age 20 years, and A is the age of the participant in years. A table of the values for T_{L1} and T_{L2} is available in Pokorny, Smith and Lutze (1987), and is reproduced in Appendix E. All adapting field values were calibrated for an observer aged 23 years because there is only about five percent variability between the ages of 18 and 25 years. Calibrations were performed using a Radoma GS-1253 spectroradiometer (Gamma Scientific, San Diego, CA) and all calibrations were done on the reflected optical light from the pellicle and transmitted light from the CRT. Table 2 is a summary of the calibrated values of each adapting field, based on the above calculations.

Photopic sawtooth stimulus design. The stimuli in the brightness task were composed of two parts: a pair of 3° dia. broadband homochromatic “blue” ($\lambda_d=452$ nm) circular pedestal background presented to the left and right of a darkened (~ 0.5 cd/m²), 1° fixation crosshair, and a

smaller, concentric 1.5° dia, “blue” circular test probe superimposed within one of the two larger 3°-dia. pedestal backgrounds. Pedestal backgrounds appeared at trial onset, and disappeared after participant responses to minimize pedestal adaptation confounds with the optical narrowband adapting fields. In other words, pedestals appeared at the onset of each trial, and disappeared at the end of each trial. The 1.5° test probe was temporally modulated either as a ramp-up or ramp-down “sawtooth” waveform, in which the ramp-up sawtooth was an incremental stimulus consisting of a gradually increasing luminance ramp from the pedestal background followed by an step off; the ramp-down sawtooth was a decremental stimulus consisting of a decreasing luminance ramp relative to the 3° pedestal background followed by an abrupt step to mean pedestal luminance (Purkiss & DeMarco, 2002; Racheva & Vassilev, 2008). The luminance of the circular 3° fields was set to 4.95 cd/m², whereas the luminance of the 1.5° test probes varied from 0 cd/m² to a maximum of 9.82cd/m², depending on contrast settings. It is to be noted that the present stimulus design focused on the “ramp” (i.e., polarity), rather than the step or transient pulse component of the sawtooth waveform. As mentioned earlier, a ramp-up/ramp-down stimulus configurations was used because a) the present study focused on short-wavelength stimuli (Racheva & Vassilev, 2008) and b) an equiluminant surround pedestal was used as a starting point, which conforms to Purkiss and Demarco (2002) conclusions on driving ON and OFF systems, specifically when used with low temporal frequency stimuli (e.g., the 500 ms presentation used by this study). Additionally, issues of salience at potential subthreshold levels when combined with the putative “pulse onset” of the pedestal led us to configure the stimulus as a “ramp” first. It is understood that this ramp-first approach is at odds with Bowen, Pokorny and Smith (1989) with respect to Fourier component analysis, however it was necessary given the limitations of the display, the need to use an aperiodic 2AFC design that required an

equiluminant starting point, and the focus on the “ramp” portion of the waveform to isolate ON and OFF activity. Further, the “ramp-first” stimulus configuration has been used in other studies (Bowen, Pokorny & Smith, 1989; Demarco, Smith & Pokorny, 1994; Racheva & Vassilev, 2008). Racheva and Vassilev (2008) also showed that for stimulus presentation times at or under 500 ms, it is the polarity of waveforms that best targets incremental or decremental systems. Thus, it was ensured that the polarity of the ramp was reversed with respect to ON and OFF selective stimuli; ON-selective stimuli ramped “up” from mean luminance, whereas OFF-selective stimuli ramped “down” from mean luminance. For details on the staircase variations in luminance, see the procedure section below. For a visual schematic of the stimulus design and temporal envelope, see Appendices F and G.

Contrast sensitivity stimulus design. Similar to the brightness stimulus design, contrast stimuli will be presented on either side of a 1° “blue” cross-hair fixation point, and will consist of vertically-oriented sine-wave luminance gratings ($\lambda_d=452$ nm, maximum peak luminance of 9.52 cd/m², minimum trough luminance approaching 0 cd/m²), spatially windowed with a two-dimensional 5.7°- dia, circular Gaussian envelope with x, y space constant values of 1.0° (Wesner & Tan, 2006). These gabors were superimposed on one of two, 5.7°-dia “blue” ($\lambda_d=452$ nm, luminance 4.95 cd/m²) pedestal backgrounds that flanked the crosshair by 5.7° (10° centre-to-centre visual angle). Relative proportion contrast of the gabors were varied based on participant response (i.e., staircase method; see procedure). The gabor contrast was defined using Michelson contrast for periodic patterns:

$$(15) \quad L_{\max} - L_{\min} / (L_{\max} + L_{\min})$$

with L_{\max} and L_{\min} representing the peak and trough “blue” phosphor luminance, respectively.

With periodic patterns the luminances are modulated through a space-averaged mean luminance;

in this case the “blue” 5.7° pedestal backgrounds (Peli & Goldstein, 1988). Three spatial frequencies (0.5, 1.0 and 2.0 cycles/degree) were used in accordance with Humanski’s and Wilson’s (1993) three-channel model of S-cone spatial vision, with optimal operating ranges determined by pilot testing. It is understood that S-cones have an operating frequency higher than 2.0 c/deg (Swanson, 1996), however the brightest adapting field condition (490r) obscured contrast gratings above 2.0 c/deg almost completely, and as such the present study was only able to sample a limited range of spatial frequencies. For a visual schematic of the stimulus designs and sequence, see Appendix H.

Procedure

Recruitment of participants. Research participants were recruited from undergraduate psychology classes. A letter (see Appendix G) was distributed to the students with the request that they go to a website to fill out a ten-item online screening questionnaire to determine their suitability for participation in the study. The online questionnaire was hosted by SurveyMonkey.com, and contained a basic demographic questionnaire inquiring about the age and sex of participants and their contact information, along with questions about the use of prescribed psychoactive medication, diagnoses of glaucoma or other ophthalmological disease, colour-blindness, and diagnoses of SAD or depression (for a copy of the online questionnaire, again see Appendix B). Once pre-screened, participants were contacted and experimental session appointments were booked. On the day of the experimental session, prior to beginning the experiment, participants were asked to sign a consent form (again, see Appendix A).

Experimental session. Prior to the experimental session, participants’ left eyes were patched, as all testing was performed using the right eye only. Basic visual acuity, colour vision, and S-cone sensitivity were assessed using the FrACT; (Bach 1996), Farnsworth D-15 colour

test, and SWAP, respectively (for a summary of the screening procedures, see the apparatus section above). All experimental testing was performed between the hours of 9:00 AM and 4:00 PM EST to exclude circadian influences on ocular responses (Fukuda et al., 2010).

Following the screening tests, participants were led to the main experimental workstation. The workstation was in a darkened room, with black baffling minimizing any light intrusion around the experimental workstation. All programs were controlled from a secondary experimenter's monitor that was not visible to participants. Participants were seated with their chair height adjusted for comfort, and placed within a chinrest assuring 75 cm viewing distance from the monitor. A test adapting field was then turned on, and the horizontal and vertical position of the chinrest was adjusted until the participants noted the centre of the optical system adapting field (indicated by a small gap) was superimposed onto the centre of the display indicated by a crosshair. Given that the optical system produced a pseudo-Maxwellian diffuse adapting field (Beer, MacLeod & Miller, 2005), precise alignment was necessary to ensure the consistency of calibrated adapting field values between subjects. Therefore, throughout the experiment, the participants were continuously monitored to ensure they were properly positioned within the chin cup and headrest.

After proper alignment, the participants were exposed to a 100 cd/m^2 , 500 nm adapting field for 3 min to minimize rod responses during the "control" experimental condition. Following this exposure, participants were blindfolded and dark-adapted for 7 minutes. Following the dark adapt, participants were asked to perform a series of practice exercises outlining the basic concept of both the brightness and contrast experimental conditions (this practice exercise was replaced by the "light-adapt" to the various adapting field conditions in subsequent blocks). In order to use experimental time effectively, each block of trials was

distinguished by the adapting field condition, in which the brightness sensitivity task was followed by the contrast sensitivity tasks. Thus, the experimental procedure took the following form: 7-min dark-adaptation period, 3-min light adaptation period, brightness tasks 1 and 2, contrast sensitivity tasks 1, 2, and 3. The order in which the blocks were presented only varied in one way, namely half the participants began the experiment with the 650 nm condition, and half began with the control condition. The other blocks were presented in the following order: 440 nm, 490p “dim” and 490r “bright”. Although there is a potential order effect confound in presenting a sequenced order of adapting field conditions, it was deemed necessary to ensure that rod-saturation via exposure to each adapting field remained as constant as possible for the entire experiment.

Experiment 1 (photopic sawtooth brightness sensitivity). A two-interwoven staircase design, using a spatial, two-alternative forced choice (2-AFC) procedure was used to assess SWL_S(OFF) and SWL_S(ON) brightness sensitivities. Each trial began with the presentation of the 1° crosshair for 125 ms. Following this, with the crosshair still on the screen, the two 3° dia. pedestal adapting fields appeared 3° to the left and right of the crosshair for 250 ms; the total “window” of the experiment did not exceed 15°, and thus no substantial effects on S-cone OFF:ON asymmetry was expected (Vassilev, Mihaylova, Racheva, Zlatkova & Anderson, 2003). With the pedestals still on the screen, an incremental or decremental 1.5° dia concentric aperiodic circular test was temporally presented as a sawtooth-modulation either within the left- or right-hand pedestal for 500 ms, making for a 2 Hz temporal frequency known to be effective for OFF systems, particularly S-OFF systems (Bowen et al., 1992; Humanski & Wilson, 1993). Participants were asked to respond by clicking a left (right) mouse button if the sawtooth modulation was located within the left (right) pedestal adapting field. For a full schematic

diagram of both incremental and decremental task outlines, see Appendices F and G. If the participants were unable to see the stimulus, they were told to guess as to its location. An interwoven two staircase design was used to vary the luminance levels within the ramp-down and ramp-up sawtooth stimuli defined above. Staircase designs are adaptive testing techniques, and in this case I used the method to vary the extrema (i.e., minima or maxima) intensities of the temporal envelope in iterating steps based on observer response. To this end, two initial points were determined by pilot testing for each test block; one very salient, and one less salient (e.g., closer to the perceptual threshold being sought) and these were used as starting seeds for the two interleaved staircases. With interleave staircases, the total luminance change from the initial seeds would increase (become more salient) or decrease (become less salient) depending upon the number of correct or incorrect responses provided. In the present study, each staircase was divided into two “phases”. In the first phase, the step-size was relatively large, allowing the algorithm to narrow-in quickly on the approximate sensitivity of the participant. In the second phase, the step size became smaller, allowing for a more precise measurement of individual sensitivity thresholds. The phases were defined by two “reversals” for the first phase and six for the second phase (i.e., the number of times the direction of the steps changes). During the first two reversals, step size was set at 5% contrast, two correct responses resulted in a single step-down (a decrease in salience), while an incorrect response resulted in two steps-up (increases in salience). During the following 4 reversals, step size was set at 1% contrast, and three successive correct responses were required for a single step-down, while an incorrect response resulted in three steps-up. Brightness sensitivity was computed as the inverse of the arithmetic mean of the last four iterated test probe values.

Finally, in order to ensure specific probing of S-ON and S-OFF cone systems, the incremental and decremental stimulus designs were separated into two separate blocks of trials within each adapting field condition for the purpose of this study.

Experiment 2 (periodic contrast sensitivity). Experiment 2 began with the presentation of a homochromatic blue crosshair (1° , $\sim 0.5 \text{ cd/m}^2$) on a black background for 250 ms. While the fixation crosshair was still on the screen, two 5.7° dia. homochromatic blue circles were presented 4° to the left and right of the crosshair. Superimposed on one of the circles was the homochromatic, “blue” sinusoidal gabor described above with center spatial frequencies of either 0.5, 1.0, or 2.0 cycles/degree visual angle. The circles and gabor were presented for a total of 500 ms before disappearing. Participants were required to press the right (left) mouse button if the gabor appeared on the right (left) side of the screen. If the participants were unable to see the stimulus, they were told to guess as to its location.

An interwoven staircase design (including step sizes, number of reversals, and sensitivity calculations) identical to that employed in the brightness sensitivity task was used to vary the relative salience of the gabors in all three blocks of trials in this part of the study. Similar to the brightness task, this part of the study was separated into three blocks, with each spatial frequency having its own trial block.

Results

Analytic Strategy

All statistics were computed using SPSS version 20 for Microsoft Windows (IBM Corp., Armonk, NY.), and graph and curve-fit procedures were generated using Kaleidagraph version 4.1 for Microsoft Windows (Synergy Software, Reading, PA).

Parametric assumptions. Normality of all variables was assessed with the Shapiro-Wilk test and visual inspection of both Q-Q plots and histograms. When normality was violated, data were inspected for outliers more than two standard deviations from the mean. A total of six participants' data were excluded from analyses to ensure normality. The assumption of equality of covariance matrices was tested using Box's M test, with no violations reported on any analyses. The assumption of sphericity was tested using Mauchly's W. In cases when the sphericity assumption was violated, the Greenhouse-Geisser epsilon was $> .75$, and thus the Greenhouse-Geisser corrected degrees of freedom were reported (Girden, 1992). Although there were no significant findings related to sex or order of presentation, when between-subject factors were included in analyses, the assumption of equality of error variances verified using Levene's test. No violations of this assumption were noted for any analyses.

The following subsections detail the individual omnibus analyses, and include details regarding post-hoc analyses and dependent variables for each analysis.

Short-wavelength automated perimetry. A 2 (Horizontal Hemiretinas; Nasal, Temporal) x 2 (Vertical Hemiretinas; Superior, Inferior) x 2 (Eccentricity; Paracentral, Peripheral) x 2 (Sex: Male, Female) mixed factorial ANOVA with three within-subject variables (horizontal hemiretinas, vertical hemiretinas, eccentricity) and one between-subject variable (sex) was conducted to examine the homogeneity of S-cone sensitivity across participants. S-

cone sensitivity (reported in decibels, or db) was computed as the inverse of the detection threshold for each probe location, and aggregate sensitivity scores were computed as the mean of individual sensitivity values in each retinal zone detailed above. A schematic representation of the retinal zones is shown in Appendix J. Bivariate Pearson correlation coefficients were computed between aggregate SWAP sensitivity values (central, paracentral, and peripheral) and threshold scores for both the brightness discrimination task (Experiment 1) and the contrast sensitivity task (Experiment 2) to ascertain whether retinal sensitivity had influence on task performance.

Photopic sawtooth brightness sensitivity. In order to accurately examine the effects of ipRGCs on conscious vision, a procedure to parse out the ipRGC's sluggish responses from the more rapid responses of traditional photoreceptors was developed. As stated in the proposed model, an analysis comparing the relative activity of S-ON and S-OFF cone pathways under the influence of different adapting fields was used to tease out the contribution of ipRGCs to chromatic perception. It is to be noted that sensitivity was calculated as $10/\text{threshold}$. Threshold was defined at the arithmetic mean of the contrast proportion of the test probe compared to the background (ranging from 0-1) of the last four reversals in any given staircase procedure.

To simplify the description of results, the following is a restatement of the primary variables and labels used in these analyses:

1. $SWL_S(\text{OFF})$ sensitivity is defined as $10/\text{threshold}$ in the "ramp-down" stimulus paradigm. It is to be noted that this term differs from the broader "S-OFF" term, which refers to S-OFF cell activity in the retina.

2. $SWL_S(\text{ON})$ sensitivity is defined as $10/\text{threshold}$ in the “ramp-up” stimulus paradigm. It is to be noted that this term differs from the broader “S-ON” term, which refers to S-ON cell activity in the retina.
3. $\delta_{\text{adapting field}}$ is defined as the ratio of $SWL_S(\text{OFF}) : SWL_S(\text{ON})$ in a particular wavelength condition (e.g., $\delta_{\text{control}} = SWL_S(\text{OFF})_{\text{control}}/SWL_S(\text{ON})_{\text{control}}$). This value was calculated for each participant prior to analysis.
4. $X_{\text{condition}}$ is defined as the quotient of $SWL_S(\text{OFF}):SWL_S(\text{ON})$ asymmetry (δ) produced by the adapting field and the individual’s baseline asymmetry (e.g., $X_{440} = \delta_{440} / \delta_{\text{control}}$). This value was calculated for each participant prior to analysis.
5. Five adapting field conditions were used in this experiment
 - 1) Control: no adapting field.
 - 2) 440 nm
 - 3) 490p: a 490 nm wavelength adapting field calibrated to match the luminance of the 440 nm condition, and thus equally excite the (L+M) cone system.
 - 4) 490r: a 490 nm wavelength adapting field calibrated to match the S-cone excitation produced by the 440 nm condition.
 - 5) 650 nm.
6. Two Orders of Presentation, in which stimulus blocks were presented as follows:
 - 1) Control, 440 nm, 490p, 490r, 650 nm.
 - 2) 650 nm, 440 nm, 490p, 490r, Control.
7. Sex, defined genetic sex, e.g., female (XX) or male (XY).

In order to adequately verify the unique contributions of ipRGCs to conscious vision, four separate levels of analysis of the photopic sawtooth brightness sensitivity task were used.

First, I compared the absolute sensitivity to both SWL_S(ON) and SWL_S(OFF) targeting stimuli across adapting field wavelength condition, presentation order, and participant sex. Second, I compared the SWL_S(OFF) : SWL_S(ON) ratio (or δ : defined in eq. 1-5 above) across adapting field wavelength conditions. Third, I compared the “ratio of ratios” (or X : defined in eq. 6-8 above) across adapting field wavelength conditions. Finally, I tested the two *a priori* listed above; a) I compared the X_{490p} and X_{490r} controlling for the 440 nm condition, and b) I compared δ_{control} and δ_{650} to ascertain the potential influence of chromophore regeneration on S-ON and S-OFF activity.

Brightness sensitivity. A 5 (Adapting Field Wavelength: Control, 440 nm, 490p, 490r, 650 nm) x 2 (Direction of Change: SWL_S(OFF), SWL_S(ON)) x 2 (Order of Presentation: Control-first, Control-last) x 2 (Sex: Female, Male) mixed factorial ANOVA with two within-subject variables (adapting field wavelength, direction of change) and two between-subject variables (order, sex) was performed to examine the effects of the various adapting fields, ramp-down and ramp-up stimulus presentation, presentation order and participant sex on perceptual brightness sensitivity. Post-hoc analyses were conducted using paired t-tests, with alpha levels adjusted according to the Bonferroni correction.

δ [SWL_S(OFF)/SWL_S(ON) asymmetry]. A follow-up comparison of the asymmetry of the SWL_S(OFF) and SWL_S(ON) sensitivity between each adapting field condition was conducted. To this end, the $\delta_{(\text{adapting field})}$ ratio defined in eqs. 1-5 above as SWL_S(OFF)/SWL_S(ON), was computed for each adapting field, and these ratios were compared across the five Adapting Field Wavelength conditions: Control, 440 nm, 490p, 490r, 650, using a repeated-measures ANOVA. Post-hoc analyses were conducted using paired t-tests, with alpha levels adjusted according to the Bonferroni correction.

$X (\delta_{condition} / \delta_{control})$. The validity of the asymmetry differences noted above was further tested by comparing the result of the 440 nm, 490p, and 490r condition's asymmetry ratio divided by the asymmetry ratio from the control condition (see eqs. 6-8) using a repeated-measures ANOVA. Post-hoc analyses were conducted using paired t-tests, with alpha levels adjusted according the Bonferroni correction.

A priori hypothesis tests. *A priori* hypotheses were devised to determine whether any difference in brightness sensitivity asymmetry exists between the 490p and 490r conditions after a participant's baseline asymmetry (the control condition), and asymmetry during the 440 nm condition were accounted for. This comparison goes to the heart of this study, as factoring out the 440 nm condition from the X -ratios of the 490p and 490r conditions should allow for a direct comparison between these two conditions based on ipRGC activity alone. The quotient of X_{490p} and X_{440} was compared to the quotient of X_{490r} and X_{440} using a t-test.

In order to test for evidence of chromophore bistability, the δ_{650} to $\delta_{control}$ were compared using a t-test.

Contrast sensitivity task. A 5 (Adapting Field Wavelength: Control, 440 nm, 490p, 490r, 650) x 3 (Spatial Frequency: 0.5 c/deg, 1.0 c/deg, 2.0 c/deg) x 2 (Presentation Order: Control-First, Control-Last) x 2 (Sex: Female, Male) mixed factorial ANOVA with two within-subject variables (adapting field wavelength, spatial frequency) and two between-subject variables (order, sex) was performed to ascertain the effects of chromatic adapting fields on visual contrast sensitivity. Again, sensitivity was calculated as $10/\text{threshold}$, with threshold defined as above. Post-hoc analyses were conducted using paired t-tests, with alpha levels adjusted according the Bonferroni correction.

Short-Wavelength Automated Perimetry

Main effects were noted for Horizontal Hemiretina [$F(1,38)=194.19$, $p<0.001$, partial $\eta^2=0.836$, obs. Power=1.00], Vertical Hemiretina [$F(1,38)=290.42$, $p<0.001$, partial $\eta^2=0.884$, obs. Power=1.00] and Eccentricity [$F(1,44)=784.32$, $p<0.001$, partial $\eta^2=0.954$, obs. Power=1.00]. Though numerous second-order interactions were found in the analysis, an interesting third-order interaction of all of the above terms was noted, namely Horizontal Hemiretina x Vertical Hemiretina x Eccentricity [$F(1, 38)=8.99$, $p=0.005$, partial $\eta^2=0.191$, obs. Power=0.832]. The individual sensitivity values for each condition are summarized in Table 3 and the interaction is illustrated in Figure 1, which shows the sensitivity thresholds for all zones. Figure 1 also suggests that all main effects and second-order interactions appear to be explained by a third order-interaction, in which the peripheral inferior-nasal region showed similar sensitivity to the paracentral region. Overall, it was found that, unsurprisingly, S-cone sensitivity decreases as stimuli move outward toward the periphery of the visual field, with the exception of stimuli in the inferior-nasal quadrant of the periphery, in which sensitivity is comparable to that in the paracentral region.

Correlation between S-cone function and task performance. No statistically significant correlations were noted between SWAP sensitivity values and brightness or contrast sensitivity scores.

Photopic Sawtooth Brightness Sensitivity

Brightness sensitivity. No significant main effect of order was noted [$F(1, 35)=1.52$, $p=0.226$], nor were any significant order factor interactions. These results indicate that the order of adapting field presentations had no effect on brightness sensitivity.

No significant main effect of sex was noted [$F(1, 35)=0.035$, $p=0.852$], however a third-order interaction of Adapting Field Wavelength x Direction of Change x Sex was found [$F(4, 140)=3.72$, $p=0.007$, partial $\eta^2=0.096$, obs. Power=0.876] showing that females had a slight sensitivity advantage for S-ON stimuli in the control condition compared to males.

A significant main effect of adapting field was found [$F(4, 140)=238.83$, $p<0.001$, partial $\eta^2=0.872$, obs. Power=1.00]. Pairwise comparisons revealed significant differences (at $p<0.001$ level) in aggregate brightness sensitivity [$SWL_S(\text{OFF})+SWL_S(\text{ON})$ combined] between all adapting field conditions except the following pairs; a) Control and 490p ($p=1.00$), and b) 440 nm and 650 nm ($p=0.14$).

A significant main effect of direction of change was also found, $F(1, 43)=46.591$, $p<0.001$, partial $\eta^2=0.520$, obs. Power=1.00, indicating greater overall sensitivity for ramp-down than ramp-up stimuli when all adapting field conditions are collapsed.

A significant Adapting Field x Direction of Change interaction was found, $F(4, 172)=5.765$, $p<0.001$, partial $\eta^2=0.141$, obs. Power=0.979. Post-hoc within subject contrasts revealed that there was a significant difference between the $SWL_S(\text{OFF})$ and $SWL_S(\text{ON})$ stimulus paradigms in three of the five of the adapting field conditions, with the 490p and 650 nm condition showing no difference. In all conditions in which a significant difference was found, the OFF stimulus paradigm showed a greater sensitivity than the ON; this trend was also noted in the non-significant comparisons. Thus, depending on the wavelength of the adapting field, the magnitude of the asymmetry between $SWL_S(\text{OFF})$ and $SWL_S(\text{ON})$ varied. Descriptive statistics are presented in Table 4, and the results of the post-hoc pairwise analysis are summarized in Table 5. Significance levels for the post-hoc pairwise comparisons were adjusted using a Bonferroni correction. Means of both $SWL_S(\text{OFF})$ and $SWL_S(\text{ON})$ sensitivities in all

adapting field conditions are shown in Figure 2, which plots the brightness sensitivities $SWL_S(\text{OFF})$ and $SWL_S(\text{ON})$ for each adapting field wavelength condition.

δ [$SWL_S(\text{OFF})/ SWL_S(\text{ON})$ asymmetry]. A significant effect of adapting field wavelength was noted [$F(3.3, 123)=10.63$, $p<0.001$, partial $\eta^2=0.223$, obs. Power=1.00], confirming the preceding result regarding the interaction of $SWL_S(\text{OFF}) : SWL_S(\text{ON})$ differences and adapting field wavelength, and indicating a significant variation between OFF-ON sensitivity asymmetries. Post-hoc pairwise t-tests were performed using a Bonferroni correction and revealed significant differences between the following pairs of conditions: Control – 490p ($p=0.002$), 440 nm – 490r ($p<0.001$), 490p – 490r ($p<0.001$), and 490r – 650 nm ($p<0.001$). Descriptive statistics for δ are presented in Table 6, and a complete summary of all pairwise comparisons is shown in Table 7. Figure 3 shows the δ -ratio for each adapting field condition and illustrates the significant differences noted above. To further elucidate the relationship between these asymmetry ratios, the difference between the δ -asymmetry ratio in the control condition and all other conditions were computed. Figure 4 illustrates the directional nature of the adapting fields' effects on the $SWL_S(\text{OFF}) : SWL_S(\text{ON})$ sensitivity ratio. Of note is the relative advantage for $SWL_S(\text{OFF})$ sensitivity in the 490r condition (indicated by a positive shift in the $SWL_S(\text{OFF}) : SWL_S(\text{ON})$ ratio with respect to the “baseline”), compared to the relative advantage for S-ON sensitivity in all other conditions (indicated by a negative shift in the $SWL_S(\text{OFF}) : SWL_S(\text{ON})$ ratio compared to the “baseline”).

X ($\delta_{\text{condition}}/ \delta_{\text{control}}$). The result of this comparison was significant [$F(1.4, 48.3)=16.92$, $p<0.001$, partial $\eta^2=0.326$, obs. Power=0.995], indicating that the difference between the aforementioned three conditions was maintained after mathematically controlling for the “control” condition. A Bonferroni-corrected post hoc analysis revealed significant differences

between all three conditions; the 490r condition showed the greatest overall asymmetry followed by the 440 nm condition, with the 490p condition showing the smallest asymmetry ratio.

Descriptive statistics for X are shown in Table 8, and a summary of the post-hoc pairwise comparisons is shown in Table 9. These results are summarized in Figure 5, which illustrates the X -ratio for each of the 440 nm, 490p, and 490r conditions and clearly shows the asymmetry differences between the various conditions.

A priori hypothesis tests. With respect to the first *a priori* test, a significant difference was noted between the (X_{490r} / X_{440}) and (X_{490p} / X_{440}) conditions, $t(38)=6.36$, $p<0.001$, indicating a significant ratio difference between the 490r and 490p conditions, with the asymmetry being more pronounced with the 490r condition.

In order to test for evidence of chromophore bistability, the δ_{650} to δ_{control} conditions were compared. No significant difference was noted between the δ_{650} and δ_{control} conditions, though the difference was approaching significance [$t(38)=1.88$, $p=0.068$], with the control condition showing the greater level of $\text{SWL}_S(\text{OFF}) : \text{SWL}_S(\text{ON})$ asymmetry.

Contrast Sensitivity Task

No main effects of order [$F(1, 35)=0.682$, $p=0.415$] or sex [$F(1,35)=1.182$, $p=0.284$] were noted, nor were any interaction with these factors significant. Main effects of both Adapting Field [$F(4, 172)=230.18$, $p<0.001$, partial $\eta^2=0.868$, obs. Power=1.00] and Spatial Frequency, $F(1.4, 48.3)=198.61$, $p<0.001$, partial $\eta^2=0.850$, obs. Power=1.00] were noted. Further, a significant Adapting Field x Spatial Frequency interaction was noted [$F(5.2, 181.9)=46.19$, $p<0.001$, partial $\eta^2=0.569$, obs. Power=1.00]. Figure 6 shows the sensitivity measurements for each adapting field wavelength condition. For clarity, double exponential functions were fit to the contrast sensitivity data using the following equation (Movshon & Kiorpes, 1988):

$$(16) \quad f(x) = k_s(\omega k_\omega)^\alpha \exp(-\beta \omega k_\omega)$$

where ω is spatial frequency; α and β are the steepnesses of the low and high frequency curve components, respectively; and k_ω and k_s are the lateral and vertical shift parameters for spatial frequency and sensitivity, respectively.

Individual sensitivity values for all levels and conditions are summarized in Table 10, and post hoc analyses of the interaction revealed many sensitivity differences between Adapting Field Wavelength conditions and Spatial Frequency levels. These differences are illustrated in Figure 7, which shows relative sensitivity across all adapting field conditions for each spatial frequency probed. All comparisons noted below were significantly different at $p < 0.005$ (Bonferroni corrected).

At the 0.5 c/deg level, there was a sensitivity advantage for the 490p condition ($M=81.94$, $SD=25.02$) compared to the control condition ($M=69.32$, $SD=16.41$), whereas the 440-nm condition ($M=71.47$, $SD=16.51$) and control conditions showed no significant difference. The 650-nm condition ($M=41.73$, $SD=13.22$) also showed significantly less sensitivity than the control condition, as did the 490r condition ($M=25.09$, $SD=9.08$).

At the 1.0 c/deg level, the 490p ($M=175.32$, $SD=45.77$) and control ($M=172.84$, $SD=46.61$) conditions showed the greatest overall sensitivity, and there was no significant difference between them. The 440 nm ($M=138.00$, $SD=36.13$), 650 nm ($M=100.26$, $SD=27.30$) and 490r ($M=33.46$, $SD=10.05$) conditions all showed significantly lower sensitivity.

At the 2.0 c/deg level, a similar sensitivity order to that found in the 1.0 c/deg condition was noted. The control condition ($M=229.36$, $SD=64.25$) showed greater sensitivity than the 490p ($M=200.32$, $SD=54.47$) condition. These two conditions were followed by the 440 nm

($M=168.86$, $SD=53.38$), the 650 nm ($M=133.54$, $SD=57.42$) and the 490r ($M=24.25$, $SD=7.55$) conditions, in that order.

Overall, the data indicate that adaptation with the 490p condition (photometrically equiluminant to the 440-nm condition) produced a sensitivity advantage over the control condition at 0.5 c/deg, but that advantage disappeared at 1.0 cycles/degree, and was reversed at 2.0 c/deg, with the control condition showing a slight sensitivity advantage at this highest spatial frequency. Also, no differences were found between the 440-nm and control condition at 0.5 c/deg, but a distinct advantage for the control condition at both 1.0 and 2.0 c/deg. The 490p condition showed a distinct advantage across all three frequencies compared to the 440-nm condition. The 650-nm condition showed a significantly lower sensitivity compared to the dim 490p, 440 nm, and control conditions across all frequencies, though there appears to be a marked suppression in the 0.5 c/deg condition. Finally, an increase in sensitivity was observed from the 0.5 to the 2.0 cycle/degree levels for all conditions except the bright 490r condition (S-cone excitation match to the 440 nm condition) which appears to conform to a “band-pass” sensitivity function, with peak sensitivity shown at 1.0 c/deg, and decreased sensitivity in both the 0.5 and 2.0 c/deg conditions.

Discussion

In this series of experiments, I set out to ascertain the potential connectivity of a novel, melanopsin-containing, intrinsically-photosensitive subclass of retinal ganglion cells. I also examined whether these ipRGCs provide measurable input to the visual cortex, and thus contribute to conscious vision. Up to this point, only scant evidence has been available supporting this notion in mammals such as mice, and even less evidence exists for this same function in primates, including humans. I have summarized previous literature showing some support for this connection in mice, including Ecker et al.'s (2010) work with mice discriminating contrast gratings, and Zaidi et al.'s (2007) case study on a human female lacking rods and cones. The present study sought to elucidate and expand upon these findings. Using a novel, hybrid system including a narrow-band-capable optical bench arrangement and a computer system used in psychophysical stimulus delivery, as well as a series of visual screening tasks and psychophysical stimuli, I sought to tease out the role of ipRGCs from that of classical photoreceptors (e.g., rods and cones) in conscious visual perception. Given Dacey et al.'s (2005) seminal work showing that at least one subtype of ipRGCs has a coextensive S-OFF/(L+M)-ON chromatic receptive field, I chose to focus on the S-cone contributions to these ganglion cells as a way to narrow my search. The following summary of the results and implications of the experiments will be divided by structure, beginning with the results of the visual screening, and subsequently discussing the findings from the psychophysical experiments.

S-Cone Sensitivity and ipRGC Function

The contribution of retinal S-cone sensitivity, defined by performance on the SWAP task, was not correlated with psychophysical task performance. Though it was reasoned that the SWAP could be used as a verification of S-cone functioning, it was found that the population that

was assessed in this study was relatively uniform, in that there was not a substantial amount of sample variance in sensitivity. As such there was no way to compare the effects of “normal” and “abnormal” S-cone functioning on the psychophysical tasks. The lack of correlation could also have been due to the fact that the psychophysical task that was used probed the asymmetry between the ON and OFF pathways, not the sensitivity of a specific retinal-based system. Thus, the absolute S-cone sensitivity of an individual participant would not necessarily have had an effect on the relative sensitivity of ON or OFF pathways. The one thing that can be said about the present SWAP findings is that despite the lack of correlations with the higher-end psychophysical discrimination findings, they did confirm intersubject consistency with early, up-front S-cone response properties. Thus, we can be confident that the findings were not influenced by intersubject S-cone variability.

One unexpected finding was the seemingly increased S-cone sensitivity noted in the inferior nasal quadrant of the periphery, compared to all other peripheral quadrants. These data seems to support a recent finding by Ortin-Martinez et al. (2010), who determined the relative distribution of cones in the mouse retina, and found that the inferior nasal quadrant contained the highest density of S-cones. These data may provide support for this sensitivity distribution in humans, however consequential functions of such anatomical heterogeneity, particularly in human, remain tentative.

ipRGC Involvement in Brightness Perception

It was initially hypothesized that the contribution of ipRGCs to conscious vision could be ascertained by examining the S-ON and S-OFF response asymmetries using five different near-monochromatic adapting field conditions. This was particularly difficult, given that the retina is a dynamic system, with multiple receptor subtypes being active in any given adapting field

condition. The task was made more challenging by the fact that the putative involvement of ipRGCs in conscious visual perception is minimal at best, and thus this study was designed to probe for particularly minute differences that may otherwise be masked or discounted as individual variability in other studies. To address this problem, I decided to compare S-cone asymmetric response properties by examining the ratio of $SWL_S(\text{OFF}) : SWL_S(\text{ON})$ sensitivities to tailored spatiotemporal stimuli superimposed onto five different chromatic and luminance adapting field conditions in an attempt to isolate potential ipRGC perceptual modulations. A more direct assessment was impossible given the potentially large sensitivity changes that were expected with the varying adapting fields among the four traditional photoreceptors.

The data revealed some pertinent information related to the experimental design. It was noted that there was indeed a sensitivity advantage for light decrements as opposed to increments in the control condition. This finding may indicate that some sensitivity asymmetry exists between S-OFF and S-ON cone pathways, which runs counter to findings about chromatic increment-decrement detection by Demarco, Smith & Pokorny (1994), but supports more recent, S-cone-specific findings by Racheva and Vassilev (2008). Conversely, it may indicate that despite this study's attempts to isolate the S-cone system, the broader bandwidth nature of the computer-generated "blue" stimulus probes might have sufficiently activated luminance as well as chromatic channels during the task and thus induced decremental bias (Bowen, Pokorny & Smith, 1989). However, the experimental design was configured to control for luminance and S-cone pathway effects using the "ratio of ratios" method described above, and as such should not have significantly impacted the present findings.

The initial hypotheses were mostly supported. Significant differences between $SWL_S(\text{OFF}) : SWL_S(\text{ON})$ asymmetry ratios (δ) were noted between the five adapting field

conditions. As expected, the overall sensitivity to the OFF:ON photopic sawtooth brightness sensitivity task varied by adapting field. A relative decline in sensitivity in all the adapting field conditions was observed relative to the control condition, which was expected given the presence of the chromatic adapting field. More importantly, the OFF:ON ratio between the five adapting field conditions differed significantly, with the δ_{490r} ratio being most exaggerated and the δ_{490p} being most suppressed. Thus, it appears as though the use of the bright 490r field preferentially favoured S-OFF activity over S-ON, which supports the idea that M2-type ipRGCs, with their putative S-OFF receptive fields, were implicated.

The *a priori* hypotheses were partially supported. As previously stated, the quotient of X_{490r}/X_{440nm} was compared to the quotient X_{490p}/X_{440nm} . This comparison controlled for both initial asymmetry (using the X-ratio factoring out the control condition) and S-cone/(L+M)-cone activation (by factoring out the X_{440nm} condition). The results showed a significant difference in asymmetry between these conditions, further supporting that the difference between these two conditions can be directly linked to ipRGC activity. The direction of the asymmetry indicates that the S-OFF sensitivity was relatively suppressed with the dim 490p condition, leading to an $X_{490p}(S-OFF : S-ON)$ ratio approaching 1:1, compared to the bright 490r condition, in which the $X_{490r}(S-OFF : S-ON)$ ratio was closer to 1.5:1. The disadvantage of using ratios becomes apparent when attempting to draw conclusions as to the direction of change in this instance. Indeed, Dacey et al. (2005) pointed out that ipRGCs (putatively the M2 subtype projecting to the dLGN), showed S-OFF response characteristics that should bias the ratio the other direction. Many reviews (Bailes & Lucas, 2010; Do & Yau, 2010; Sand et al., 2012; Schmidt, Chen & Hattar, 2011) have identified that ipRGCs, like other ganglion cells, depolarize when excited by light input as well as cone input via bipolar cells, and it is the sum of these signals that is

transmitted to the brain. Thus, one must consider that any directional change in ON or OFF sensitivity, resulting in an overall change in OFF:ON asymmetry, may be the result of a relative suppression or potentiation of either the OFF or ON response, or a combination of the two. To illustrate this point, if the default OFF:ON ratio in this task (measured by the control condition) was approximately 1.33:1, both an increase in relative S-ON sensitivity, or a decrease in relative S-OFF sensitivity, or both, could account for a 1:1 ratio in the 490p condition. Similarly, a relative decrease in S-ON sensitivity, or a relative increase in S-OFF sensitivity, could account for the 1.5:1 ratio in the 490r. At this point, it may be prudent to reiterate the unique influences of the 490r and 490p conditions after controlling for baseline asymmetry and the influence of the 440 nm field. The 490r condition, since it was radiometrically matched to the S-cone excitation in the 440-nm condition, reflected the combined remaining influences of ipRGC and (L+M)-cones. Similarly, the 490p condition, since it was photometrically matched to (L+M), reflected the combined remaining influences of ipRGCs and S-cones. One could infer that the relative potentiation of S-OFF sensitivity in the bright 490r condition is due to an increased response from ipRGCs, with the signal from extrinsic cone responses being added to the intrinsic S-OFF signals of ipRGCs. One could safely argue this position because the 490r condition was the only condition to show an *increase* in asymmetry compared to the control condition (see Figure 4). Since the presentation of an adapting field increased the mean luminance of the task, one would have expected a monotonic relationship between the control, 490p and 490r conditions and a “decrement” or OFF advantage. Because a decreased sensitivity to decremental stimuli was observed with a 490p field, it can tentatively be concluded that another factor, such as the S-OFF receptive field of ipRGC, must be responsible for this non-monotonic sign change in sensitivity direction. Further, because the 490r condition was matched to the 440 nm condition in terms of

S-cone excitation, differential S-cone activity can safely be discounted as the source of this asymmetry. Another possibility is that the (L+M) component remaining in the 490r term was responsible for the asymmetry shift; however, since this condition showed increased asymmetry compared to the control condition, whereas all other adapting fields produced decreases in asymmetry, one could safely assume that (L+M) luminance channels were not responsible for restoring the “edge” to decremental or OFF stimuli (Bowen, Pokorny & Smith, 1989), as this condition would have seen the greatest suppression in the (L+M) channel, owing to the fact that it was 25 times “brighter” than any other adapting field used. This final assumption is further supported by the notion that short-wavelength-weighted, as opposed to luminance-dependent stimuli were used.

It is proposed that the relative suppression of S-OFF functioning with the dim 490p condition may simply be due to cone adaptation. This conclusion is logical when both the asymmetry patterns for the 490p and 440 nm conditions are examined. The asymmetry (δ) ratio difference between these two conditions was approaching significance despite a conservative Bonferroni correction applied to the data ($p = 0.009$). As the two conditions did not vary in terms of luminance (they were luminance matched), the difference in asymmetry between the conditions should be due to influence from ipRGC and S-cones. With the 440-nm condition, there was a significant difference between OFF and ON sensitivity, with the OFF sensitivity being favoured; which is logical given that the 440 nm adapting would “knock out” S-cones, and thus suppress their sensitivity. With the 490p condition, there was relative increase in sensitivity to both the ON and OFF stimuli compared to the 440 nm condition; however there was no significant difference between the ON and OFF stimuli within the condition itself. This may be due to less interference with the S-cone pathway from a 490 nm adapting field, as well as less

robust input from ipRGCs. This position seems logical given that the maximum operating radiance level of ipRGC is 10^{16} photons/cm²/sec compared to the radiance of the 490p condition (2.6×10^{12} photons/cm²/sec).

A second *a priori* hypothesis, relating to melanopsin's possible long-wavelength dependent bistability, was examined by comparing SWL_S(OFF) : SWL_S(ON) sensitivity ratios between the control and 650 nm conditions. There was no significant asymmetry change between the two conditions, though the difference was approaching significance, and demonstrated a relative potentiation of S-OFF sensitivity in the 650-nm condition. This result seems inconsistent with the aforementioned "blockade" response of a regenerating chromophore, and as such its interpretation can only be tentative at this time. Instead of a melanopsin-driven response, this asymmetry change may be due to the potential interaction between S-cones and L-cones (Shevell, 1992; Sustar, Hawlina & Breceelj, 2011). Also, Ripamonti, Woo, Crowther and Stockman (2009) reported that S-cones could contribute to luminance detection under intense "red" (610 nm) light. That said, the present study's "red" light luminance was only ~ 2 cd/m² and therefore was not likely to induce the slight asymmetric detection shifts. It is also possible that the 650-nm field reduced the influence of (L+M) cones, and thus the "flattening" of the asymmetry is a representation of the equal sensitivity of S-ON and S-OFF systems to chromatic, as opposed to luminance-based stimuli (Demarco, Smith & Pokorny, 1994).

IpRGC Involvement in Contrast Sensitivity

Ecker et al. (2010) initially used low frequency contrast gratings compared to equiluminant backgrounds to ascertain whether rodless-coneless mice could navigate a water maze, with their results suggesting that ipRGCs could code for contrast, and thus be used to communicate higher-order visual information. The same five adapting fields as above were

used, and their influence on sensitivity to vertical contrast gratings was examined at three spatial resolutions: 0.5, 1.0 and 2.0 cycles/degree visual angle (c/deg). The data conform to the expected pattern outlined above, with the bright 490r field causing the greatest suppression in S-cone sensitivity, while the 440 nm and dim 490p fields causing suppression consistent with their relative potential S-cone excitation (i.e., the 440 nm field, as it is closer to S-cones' peak sensitivity, would be expected to suppress S-cone sensitivity more than its luminance-matched 490p field).

Curiously, there appears to be a sensitivity advantage conferred by the dim 490p adapting field at the low spatial frequencies (particularly at 0.5 c/deg) that disappears at higher frequencies. Though this difference may have been expected when comparing the dim 490p condition to the 440 nm condition (due to the decreased effect of the adapting field on S-cones), it is surprising that the 490p field showed such a robust sensitivity advantage compared to the control condition, which presumably would have shown the highest sensitivity across all conditions. Further, the control condition did not differ substantially from the 440 nm condition, which suggests that the mechanism by which the 490p advantage was conferred was not S-cone related, but likely related to luminance perception.

A decline in sensitivity was noted with the long-wavelength, 650-nm adapting field, demonstrated by lower contrast sensitivities than all other conditions except the bright 490r field, and a pronounced decline at 0.5 c/deg. This relative loss in sensitivity suggests that long-wavelength-light-induced chromophore regeneration, or involvement from other retinal feedback systems (e.g., amacrine cells), may play a modulatory role in spatial perception. Another possibility is that the 650 nm field partially adapted the L-cones, and thus reduced the overall spatial acuity of the observer (Cicerone & Nerger, 1989). Since L-cones account for

approximately two-thirds of the cones in the fovea (Vimal, Pokorny, Smith, & Shevell, 1989), suppressing their activity, even with a relatively dim (2.0 cd/m^2) field, may have been enough to reduce the observer's spatial contrast sensitivity. That said, it is unclear whether the magnitude of such suppression would be relatively equal across all three wavelengths, and whether this hypothesis accounts for the more pronounced suppression noted at 0.5 c/deg . Thus, I argue that the noted suppression may in fact be indicative of a "blockade" response produced by *in vivo* long-wavelength dependent melanopsin regeneration within the ipRGCs in this condition.

Both the increased sensitivity in the 490p condition and the decreased sensitivity in the 650-nm condition, taken together, suggest an involvement of ipRGCs in the perception of spatial contrast. Since the differences reported exist only in the low spatial frequency condition (0.5 c/deg), it is suggested that ipRGCs are primarily involved in the communication of low frequency contrast via the "magno-type" koniocellular pathways (Hendry & Reid, 2000). Though it is tempting to draw further conclusions based on the apparent "high-pass" characteristics of the sensitivities in all conditions except the 490r, it is important to reiterate that we sampled a relatively limited and truncated range of spatial frequencies, and as such conclusions based on these may not be completely reliable. If higher spatial frequencies had been sampled, it is expected that the sensitivity curves produced by the various adapting fields would likely conform to a bandpass pattern.

Finally, the bright 490 nm condition exhibits "band-pass" sensitivity qualities, which may indicate preferential activation of S-OFF pathways (Tailby et al., 2008), and thus potentially implicate ipRGCs and the koniocellular visual pathway (Szmajda, Buzas, FitzGibbon & Martin, 2006; Hendry & Reid, 2000). Szmajda and colleagues proposed that S-OFF ganglion cells' sluggish light-response properties, large receptive fields, and lower-frequency "sustained" firing

patterns meant that they used the koniocellular pathway to communicate information to the cortex. They also argued that there was negligible input from ipRGCs to chromatic visual perception, which runs counter to this study's findings. Indeed, it was noted that ipRGC-selective adapting fields produced marked differences to $SWL_S(\text{OFF}) : SWL_S(\text{ON})$ sensitivity asymmetries as well as changes in spatial contrast sensitivity under 2.0 cycles/degree. That said, the limit of ipRGC spatial resolution may only be 0.3-0.5 cycles/degree visual angle (Brown et al., 2010), and as such any conclusions based on these data are speculative, as the spatial resolution of human ipRGC channels is unknown. Further, the band pass quality of this curve may simply be an indication of luminance channel involvement, as the 490r field was very intense compared to both the other adapting field and the stimulus.

Implications of Data in the Proposed Model

The present data support the notion that ipRGCs contribute in some manner to both brightness perception and pattern contrast sensitivity, and thus implicate ipRGC communication along the whole of the retinogeniculostriate pathway. The data show that ipRGCs influence S-cone communication, and thus may depend upon, or make connections with, the koniocellular pathway to transmit information to the cortex. As S-cones are not thought to significantly contribute to brightness perception, the findings of this study pose new questions as to the source of brightness information processing.

Brown et al. (2010) posited an irradiance-dependent switch in which ipRGCs code for sustained luminance levels beyond a certain threshold (approximately 10^{12} photons/cm²/sec), which coincides with the threshold for ipRGC activity. Brown and his colleagues also questioned whether ipRGCs communicate perceptual information besides ambient luminance, and to what degree and spatial resolution. Indeed, they noted that higher colour temperature

light (e.g., “bluer” or shorter-wavelength light) appears brighter to human observers than other colours, even when photometrically matched suggesting that either S-cones contribute to luminance in their own right, or that another photoreceptor, such as ipRGC, is responsible for some part of the “brightness” percept. Along these same lines, they further noted that ipRGCs signal to all LGN neurons with “sustained” response phenotypes, and concluded that these cells effectively drive the spatial average or ambient “brightness” mapping of a visual image, allowing traditional photoreceptors to generate more fine-tuned images. Overall, these results suggest that ipRGCs have a brightness gain relationship to traditional photoreceptors, and that they are involved in the conscious percept of “brightness”.

Viewed together, these data provide support for both Brown et al.’s (2010) and Dacey et al.’s (2005) conclusions on ipRGC functioning, however they fall short of providing conclusive evidence of higher resolution spatial perception. Dacey and colleagues reported the existence of S-OFF receptive fields in humans. They noted that these S-OFF systems have limited input into the conscious visual system, likely via the koniocellular pathway, and that these S-OFF systems appear to share many of the ipRGC’s response characteristics. That said, some new questions need to be asked about the origins of brightness information processing and the involvement of both S-cones and the koniocellular pathway in the transmission of this information. Since the results seem to confirm an extrinsic, S-OFF/(L+M)-ON receptive field in ipRGCs in humans, concurring with Dacey et al.’s (2005) findings, it can be assumed that at least some of the “brightness” information being transmitted by ipRGC to the dLGN and cortex must travel along the KC-pathway. Since previous reviews mention only the magnocellular and parvocellular pathways in the communication of brightness information (e.g., Eisner & MacLeod, 1980; Lennie, Pokorny & Smith, 1993), the present findings are seemingly at odds with traditional

models of brightness perception, particularly when dealing with incremental versus decremental sensitivities. How ipRGCs communicate this brightness information remains unclear. It is possible that ipRGC-specific sublaminae of the “magno-type” KC-pathway may exist, and that these neurons may “cross-talk” with parvo- and magnocellular LGN layers to communicate the aforementioned coarse brightness map to the cortex. Hendry and Reid (2000) reported that a small subpopulation of K-cells exists in the magno- and parvocellular layers of the LGN, and are particularly concentrated between parvocellular layers 3 and 4. There also exist K-cell “bridges” across the other layers of the LGN, with the largest bridge across magnocellular layer 1. As the magnocellular layers are primarily responsible for relaying brightness and motion information to the visual cortex, these bridges could be part of the pathway by which ipRGCs, via the “magno-type” KC-pathway, transmit visual information to V1, and thus contributes to conscious vision. However these pathways may be relatively limited in terms of spatial resolution, a concept supported by the relative robustness of the brightness sensitivity asymmetry findings, and the seemingly low spatial sensitivity of ipRGC indicated by the contrast sensitivity findings.

Another possibility is that “brightness” or radiance information is processed at the level of the LGN, rather than the cortex. Kastner, Schneider and Wunderlich (2006) noted that organization of the LGN is far more complex than originally thought, and concluded that it should be considered an early processing centre for visual attention and awareness. With this in mind, it is not far-fetched to hypothesize that signals from ipRGCs, communicate with the KC-pathway and combined with traditional (L+M) signals from the magno- and parvocellular pathways at the level of the LGN to create a “brightness” composite; one band of information communicating coarse radiance information, and the other delivering more fine-tuned chromatic information.

Limitations

This study sought preliminary data related to the role of ipRGCs in human conscious visual perception, and despite attempts to reduce confounding variables, a few limitations of the present design were noted.

First, the range and intensity of stimuli that were feasible to use was limited. Given equipment limits, the maximum luminance produced on the “blue” channel of the monitor was $\sim 12 \text{ cd/m}^2$, and as such, I was unable to calibrate the adapting fields to levels that would have been most optimal for ipRGC functioning, since those radiance levels would have completely obscured the stimuli. Further, the use of narrowband adapting fields calibrated to S-cone output on the tritan axis limited their range substantially, as the luminance-matched 490 nm condition was required to be “bright” enough to adequately excite ipRGCs, while the radiance-matched 490 nm condition needed to be “dim” enough to allow stimuli to be seen through it. This adapting field conundrum was further exacerbated during the CSF task, as the frequency of the gratings that would not be obscured by the bright 490 nm adapting field was also restricted. As such, I was unable to sample a broad range of spatial frequencies in all conditions, potentially limiting the studies’ ability to draw conclusions about the effects of the other adapting fields on higher frequency contrast sensitivity.

Second, up to five subtypes of ipRGCs are known to exist in mice, and recent studies have suggested that the same subtypes may also exist in humans (e.g., Schmidt, Do & Dacey, 2011). Though the functional distinctions between the M1 and M2 subtypes are clear, little is known about the M3-M5 subtypes, except that they may functionally overlap with the M2 subtype (hence the designation “non-M1” used by some authors). As such, though the proposed

model and conclusions are based on the assumption that the stimuli were targeting M2 ipRGCs, the tasks may have involved up to three other ipRGC subtypes.

Third, due the configuration of the apparatus, I was unable to control for pupil size via the use of an artificial pupil. The generated adapting field was Newtonian derived from a holographic diffused pupillary image (Beer, MacLeod & Miller, 2005) reflected via a pellicle beam splitter to overlap with the entire stimulus presentation once participants were properly aligned. This, in conjunction with the spacing of the optical components, did not allow for the use of an artificial pupil.

Fourth, I did not include an additional set of conditions in which the luminance of the 490r field was matched across wavelengths. Since the primary focus was on S-cone pathways, it was felt that the double-control for S-cone and (L+M)-cone activity compared to the 440 nm condition was sufficient to draw conclusions. In line with this, the results did not indicate a monotonic relationship between mean luminance and asymmetry when comparing both 490 nm conditions to the control condition, thus rendering this point moot.

Fifth, as stated above, I was limited in the range of spatial frequencies I was able to sample, given the relative intensity of some of the adapting field conditions compared to the stimuli, as well as time constraints. Although the results were able to show preliminary evidence for the potential spatial tuning properties of ipRGCs, an expanded sample of spatial frequencies might shed further light on ipRGC's influence on spatial contrast sensitivity.

Finally, no correlation was found between S-cone sensitivity assessed by the SWAP and psychophysical task performance. Since the SWAP data were relatively uniform across participants, and that all participants showed healthy S-cone functioning, the present study was unable to address the effects of “unhealthy” S-cones to healthy ones in the present paradigm.

That said, we can safely say that the findings were in no way confounded by intersubject variability in S-cone functioning.

Future Directions

The present data seem to support the idea that the unique S-OFF contributions of ipRGCs to the conscious visual system can be psychophysically measured using sawtooth-brightness sensitivity tasks and specially calibrated adapting fields. With this in mind, there are many avenues with which to continue this line of research.

First and foremost, a confirmation of the initial findings would aid in solidifying the role of ipRGCs in conscious visual perception. One method of achieving this would involve using different radiance levels in the tritan pair conditions (440 and 490 nm) in order to verify whether a linear relationship exists between adapting field radiance and OFF:ON asymmetry. In addition to this, there is a need to further explore the contributions of ipRGCs to visual contrast sensitivity. To accomplish this, the overall intensity of the gabors relative to the adapting fields needs to be increased. Although technically challenging, this would be useful in revealing ipRGC contributions at peak excitation levels. Future studies might also consider the spatial orientations of the gabors other than vertical as a potential variable. It may be interesting to ascertain whether ipRGCs are preferentially sensitive to particular orientations, since this might help localize the hierarchical nature of these cell pathways (Edden, Muthukumaraswamy, Freeman, & Singh 2009). Further, and in line with the SWAP findings from the present study, it may be interesting to explore the retinal connectivity of ipRGCs in persons lacking one or more of the traditional photopigments (cyanolabe, erythrolabe, and chlorolabe); indeed, these persons may offer a unique view of ipRGC connectivity confounded by fewer colour dimensions.

The current paradigm could also be used to verify the role of ipRGCs in certain ocular and psychological illnesses. La Morgia et al. (2011) extensively reviewed the role of melanopsin in a variety of disorders, most of which are accessible using this methodology. For example, the balance of S-cone versus ipRGC activity in the ON:OFF sawtooth brightness task could be ascertained by comparing a control group to a group with glaucoma, in which S-cone function is suppressed. Further, should this paradigm be successfully supported in follow-up studies, it could be used to assess the putative dysfunction of ipRGCs in seasonal affective disorder (SAD) or migraine sufferers. It may also be useful to expand on the current study and examine the effects of aging on ipRGCs. Feigl et al. (2012) noted that ipRGC function is affected in type II diabetes, and this experimental procedure may be useful in probing differential aspects of that dysfunction in addition to other established tasks (e.g., post-illumination pupil response), especially considering that the present paradigm putatively focuses on M2 ipRGCs, as opposed to the vegetative visual function measures of M1 cells.

Finally, in order to get a more complete picture of the ipRGC/melanopsin network, it may be worthwhile to explore the corticogeniculate feedback system in relation to ipRGCs. Since this study and many others have focused on the feedforward input of ipRGCs to the thalamus and other cortical areas, it would be interesting to establish the existence and role of any feedback pathways or other modulators to the ipRGCs themselves. One possible chemical modulator along this line is estradiol (estrogen); estrogen receptors modulate transcription of *Brn3b*, which is known to be involved in ipRGC expression (Budhram-Mahadeo, Parker & Latchman, 1998). Estradiol is also known to be involved with early visual functioning, specifically spatial and chromatic contrast sensitivity (Richards, 2011). Another possible neuromodulator, melatonin, has shown some evidence of feedback to the retina (Li et al, 2012). As melatonin production

appears to be directly influenced by ipRGC activity (Gooley et al, 2010), the details and functions of this feedback system could be very relevant to the future study of these cells.

Conclusion

This study set out to test the limits of the hypothesis that a novel, melanopsin containing retinal ganglion cell (ipRGC) contributes to conscious vision. This was done in order to advance the current understanding of these new retinal elements, and potentially offer a paradigm with which to further explore their functioning. A novel, hybrid stimulus delivery paradigm employing both computer generated stimuli and narrow-band monochromatic adapting fields was developed, aimed at exploring the contributions of ipRGCs to conscious vision via detectable differences in the asymmetry of S-ON and S-OFF responses, as well as differences in contrast sensitivity.

The present study's data support the notion that the M2 subclass of ipRGC do actively contribute to conscious image formation, and, in line with Brown et al. (2010), this function appears to be limited to "brightness" or radiance detection and low spatial frequency pattern vision. An S-cone weighted stimulus was used, and the present findings seem to indicate that some of the information transmitted by ipRGCs may follow a sub-division of the koniocellular pathway, and thus may speak to brightness signal integration at the level of the LGN rather than V1. Because current research does not support the notion of brightness coding by S-cones, except under specific M- and L-cone adaptation conditions (e.g., intense "red" light; Ripamonti, Woo, Crowther, & Stockman, 2009) or while using "flicker" brightness probes (Teufel & Wehrhahn, 2000), the present results may be indicative of an as-yet-undiscovered visual pathway for the communication of brightness information. Finally, although the findings in this line are preliminary, there may be some noticeable modulatory input from ipRGCs in more complex visual tasks involving contrast discrimination, particularly for low spatial frequencies.

References

- Altimus, C. M., Guler, A. D., Villa, K. L., McNeill, D. S., LeGates, T. A., & Hattar, S. (2008). Rods-cones and melanopsin detect light and dark to modulate sleep independent of image formation. *Proceedings of the National Academy of Sciences of the United States of America*, *105*(50), 19998-20003. doi:10.1073/pnas.0808312105
- Bach, M. (1996). The “Freiburg visual acuity test” – automatic measurement of visual acuity. *Optometry and Vision Science*, *73*, 49–53. doi:10.1097/00006324-199601000-00008
- Bailes, H. J., & Lucas, R. J. (2010). Melanopsin and inner retinal photoreception. *Cellular and Molecular Life Sciences*, *67*(1), 99-111. doi:10.1007/s00018-009-0155-7
- Barnard, A. R., Hattar, S., Hankins, M. W., & Lucas, R. J. (2006). Melanopsin regulates visual processing in the mouse retina. *Current Biology*, *16*(4), 389-395. doi:10.1016/j.cub.2005.12.045
- Beck, A. T., Steer, R. A., & Brown, G. K. (1996). *Manual for the Beck Depression Inventory-II*. San Antonio, TX: Psychological Corporation.
- Beer, R. D., MacLeod, D. I. A., & Miller, T. P. (2005). The Extended Maxwellian View (BIGMAX): A high-intensity, high-saturation color display for clinical diagnosis and vision research. *Behavior Research Methods*, *37*(3), 513-521.
- Berson, D. M., Castrucci, A. M., & Provencio, I. (2010). Morphology and Mosaics of Melanopsin-Expressing Retinal Ganglion Cell Types in Mice. *Journal of Comparative Neurology*, *518*(13), 2405-2422. doi:10.1002/cne.22381
- Berson, D. M., Dunn, F. A., & Takao, M. (2002). Phototransduction by retinal ganglion cells that set the circadian clock. *Science*, *295*(5557), 1070-1073. doi:10.1126/science.1067262

- Birch, J. (1997). Efficiency of the Ishihara test for identifying red-green colour deficiency. *Ophthalmic and Physiological Optics*, *17*(5), 403-408. doi:10.1046/j.1475-1313.1997.97000227.x
- Boudard, D. L., Mendoza, J., & Hicks, D. (2009). Loss of photic entrainment at low illuminances in rats with acute photoreceptor degeneration. *European Journal of Neuroscience*, *30*(8), 1527-1536. doi:10.1111/j.1460-9568.2009.06935.x
- Bowen, R. W., Pokorny, J. & Smith, V. C. (1989). Sawtooth contrast sensitivity: decrements have the edge. *Vision Research*, *29*(11), 1501-1509. doi:10.1016/0042-6989(89)90134-X
- Bowen, R. W., Pokorny, J., Smith, V. C., & Fowler, M. A. (1992). Sawtooth contrast sensitivity: effects of mean illuminance and low temporal frequency. *Vision Research*, *32*(7), 1239-1247. doi:10.1016/0042-6989(92)90218-8
- Boynton, R. M. (1979). *Human Color Vision*. Holt, Rinehart, Wilson: USA.
doi:10.1002/col.5080050321
- Brainard, G.C., Sliney, D., Hanifin, J.P., Glickman, G., Byrne, B., Greeson, J.M., ... Rollag, M.D. (2008). Sensitivity of the human circadian system to short-wavelength (420-nm) light. *Journal of Biological Rhythms*, *23*, 379–386. doi:10.1177/0748730408323089
- Brown, T.M., Gias, C., Hatori, M., Keding, G., Semo, M., Coffey, P., ... Lucas, R. (2010). Melanopsin contributions to irradiance coding in the thalamo-cortical visual system. *PLOS Biology*, *8*(12), 1-14. doi:10.1371/journal.pbio.1000558
- Bubl, E., Kern, E., Ebert, D., Bach, M., van Elst, L.T. (2010). Seeing gray when feeling blue? Depression can be measured in the eye of the diseased. *Biological Psychiatry*, *68*(2), 205-208. doi:10.1016/j.biopsych.2010.02.009

- Budhram-Mahadeo, V., Parker, M., & Latchman, D. S. (1998). POU transcription factors Brn-3a and Brn-3b interact with the estrogen receptor and differentially regulate transcriptional activity via an estrogen response element. *Molecular Cell Biology*, *18*(2), 1029-1041.
- Calkins, D. J. (2001). Seeing with S cones. *Progress in Retinal and Eye Research*, *20*(3), 255-287. doi:10.1016/j.preteyeres.2001.01.003
- Calkins, D. J. & Sterling, P. (2007). Microcircuitry for two types of achromatic ganglion cell in primate fovea. *Journal of Neuroscience*, *27*(10), 2646–2653.
doi:10.1523/jneurosci.4739-06.2007
- Celesia, G.G. & DeMarco, P.J. (1994). Anatomy and physiology of the visual system. *Journal of Clinical Neurophysiology*, *11*, 482-492. doi:10.1097/00004691-199409000-00003
- Chen, S. K., Badea, T. C., & Hattar, S. (2011). Photoentrainment and pupillary light reflex are mediated by distinct populations of ipRGCs. *Nature*, *476*, 92-96.
doi:10.1038/nature10206
- Cheng, N., Tsunenari, T., & Yau, K. W. (2009). Intrinsic light response of retinal horizontal cells of teleosts. *Nature*, *460*(7257), 899-U139. doi:10.1038/nature08175
- Cheong, S. K., Tailby, C., Martin, P. R., Levitt, J. B., & Solomon, S. G. (2011). Slow intrinsic rhythm in the koniocellular visual pathway. *Proceedings of the National Academy of Sciences of the United States of America*, *108*(35), 14659-14663.
doi:10.1073/pnas.1108004108
- Cicerone, C. M., & Nerger, J. L. (1989). The relative numbers of long-wavelength-sensitive to middle-wavelength-sensitive cones in the human fovea centralis. *Vision Research*, *26*(1), 115-128. doi:10.1016/0042-6989(89)90178-8

- Dacey, D. M., Liao, H. W., Peterson, B. B., Robinson, F. R., Smith, V. C., Pokorny, J., ... Gamlin, P. D. (2005). Melanopsin-expressing ganglion cells in primate retina signal colour and irradiance and project to the LGN. *Nature*, *433*(7027), 749-754.
doi:10.1038/nature03387
- Dacey, D. M., Peterson, B. B., Liao, H.-W., & Yau, K.-W. (2006). Two types of melanopsin-containing ganglion cells in the primate retina: links to dopaminergic amacrine and DB6 cone bipolar cells. *Investigative Ophthalmology and Vision Science*, *47*, E-Abstract 3111.
- De Groot, S. G. D., & Gebhard, J. W. (1952). Pupil size as determined by adapting luminance. *Journal of the Optical Society of America*, *42*(7), 492-495. doi:10.1364/JOSA.42.000492
- DeMarco, P.J., Hughes, R.A. and Purkiss, T.J. (2000). Increment and decrement detection on temporally modulated fields. *Vision Research*, *40*, 1907-1919. doi:10.1016/S0042-6989(00)00033-X
- DeMarco, P.J., Smith, V.S. & Pokorny, J. (1994). Effect of sawtooth polarity on chromatic and luminance detection. *Visual Neuroscience*, *11*, 491-499.
doi:10.1017/S0952523800002418
- Do, M. T. H., Kang, S. H., Xue, T., Zhong, H. N., Liao, H. W., Bergles, D. E., & Yau, K.-W. (2009). Photon capture and signaling by melanopsin retinal ganglion cells. *Nature*, *457*(7227), 281-U282. doi:10.1038/nature07682
- Do, M. T. H. & Yau, K.-W. (2010). Intrinsically photosensitive retinal ganglion cells. *Physiology Reviews*, *90*, 1547-1581. doi:10.1152/physrev.00013.2010.
- Dollet, A., Albrecht, U., Cooper, H. M., & Dkhissi-Benyahya, O. (2010). Cones Are Required for Normal Temporal Responses to Light of Phase Shifts and Clock Gene Expression. *Chronobiology International*, *27*(4), 768-781. doi:10.3109/07420521003695704

- Doyle, S. E., Castrucci, A. M., McCall, M., Provencio, I., & Menaker, M. (2006). Nonvisual light responses in the Rpe65 knockout mouse: Rod loss restores sensitivity to the melanopsin system. *Proceedings of the National Academy of Sciences of the United States of America*, *103*(7), 10432-10437. doi:10.1073/pnas.0600934103
- Ebihara, S., & Tsuji, K. (1980). Entrainment of the circadian activity rhythm to the light cycle – Effective light-intensity for a zeitgeber in the retinal degenerate C3H mouse and the normal C57BL mouse. *Physiology and Behavior*, *24*(3), 523-527. doi:10.1016/0031-9384(80)90246-2
- Ecker, J. L., Dumitrescu, O. N., Wong, K. Y., Alam, N. M., Chen, S. K., LeGates, T., ... Hattar, S. (2010) Melanopsin-Expressing Retinal Ganglion-Cell Photoreceptors: Cellular Diversity and Role in Pattern Vision. *Neuron*, *67*(1), 49-60. doi:10.1016/j.neuron.2010.05.023
- Edden, R. A. E., Muthukumaraswamy, S. D., Freeman, T. C. A., & Singh, K. D. (2009). Orientation discrimination performance is predicted by GABA concentration and gamma oscillation frequency in human primary visual cortex. *Journal of Neuroscience*, *29*(15), 15721-15726. doi:10.1523/jneurosci.4426-09.2009
- Eisner, A. & MacLeod, D. I. A. (1980). Blue-sensitive cones do not contribute to luminance. *Journal of the Optical Society of America*, *70*(1), 121-123. doi:10.1364/JOSA.70.000121
- Famiglietti E.V. Jr., & Kolb H. (1976) Structural basis for ON- and OFF-center responses in retinal ganglion cells. *Science*, *194*, 193–195. doi:10.1126/science.959847

- Feigl, B., Zele, A. J., Fader, S. M., Howes, A. N., Hughes, C. E., Jones, K. A., & Jones, R. (2012). The post-illumination pupil response of melanopsin expressing intrinsically photosensitive retinal ganglion cells in diabetes. *Acta Ophthalmologica*, *90*, e230-e234. doi:10.1111/j.1755-3768.2011.02226.x
- Figueiro, M. G., Bierman, A., & Rea, M. S. (2008). Retinal mechanisms determine the subadditive response to polychromatic light by the human circadian system. *Neuroscience Letters*, *438*(2), 242-245. doi:10.1016/j.neulet.2008.04.055
- Figueiro, M. G., Bullough, J. D., Parsons, R. H., & Rea, M. S. (2004). Preliminary evidence for spectral opponency in the suppression of melatonin by light in humans. *Neuroreport*, *15*(2), 313-316. doi:10.1097/01.wnr/0000109799.20952.0f
- Foster, R. G., Provencio, I., Hudson, D., Fiske, S., Degrip, W., & Menaker, M. (1991). Circadian photoreception in the retinally degenerate mouse (rd/rd). *Journal of Comparative Physiology A – Sensory, Neural and Behavioral Physiology*, *169*(1), 39-50. doi:10.1007/BF00198171
- Freedman, M. S., Lucas, R. J., Soni, B., von Shantz, M., Munoz, M., David-Gray, Z., & Foster, R. (1999). Regulation of mammalian circadian behavior by non-rod, non-cone, ocular photoreceptors. *Science*, *284*, 502-504. doi:10.1126/science.284.5413.502
- Fu, Y. B., Zhong, H. N., Wang, M. H. H., Luo, D. G., Liao, H. W., Maeda, H., et al. (2005). Intrinsically photosensitive retinal ganglion cells detect light with a vitamin A-based photopigment, melanopsin. *Proceedings of the National Academy of Sciences of the United States of America*, *102*(29), 10339-10344. doi:10.1073/pnas.0501866102

- Fukuda, Y., Tsujimura, S., Higuchi, S., Yasukouchi, A., & Morita, T. (2010). The ERG responses to light stimuli of melanopsin-expressing retinal ganglion cells that are independent of rods and cones. *Neuroscience Letters*, *479*(3), 282-286. doi:10.1016/j.neulet.2010.05.080
- Gamlin, P. D. R., McDougal, D. H., Pokorny, J., Smith, V. C., Yau, K. W., & Dacey, D. M. (2007). Human and macaque pupil responses driven by melanopsin-containing retinal ganglion cells. *Vision Research*, *47*(7), 946-954. doi:10.1016/j.visres.2006.12.015
- Girden, E. (1992). *ANOVA: Repeated measures*. Newbury Park, CA: Sage.
- Gooley, J. J., Rajaratnam, S. M. W., Brainard, G. C., Kronauer, R. E., Czeisler, C. A., & Lockley, S. W. (2010). Spectral Responses of the Human Circadian System Depend on the Irradiance and Duration of Exposure to Light. *Science Translational Medicine*, *2*(31), 31-33. doi:10.1126/scitranslmed.3000741
- Graham, D. M., Wong, K. Y., Shapiro, P., Frederick, C., Pattabiraman, K., & Berson, D. M. (2008). Melanopsin ganglion cells use a membrane-associated rhabdomeric phototransduction cascade. *Journal of Neurophysiology*, *99*(5), 2522-2532. doi:10.1152/jn.01066.2007.
- Guler, A. D., Ecker, J. L., Lall, G. S., Haq, S., Altimus, C. M., Liao, H.-W., ... Hattar, S. (2008). Melanopsin cells are the principal conduits for rod-cone input to non-image-forming vision. *Nature*, *453*, 102-107. doi:10.1038/nature06829
- Hankins, M. W., & Lucas, R. J. (2002). The primary visual pathway in humans is regulated according to long-term light exposure through the action of a nonclassical photopigment. *Current Biology*, *12*(3), 191-198. doi:10.1016/S0960-9822(02)00659-0
- Hankins, M. W., Peirson, S. N., & Foster, R. G. (2008). Melanopsin: an exciting photopigment. *Trends in Neurosciences*, *31*(1), 27-36. doi:10.1016/j.tins.2007.11.002

- Hattar, S., Kumar, M., Park, A., Tong, P., Tung, J., Yau, K. W., & Berson, D. M. (2006). Central projections of melanopsin-expressing retinal ganglion cells in the mouse. *Journal of Comparative Neurology*, *497*(3), 326-349. doi:10.1002/cne.20970
- Hattar, S., Liao, H. W., Takao, M., Berson, D. M., & Yau, K. W. (2002). Melanopsin-containing retinal ganglion cells: Architecture, projections, and intrinsic photosensitivity. *Science*, *295*(5557), 1065-1070. doi:10.1126/science.1069609
- Hattar, S., Lucas, R. J., Mrosovsky, N., Thompson, S., Douglas, R. H., Hankins, M. W., et al. (2003). Melanopsin and rod-cone photoreceptive systems account for all major accessory visual functions in mice. *Nature*, *424*(6944), 76-81. doi:10.1038/nature01761
- Hendry, S. H. C. & Reid, R. C. (2000). The koniocellular pathway in primate vision. *Annual Review of Neuroscience*, *23*, 127-153. doi:10.1146/annurev.neuro.23.1.127
- Humanski, R. A. & Wilson, H. R. (1993). Spatial frequency adaptation: evidence for a multiple-channel model of short-wavelength-sensitive-cone spatial vision. *Vision Research*, *33*(5-6), 665-675. doi:10.1016/0042-6989(93)90248-U
- IBM Corp. Released 2011. IBM SPSS Statistics for Windows, Version 20.0. Armonk, NY: IBM Corp.
- Ichinose, T. & Lukasiewicz, P.D. (2007). Ambient light regulates sodium channel activity to dynamically control retinal signaling. *The Journal of Neuroscience*, *27*(17), 4756 – 4764. doi:10.1523/jenurosci.0183-07.2007
- Jain, V., Ravindran, E., & Dhingra, N. K. (2012). Differential expression of Brn3 transcription factors in intrinsically photosensitive retinal ganglion cells in mouse. *Journal of Comparative Neurology*, *520*(4), 742-755. doi:10.1002/cne.22765

- Kastner, S., Schneider, K. A., & Wunderlich, L. (2006). Beyond a relay nucleus: neuroimaging views on the human LGN. *Progress in Brain Research, 155*, 125-143.
doi:10.1016/S0079-6123(06)55008-3
- Keeler, C. E. (1924). The inheritance of a retinal abnormality in white mice. *Proceedings of the National Academy of Sciences of the United States of America, 10*, 329-333.
doi:10.1073/pnas.10.7.329
- Keeler, C. E. (1927). The reflex to the light in the mouse at the retina without rods. *Comptes Rendus des Seances de la Societe de Biologie et de ses Filiales, 96*, 10.
- Keeler, C. E., Sutcliffe, E., & Chaffee, E. L. (1928). Normal and "rodless" retinæ of the house mouse with respect to the electromotive force generated through stimulation by light. *Proceedings of the National Academy of Sciences of the United States of America, 14*, 477-484. doi:10.1073/pnas.14.6.477
- Kimura, E., & Young, R. S. L. (2010). Sustained pupillary constrictions mediated by an L- and M-cone opponent process. *Vision Research, 50*(5), 489-496.
doi:10.1016/j.visres.2010.01.001
- La Morgia, C., Ross-Cisneros, F. N., Hannibal, J., Montagna, P., Sadun, A., & Carelli, V. (2011). Melanopsin-expressing retinal ganglion cells: implications for human diseases. *Vision Research, 51*, 296-302. doi:10.1016/j.visres.2010.07.023
- Lall, G. S., Revell, V. L., Momiji, H., Al Enezi, J., Altimus, C. M., Guler, A. D., et al. (2010). Distinct Contributions of Rod, Cone, and Melanopsin Photoreceptors to Encoding Irradiance. *Neuron, 66*(3), 417-428. doi:10.1016/j.neuron.2010.04.037
- Lennie, P., Pokorny, J., & Smith, V. (1993). Luminance. *Journal of the Optical Society of America A – Optics, Image Science, and Vision, 10*(6), 1283-1293. doi:10.1364/JOSAA.10.001283

- Li, X., Montgomery, J., Cheng, W., Noh J. H., Hyde, D. R., & Li, L. (2012). Pineal Photoreceptor Cells Are Required for Maintaining the Circadian Rhythms of Behavioral Visual Sensitivity in Zebrafish. *PLoS ONE* 7(7), e40508.
doi:10.1371/journal.pone.0040508
- Logvinenko AD (2005) Does luminance contrast determine lightness? *Journal of Spatial Vision*, 18, 337–345. doi:10.1163/1568568054089357
- Lucas, R. J., Freedman, M. S., Munoz, M., Garcia-Fernandez, J. M., & Foster, R. G. (1999). Regulation of the mammalian pineal by non-rod, non-cone, ocular photoreceptors. *Science*, 284, 505-507. doi:10.1126/science.284.5413.505
- Lucas, R. J., Douglas, R. H., & Foster, R. G. (2001). Characterization of an ocular photopigment capable of driving pupillary constriction in mice. *Nature Neuroscience*, 4(6), 621-626.
doi:10.1038/88443
- Lupi, D., Oster, H., Thompson, S., & Foster, R. G. (2008). The acute light-induction of sleep is mediated by OPN4-based photoreception. *Nature Neuroscience*, 11(9), 1068-1073.
doi:10.1038/nn.2179
- Mawad, K., & Van Gelder, R. N. (2008). Absence of long-wavelength photic potentiation of murine intrinsically photosensitive retinal ganglion cell firing in vitro. *Journal of Biological Rhythms*, 23(5), 387-391. doi:10.1177/0748730408323063
- McDougal, D. H., & Gamlin, P. D. (2010). The influence of intrinsically-photosensitive retinal ganglion cells on the spectral sensitivity and response dynamics of the human pupillary light reflex. *Vision Research*, 50(1), 72-87. doi:10.1016/j.visres.2009.10.012

- McNeill, D. S., Sheely, C. J., Ecker, J. L., Badea, T. C., Morhardt, D., Guido, W., & Hattar, S. (2011). Development of melanopsin-based irradiance detecting circuitry. *Neural Development*, 6, a8. doi:10.1186/1749-8104-6-8.
- Melyan, Z., Tarttelin, E. E., Bellingham, J., Lucas, R. J., & Hankins, M. W. (2005). Addition of human melanopsin renders mammalian cells photoresponsive. *Nature*, 433, 741-745. doi:10.1038/nature03344
- Movshon, J. A., & Kiorpes, L. (1988). Analysis of the development of spatial contrast sensitivity in monkey and human infants. *Journal of the Optical Society of America A*, 5(12), 2166-2172. doi:10.1364/JOSAA.5.002166
- Mure, L. S., Cornut, P. L., Rieux, C., Drouyer, E., Denis, P., Gronfier, C., et al. (2009). Melanopsin Bistability: A Fly's Eye Technology in the Human Retina. *Plos ONE*, 4(6), e5991. doi:10.1371/journal.pone.0005991
- Mure, L. S., Rieux, C., Hattar, S., & Cooper, H. M. (2007). Melanopsin-dependent nonvisual responses: Evidence for photopigment bistability in vivo. *Journal of Biological Rhythms*, 22, 411-424. doi:10.1177/0748730407306043
- Nadal-Nicolas, F. M., Jimenez-Lopez, M., Salinas-Navarro, M., Sobrado-Calvo, P., Alburquerque-Bejar, J. J., Vidal-Sanz, M. & Agudo-Barriuso, M. (2012). Whole Number, Distribution and Co-Expression of Brn3 Transcription Factors in Retinal Ganglion Cells of Adult Albino and Pigmented Rats. *Plos ONE*, 7(11), 1-16. doi:10.1371/journal.pone.0049830

- Neumann, S., Haverkamp, S., & Auferkorte, O.N. (2011). Intrinsically photosensitive retinal ganglion cells of the primate retina express distinct combinations of inhibitory neurotransmitter receptors. *Journal of Neuroscience*, *199*, 24-31.
doi:10.1016/j.neuroscience.2011.10.027
- Ortin-Martinez, A., Jimenez-Lopez, M., Nadal-Nicolas, F. M., Salinas-Navarro, M., Alarcon-Martinez, L., ... Argudo-Barriuso, M. (2010). Automated quantification and topographical distribution of the whole population of S- and L-cones in adult albino and pigmented rats. *Investigative Ophthalmology*, *51*(6), 3171-3183. doi:10.1167/iovs.09-4861
- Panda, S., Nayak, S. K., Campo, B., Walker, J. R., Hogenesch, J. B., & Jeglia, T. (2005). Illumination of the melanopsin signalling pathway. *Science*, *307*, 600-604.
doi:10.1126/science.1105121
- Paul, K. N., Saafir, T. B., & Tosini, G. (2009). The role of retinal photoreceptors in the regulation of circadian rhythms. *Reviews in Endocrine & Metabolic Disorders*, *10*(4), 271-278.
doi:10.1007/s11154-009-9120-x
- Peli, E., & Goldstein, R. B. (1988). Contrast in images. SPIE: *Visual Communication and Image Processing*, 1001, 521-528.
- Percival, K. A., Martin, P. R., & Grunert, U. (2011). Synaptic inputs to two types of koniocellular pathway ganglion cells in marmoset retina. *Journal of Comparative Neurology*, *519*(11), 2135-2153. doi:10.1002/cne.22586
- Perez-Leon, J. A., Warren, E. J., Allen, C. N., Robinson, D. W., & Brown, R. L. (2006). Synaptic inputs to retinal ganglion cells that set the circadian clock. *European Journal of Neuroscience*, *24*(4), 1117-1123. doi:10.1111/j.1460-9568.2006.04999.x

- Pickard, G. E., & Sollars, P. J. Intrinsically photosensitive retinal ganglion cells. *Science China-Life Sciences*, 53(1), 58-67. doi:10.1007/s1142-010-0024-5
- Pires, S. S., Hughes, S., Turton, M., Melyan, Z., Peirson, S. N., Zheng, L., ... Halford, S. (2009). Differential expression of two distinct functional isoforms of melanopsin (Opn4) in the mammalian retina. *Journal of Neuroscience*, 29(39), 12332-12342. doi:10.1523/jneurosci.2036-09.2009
- Pokorny, J., Smith, V. C., & Lutze, M. (1987). Aging of the human lens. *Applied Optics*, 26(8), 1437-1440. doi:10.1364/AO.26.001437
- Provencio, I., Jiang, G. S., De Grip, W. J., Hayes, W. P., & Rollag, M. D. (1998). Melanopsin: An opsin in melanophores, brain, and eye. *Proceedings of the National Academy of Sciences of the United States of America*, 95(1), 340-345. doi:10.1073/pnas.95.1.340
- Provencio, I., Rodriguez, I. R., Jiang, G. S., Hayes, W. P., Moreira, E. F., & Rollag, M. D. (2000). A novel human opsin in the inner retina. *Journal of Neuroscience*, 20(2), 600-605.
- Provencio, I., Rollag, M. D., & Castrucci, A. M. (2002). Anatomy: Photoreceptive net in the mammalian retina - This mesh of cells may explain how some blind mice can still tell day from night. *Nature*, 415, 493-493. doi:10.1038/415493a
- Purkiss, T.J. and DeMarco, P.J. (2002). Adaptation of spatiotemporal mechanisms by increment and decrement stimuli. *Journal of the Optical Society of America*, 19, 1475-1483. doi:10.1364/josaa.19.001475
- Qiu, X. D., Kumbalasiri, T., Carlson, S. M., Wong, K. Y., Krishna, V., Provencio, I., & Berson, D. M. (2005). Induction of photosensitivity by heterologous expression of melanopsin. *Nature*, 433, 745-749. doi:10.1038/nature03345

- Racheva, K. & Vassilev, A. (2008). Sensitivity to stimulus onset and offset in the S-cone pathway. *Vision Research*, 48(9), 1125-1136. doi:10.1016/j.visres.2008.02.001
- Rea, M. S., Figueiro, M. G., Bullough, J. D., & Bierman, A. (2005). A model of phototransduction by the human circadian system. *Brain Research Reviews*, 50(2), 213-228. doi:10.1016/j.brainresrev.2005.07.002
- Reuss, S. (2010). Pineal ribbon synapses: regulated by the gland's central innervation. *Neuro Endocrinology Letters*, 31(6), 761-765.
- Richards, M. (2011). *Visuoperceptual task performance across the menstrual cycle in women with and without premenstrual symptoms: Potential influences of estradiol and estradiol sensitivity on retinogeniculostriate, extrastriate, and elementary retinal-based smooth pursuit pathways*. (Unpublished doctoral dissertation). Lakehead University, Thunder Bay, Canada
- Ripamonti, C., Woo, W. L., Crowther, E., & Stockman, A. (2009). The S-cone contribution to luminance depends on the M- and L-cone adaptation levels: Silent surrounds? *Journal of Vision*, 9(3), 1-16. doi:10.1167/9.3.10
- Roveri, L., DeMarco, P.J. & Celesia, G.C. (1997). An electrophysiological metric of activity within the ON- and OFF-pathways in humans. *Vision Research*, 37, 669-674. doi:10.1016/S0042-6989(96)00212-X
- Rovsing, L., Rath, M. F., Lund-Andersen, C., Klein, D. C., & Moller, M. A neuroanatomical and physiological study of the non-image forming visual system of the cone-rod homeobox gene (Crx) knock out mouse. *Brain Research*, 1343, 54-65. doi:10.1016/j.brainres.2010.04.066

- Ruggiero, L., Allen, C. N., Brown, R. L., & Robinson, D. W. (2010). Mice with early retinal degeneration show differences in neuropeptide expression in the suprachiasmatic nucleus. *Behavioral and Brain Functions*, 6(36), 1-7. doi:10.1186/1744-9081-6-36
- Ruggiero, L., Allen, C. N., Brown, R. L., & Robinson, D. W. (2009). The development of melanopsin-containing retinal ganglion cells in mice with early retinal degeneration. *European Journal of Neuroscience*, 29(2), 359-367. doi:10.1111/j.1460-9568.2008.06589.x
- Sand, A., Schmidt, T. M., & Kofuji, P. (2012). Diverse types of ganglion cell photoreceptors in the mammalian retina. *Progress in Retinal and Eye Research*, 31, 287-302. doi:10.1016/j.preteyeres.2012.03.003
- Schmidt, T.M., Chen, S.-K., & Hattar, S. (2011). Intrinsically photosensitive retinal ganglion cells: many subtypes, diverse functions. *Trends in Neuroscience*, 34(11), 572-580. doi:10.1016/j.tins.2011.07.001
- Schmidt, T. M., Do, M. T. H., Dacey, D., Lucas, R., Hattar, S., & Matynia, A. (2011). Melanopsin-positive intrinsically photosensitive retinal ganglion cells: from form to function. *Journal of Neuroscience*, 31(45), 16094-16101. doi:10.1523/jneurosci.4132-11.2011
- Schmidt, T. M., & Kofuji, P. (2009). Functional and Morphological Differences among Intrinsically Photosensitive Retinal Ganglion Cells. *Journal of Neuroscience*, 29(2), 476-482. doi:10.1523/JNEUROSCI.4117-08.2009
- Schmidt, T. M., Taniguchi, K., & Kofuji, P. (2008). Intrinsic and extrinsic light responses in melanopsin-expressing ganglion cells during mouse development. *Journal of Neurophysiology*, 100(1), 371-384. doi:10.1152/jn.00062.2008

- Sekaran, S., Foster, R.G., Lucas, R.J. & Hankins, M.W. (2003). Calcium imaging reveals a network of intrinsically light-sensitive inner-retinal neurons. *Current Biology*, 13(15), 1290-1298. doi:10.1016/S0960-9822(03)00510-4
- Sharpe, L. T., Stockman, A., Knau, H., & Jagle, H. (1998). Macular pigment densities derived from central and peripheralspectral sensitivity differences. *Vision Research*, 38, 3233-3239. doi:10.1016/S0042-6989(97)00457-4
- Shevell, S. K. (1992). Redness from short-wavelength-sensitive cones does not induce greenness. *Vision Research*, 32(8), 1551-1556. doi:10.1016/0042-6989(92)90210-A
- Smith, V. C. & Pokorny, J. (1996). The design and use of a cone chromaticity space: a tutorial. *Color Research and Application*, 21(5), 375-383. doi:10.1002/(SICI)1520-6378(199610)21:5<375::AID-COL6>3.0.CO;2-V
- Smith, V. C., Pokorny, J., Gamlin, P. D., Packer, O. S., Peterson, B. B., & Dacey, D. M. (2003). Functional architecture of the photoreceptive ganglion cell in primate retina: Spectral sensitivity and dynamics of the intrinsic response. *Investigative Ophthalmology & Visual Science*, 44, Suppl. 2, U731-U731.
- Stockman, A., Macleod, D. I. A., & Johnson, N. E. (1993). Spectral sensitivities of the human cones. *Journal of the Optical Society of America*, 10(12), 2491-2521. doi:10.1364/JOSAA.10.002491
- Sustar, M., Hawlina, M., & Breclj, J. (2011). Electroretinographic evaluation of the retinal S-cone system. *Documenta Ophthalmologica*, 123(3), 199-210. doi:10.1007/s10633-011-9299-5
- Swanson, W. H. (1996). S-cone spatial contrast sensitivity can be independent of pre-receptoral factors. *Vision Research*, 36(21), 3549-3555. doi:10.1016/0042-6989(96)00047-8

Synergy Software Corp.. Released 2012. Kaleidagraph version 4.1 for Microsoft Windows.

Reading, PA: Synergy Software.

Szabo, Z., Antal, A., Tokaji, Z., Kalman, J., Keri, S., Benedek, G., et al. (2004). Light therapy increases visual contrast sensitivity in seasonal affective disorder. *Psychiatry Research*, *126*(1), 15-21. doi:10.1016/j.psychres.2003.12.013

Szmajda, B. A., Buzas, P., FitzGibbon, T., & Martin, P. R. (2006). Geniculocortical relay of blue-off signals in the primate visual system. *Proceedings of the National Academy of Sciences of the United States of America*, *103*(51), 19512-19517. doi:10.1073/pnas.0606970103.

Tailby, C., Szmajda, B. A., Buzas, P., Lee, B. B., & Martin, P. R. (2008). Transmission of blue (S) cone signals through the primate lateral geniculate nucleus. *London Journal of Physiology*, *586*(24), 5947-5967. doi:10.1113/jphysiol.2008.161893

Tailby, C., Solomon, S.G., & Lennie, P. (2008). Functional asymmetries in visual pathways carrying s-cone signals in macaque. *The Journal of Neuroscience*, *28*(15), 4078-4087. doi:10.1523/jneurosci.5338-07.2008

Teufel, H. J., & Wehrhahn, C. (2000). Evidence for the contribution of S cones to the detection of flicker brightness and red-green. *Journal of the Optical Society of America A*, *17*(6), 994-1006. doi:10.1364/JOSAA.17.000994

Thapan, K., Arendt, J., & Skene, D.J. (2001). An action spectrum for melatonin suppression: evidence for a novel non-rod, non-cone photoreceptor system in humans. *Journal of Physiology*, *535*, 261-267. doi:10.1111/j.1469-7793.2001.t01-1-00261.x

Thompson, S., Recober, A., Vogel, T.W., Kuburas, A., Owens, J.A., Sheffield, V.C., Russo, A.F., & Stone, E.M. (2010). Light aversion in mice depends on non-image-forming irradiance detection. *Behavioural Neuroscience*, *124*(6), 821-827. doi:10.1037/a0021568

- Tsai, J. W., Hannibal, J., Hagiwara, G., Colas, D., Ruppert, E., Ruby, N. F., ... Bourgin, P. (2009). Melanopsin as a sleep modulator: circadian gating of the direct effects of light on sleep and altered sleep homeostasis in *Opn4^{-/-}* mice. *PLOS Biology*, 7(6), 1-13.
doi:10.1371/journal.pbio.1000125
- Tsujimura, S. I., Ukai, K., Ohama, D., Nuruki, A., & Yunokuchi, K. (2010). Contribution of human melanopsin retinal ganglion cells to steady-state pupil responses. *Proceedings of the Royal Society B-Biological Sciences*, 277(1693), 2485-2492.
doi:10.1098/rspb.2010.0330
- Tu, D.C., Zhang, D., Demas, J., Slutsky, E.B., Provencio, I., Holy, T.E., Van Gelder, R.N. (2005) Physiologic diversity and development of intrinsically photosensitive retinal ganglion cells. *Neuron*, 48, 987–999. doi:10.1016/j.neuron.2005.09.031
- Vassilev, A., Mihaylova, M. S., Racheva, K., Zlatkova, M. & Anderson, R. S. (2003). Spatial summation of s-cone ON and OFF signals : effects of retinal eccentricity. *Vision Research*, 43(27), 2875-2884. doi:10.1016/j.visres.2003.08.002
- Vigh, B., Manzano, M. J., Zadori, A., Frank, C.L., Lukats, A., Rohlich, P., ... David, C. (2002). Nonvisual photoreceptors of the deep brain, pineal organs and retina. *Histology and Histopathology*, 17, 555-590.
- Vimal, R., Pokorny, J., Smith, V., & Shevell, S. (1989). Foveal cone thresholds. *Vision Research*, 29(1), 61-78.
- Viney, T.J., Balint, K., Hillier, D., Siebert, S., Boldogkoi, Z., Enquist, L.W., Meister M., Cepko, C.L., Roska, B. (2007). Local retinal circuits of melanopsin-containing ganglion cells identified by transsynaptic viral tracing. *Current Biology*, 17, 981–988.
doi:10.1016/j.cub.2007.04.058

- Vugler, A.A., Redgrave, P., Semo, M., Lawrence, J., Greenwood, J., Coffey, P.J. (2007). Dopamine neurones form a discrete plexus with melanopsin cells in normal and degenerating retina. *Experimental Neurology*, *205*, 26–35.
doi:10.1016/j.expneurol.2007.01.032
- Walker, M. T., Brown, R. L., Cronin, T. W., & Robinson, P. R. (2008). Photochemistry of retinal chromophore in mouse melanopsin. *Proceedings of the National Academy of Sciences of the United States of America*, *105*(26), 8861-8865. doi:10.1073/pnas.0711397105
- Warren, E. J., Allen, C. N., Brown, R. L., & Robinson, D. W. (2003). Intrinsic light responses of retinal ganglion cells projecting to the circadian system. *European Journal of Neuroscience*, *17*(9), 1727-1735. doi:10.1046/j.1460-9568.2003.02594.x
- Weng, S. J., Wong, K. Y., & Berson, D. M. (2009). Circadian Modulation of Melanopsin-Driven Light Response in Rat Ganglion-Cell Photoreceptors. *Journal of Biological Rhythms*, *24*(5), 391-402. doi:10.1177/0748730409343767
- Wesner, M. F., & Tan, J. (2006). Contrast sensitivity in seasonal and nonseasonal depression. *Journal of Affective Disorders*, *95*(1-3), 19-28. doi:10.1016/j.jad.2006.03.028
- Witkovsky, P. (2004). Dopamine and retinal function. *Documenta Ophthalmologica*, *108*, 17-20. doi:10.1023/B:DOOP.0000019487.88486.0a
- Zaidi, F. H., Hull, J. T., Peirson, S. N., Wulff, K., Aeschbach, D., Gooley, J. J., et al. (2007). Short-wavelength light sensitivity of circadian, pupillary, and visual awareness in humans lacking an outer retina. *Current Biology*, *17*(24), 2122-2128.
doi:10.1016/j.cub.2007.11.034

Zhang, D. Q., Wong, K. Y., Sollars, P. J., Berson, D. M., Pickard, G. E., & McMahon, D. G.

(2008). Intraretinal signaling by ganglion cell photoreceptors to dopaminergic amacrine neurons. *Proceedings of the National Academy of Sciences of the United States of America*, *105*(37), 14181-14186. doi:10.1073/pnas.0803893105

Zhu, Y., Tu, D. C., Denner, D., Shane, T., Fitzgerald, C., & Van Gelder, R. N. (2007).

Melanopsin-dependent persistence and photopotential of murine papillary light responses. *Investigative Ophthalmology & Visual Science*, *48*(3), 1268-1275.
doi:10.1167/iovs.06-0925

Table 1

Summary of morphological characteristics, response characteristics, and connectivity of ipRGC subtypes.

Subtype	Genetic Markers	Melanopsin Concentration	Dendritic Stratification	Dendritic field size	Dendritic Complexity	Soma Size	Light Response (Intrinsic)	Light Response (Synaptic)	Membrane Properties	Retinal Connections	Cortical Projections
M1, M1*	Brn3b- Brn3b+ Opn4S Opn4L	Highest Concentration	Outer IPL (OFF)	Mice: 275-377 μm Primates: 400-1200 μm	Least Complex	Mice: 13-17 μm	Large, Most sensitive	ON-Predominant Weak OFF under pharmacological blockade of DA-Amacrine cells Small and sustained	Higher cone input resistance (~710 M Ω) More depolarized resting membrane potential (-48 mV) Lower maximum spike rate (~80 Hz)	DA-amacrine cells in outer IPL Type II and A18 amacrine cells OFF/ON cone bipolar cells (both synapse in outer/OFF IPL) DB1 bipolar cells? Giant Bistratified Bipolar Cells?	SCN (Brn3b-) OPN Shell (Brn3b+)
M2	Brn3b+ Opn4L	Moderate	Inner IPL (ON)	Mice: 310-425 μm Primates: 400-1200 μm ?	>M1	Mice: 15-22 μm	Small, Lowest sensitivity	ON-Predominant Large and sustained	Lower cone input resistance (~216 M Ω) More hyperpolarized resting membrane potential (-66 mV) Higher maximum spike rate (~240 Hz)	DB6 bipolar cell Monostratified amacrine cells Type II amacrine cells (rods) DB1 Bipolar Cells? Giant Bistratified Bipolar Cells?	dLGN Superior Colliculus OPN Core OPN Core
M3	Brn3b+ Opn4S Opn4L	Moderate	Inner and Outer IPL (ON-OFF)	Mice: 449-477 μm	=M2	Mice: 17-18 μm	Small, Intermediate Sensitivity	ON-Predominant Large and sustained	Lower input resistance (? M Ω) More hyperpolarized resting membrane potential (? mV)	Unknown	Unknown
M4	Brn3b+ Opn4?	Lowest Concentration	Inner IPL (ON)	Mice: 302-444 μm	>M2	Mice: 17-22 μm	Small, Insensitive	Unknown	Unknown	Unknown	Presumed similar to M2
M5	Brn3b+ Opn4?	Lowest Concentration	Inner IPL (ON)	Mice: 149-217 μm	Most Complex	Unknown	Small, Insensitive	Unknown	Unknown	Unknown	Presumed similar to M2

* Some data and table formatting taken from Schmidt, Chen and Hattar (2011), and additional data summarized from Bailes and Lucas (2010), Do and Yan (2010), and Sand, Schmidt and Kofuji (2012).

Table 2

Adapting Field Calibration Values

Wavelength Condition	Radiance (at Cornea)	Luminance (at Cornea)	Retinal Luminance*
440 nm	2.0×10^{13} photons/cm ² /s	1.6 cd/m ²	7.6 td
490 nm Bright (Radiometric S-Cone Match)	7.62×10^{13} photons/cm ² /s	50 cd/m ²	155.8 td
490 nm Dim (Photometric (L+M)-Cone Match)	2.6×10^{12} photons/cm ² /s	1.6 cd/m ²	7.6 td
650 nm	1.0×10^{13} photons/cm ² /s	2.0 cd/m ²	9.3 td

*Retinal trolands estimates based on De Groot & Gebhardt (1952).

Table 3

Descriptive Statistics of Short-Wavelength Automated Perimetry sensitivity (in dB) across conditions.

Eccentricity	Vertical Hemiretina	Horizontal Hemiretina	Min	Max	M	SD
Central			24.57	32.05	29.64	1.76
Paracentral	Superior	Nasal	17.44	29.25	24.19	2.93
		Temporal	13.69	30.50	24.66	3.03
	Inferior	Nasal	21.60	31.47	28.50	2.29
		Temporal	22.06	31.81	28.27	2.30
Peripheral	Superior	Nasal	6.50	22.94	14.86	4.34
		Temporal	1.22	20.44	10.08	4.01
	Inferior	Nasal	15.83	29.33	22.85	3.29
		Temporal	8.06	21.06	15.57	3.58

Table 4

Descriptive Statistics of photopic brightness sensitivity for both ON and OFF sawtooth conditions across all adapting field conditions.

Adapting Field	OFF/ON	Min	Max	M	SD
Control	ON	38.68	121.21	80.14	21.83
	OFF	45.05	176.99	101.61	26.54
440 nm	ON	37.31	109.29	64.39	19.55
	OFF	48.08	101.52	74.41	14.21
490p	ON	44.94	132.45	85.56	21.49
	OFF	54.20	129.03	89.73	19.01
490r	ON	10.17	23.56	13.78	3.01
	OFF	13.73	31.45	20.78	4.94
650 nm	ON	36.83	112.99	60.99	18.24
	OFF	34.90	135.14	68.52	24.25

Table 5

Summary table of post-hoc pairwise analysis comparing SWL_S(OFF) sensitivity to SWL_S(ON) sensitivity across all adapting fields conditions.

Pair			<i>M Diff.</i>	<i>t</i>	<i>df</i>	<i>p</i>
1	SWL _S (OFF) _{control}	SWL _S (ON) _{control}	21.47	4.82	38	<0.001*
2	SWL _S (OFF) ₄₄₀	SWL _S (ON) ₄₄₀	10.02	3.72	38	0.001*
3	SWL _S (OFF) _{490p}	SWL _S (ON) _{490p}	4.17	1.70	38	0.098
4	SWL _S (OFF) _{490r}	SWL _S (ON) _{490r}	7.00	9.09	38	<0.001*
5	SWL _S (OFF) ₆₅₀	SWL _S (ON) ₆₅₀	7.54	2.28	38	0.029

* Denotes significance at $p < 0.01$ (Bonferroni-corrected for five pairwise comparisons)

Table 6

Descriptive Statistics of δ [SWL_S(OFF) : SWL_S(ON)] asymmetry ratios across all adapting fields conditions.

$\delta_{\text{adapting field}}$	<i>Min</i>	<i>Max</i>	<i>M</i>	<i>SD</i>
δ_{control}	0.66	2.39	1.33	0.392
δ_{440}	0.76	1.86	1.22	0.303
δ_{490p}	0.73	1.79	1.08	0.227
δ_{490r}	0.81	2.39	1.54	0.360
δ_{650}	0.57	2.97	1.16	0.417

Table 7

Summary table of post-hoc pairwise analysis comparing δ [SWL_S(OFF) : SWL_S(ON)]

asymmetry ratios across all adapting fields conditions.

Pair			<i>M Diff.</i>	<i>t</i>	<i>df</i>	<i>p</i>
1	δ_{control}	δ_{440}	0.107	1.44	38	0.158
2	δ_{control}	$\delta_{490\text{p}}$	0.244	3.36	38	0.002*
3	δ_{control}	$\delta_{490\text{r}}$	-0.215	2.23	38	0.032
4	δ_{control}	δ_{650}	0.166	1.88	38	0.068
5	δ_{440}	$\delta_{490\text{p}}$	0.137	2.76	38	0.009
6	δ_{440}	$\delta_{490\text{r}}$	-0.321	4.44	38	<0.001*
7	δ_{440}	δ_{650}	0.058	0.740	38	0.464
8	$\delta_{490\text{p}}$	$\delta_{490\text{r}}$	-0.458	6.74	38	<0.000*
9	$\delta_{490\text{p}}$	δ_{650}	-0.077	0.949	38	0.349
10	$\delta_{490\text{r}}$	δ_{650}	0.381	4.60	38	<0.001*

* Denotes significance at $p < 0.005$ (Bonferroni-corrected for ten pairwise comparisons).

Table 8

Descriptive Statistics of X ($\delta_{\text{adapting field}}/\delta_{\text{control}}$) asymmetry ratios across all adapting fields conditions.

$X_{\text{adapting field}}$	<i>Min</i>	<i>Max</i>	<i>M</i>	<i>SD</i>
X_{440}	.44	1.75	.9875	.33799
X_{490p}	.42	1.54	.8833	.30385
X_{490r}	.50	3.62	1.2898	.61113

Table 9

Summary table of post-hoc pairwise analysis comparing X ($\delta_{\text{adapting field}} / \delta_{\text{control}}$) asymmetry ratios across all adapting fields conditions.

Pair			<i>M Diff.</i>	<i>t</i>	<i>df</i>	<i>p</i>
1	X ₄₄₀	X _{490p}	0.104	2.74	38	0.009*
2	X ₄₄₀	X _{490r}	-0.302	3.85	38	<0.001*
3	X _{490p}	X _{490r}	-0.215	5.35	38	<0.001*

* Denotes significance at $p < 0.017$ (Bonferroni-corrected for three pairwise comparisons)

Table 10

Descriptive statistics for all conditions in the contrast sensitivity task (CSF).

Condition	Gabor center frequencies(c/deg)	<i>Min</i>	<i>Max</i>	<i>M</i>	<i>SD</i>
Control	0.5	40.49	113.64	69.32	16.41
	1.0	75.47	298.51	172.84	46.61
	2.0	136.05	377.36	229.36	64.25
440 nm	0.5	45.56	109.29	71.47	16.51
	1	74.07	240.96	138.00	36.13
	2	61.73	344.83	163.86	53.38
490p (dim)	0.5	46.40	137.93	81.94	25.02
	1	102.56	307.69	175.32	45.77
	2	87.34	298.51	200.32	54.47
490r (bright)	0.5	11.93	59.52	25.09	9.08
	1	16.91	63.49	33.46	10.05
	2	10.31	46.51	24.25	7.55
650 nm	0.5	22.10	82.64	41.73	13.22
	1	40.24	183.49	100.26	27.30
	2	40.65	235.29	133.54	57.42

Figure 1. Mean Sensitivity Between Tested Zones in Short-Wavelength Automated Perimetry (SWAP) Plotted as a Function of Horizontal Hemiretina, Vertical Hemiretina, and Retinal Eccentricity.

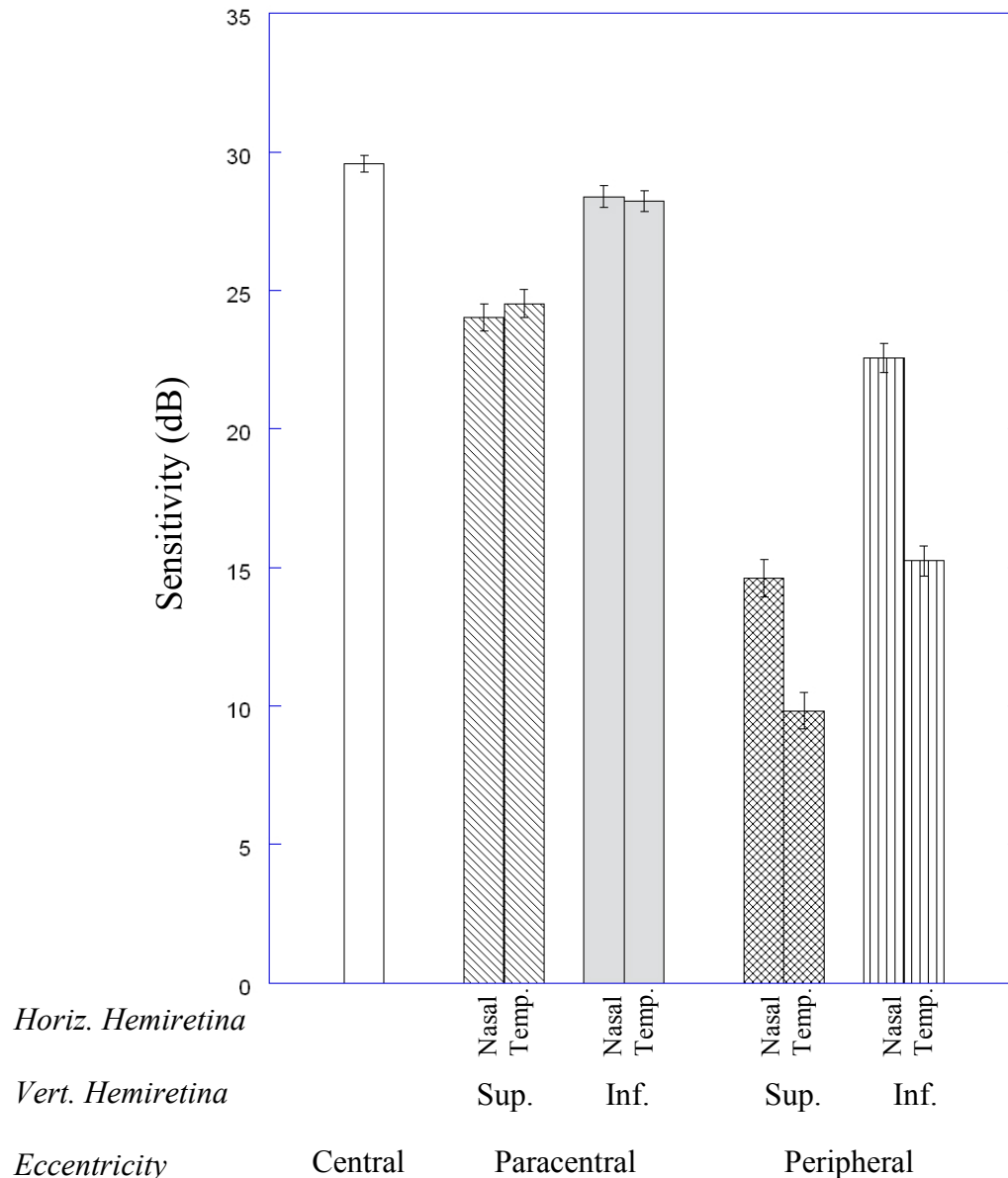


Figure 1. Mean sensitivity (in dB) between tested zones in Short-Wavelength Automated Perimetry (SWAP) plotted as a function of horizontal hemiretina, vertical hemiretina, and retinal eccentricity. Each pair of bars indicates a vertical hemiretina, and horizontal hemiretinas are shown as nasal (left) and temporal (right) in each pair. Central field sensitivity was included on the left for reference. Error bars are \pm SEM.

Figure 2. Mean OFF and ON Sensitivity in Photopic Sawtooth Brightness Task as a Function Adapting Field Condition.

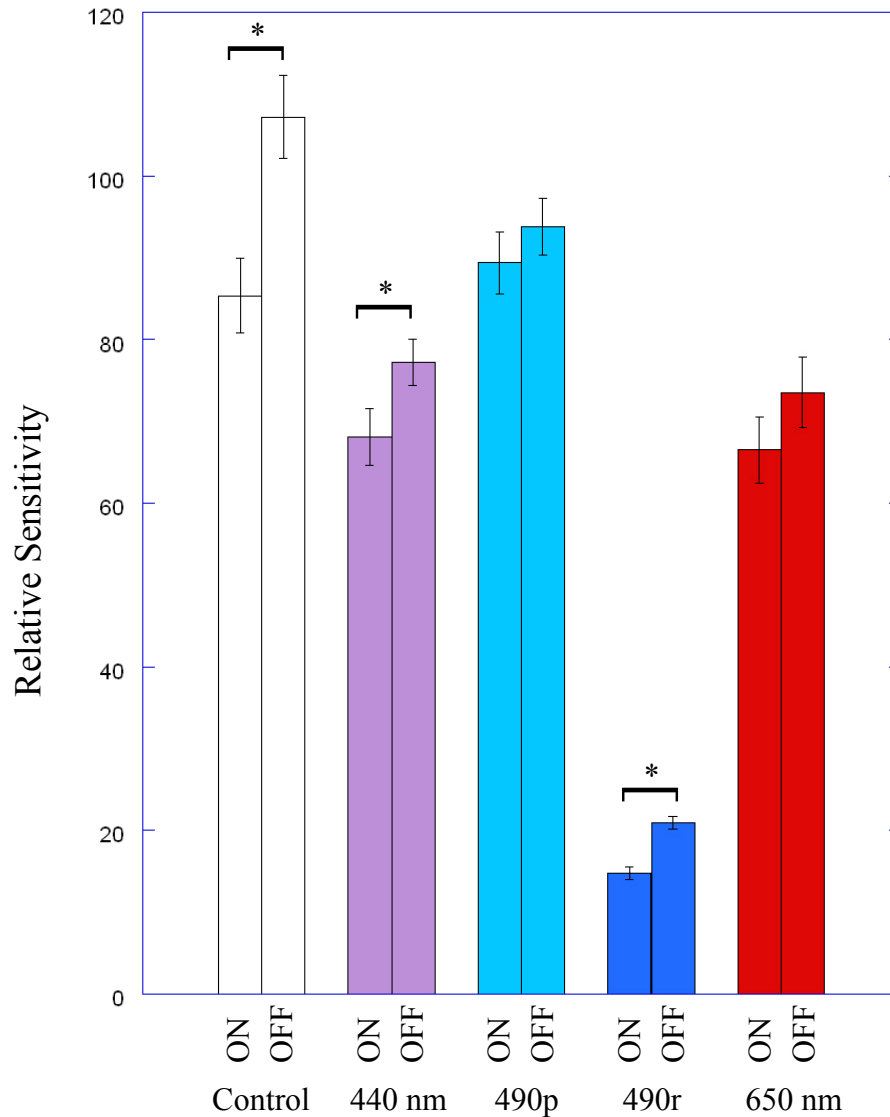


Figure 2. Mean OFF and ON sensitivity (defined as $10/\text{threshold}$) in photopic sawtooth brightness task plotted as a function adapting field condition. Note that the ‘ δ ’ measures in Fig. 3 were calculated as the ratio of OFF to ON sensitivity for each group of columns. Asterisk (*) denotes significant differences between OFF and ON sensitivity in a particular adapting field condition. Error bars are \pm SEM

Figure 3. Mean δ [$S(\text{OFF})_{\text{adapting field}}/S(\text{ON})_{\text{adapting field}}$] Asymmetry Ratios as a Function of Adapting Field Condition.

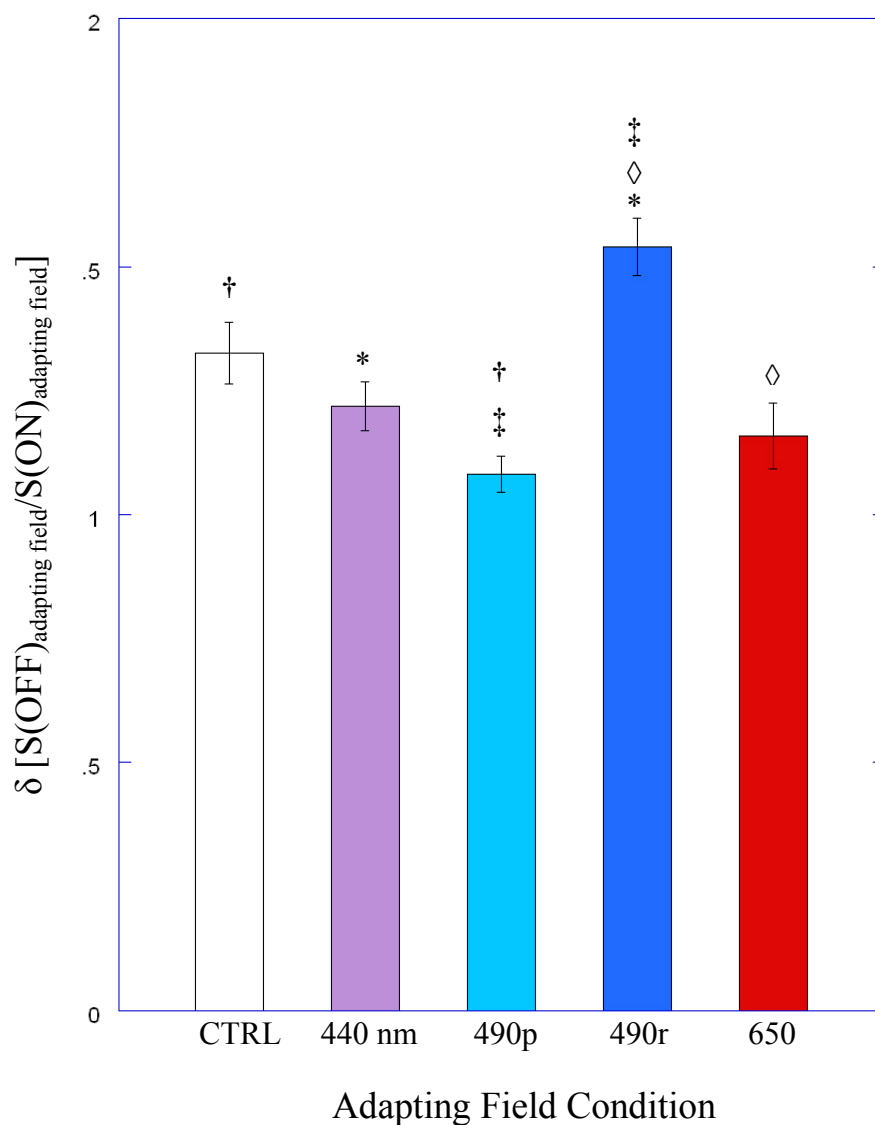


Figure 3. Mean δ [$S(\text{OFF})_{\text{adapting field}}/S(\text{ON})_{\text{adapting field}}$] asymmetry ratios as a function of adapting field condition. Note that the ‘ δ ’/‘ δ ’ measures in Fig. 4 were calculated as the δ value in each adapting field condition divided by the control δ value. Significant differences were found between the following conditions: Control – 490p ($p=0.002$, denoted by †), 440 nm – 490r ($p<0.001$, denoted by *), 490p – 490r ($p<0.001$, denoted by ‡), and 490r – 650 nm ($p<0.001$, denoted by ◇). Error bars are \pm SEM.

Figure 4. Mean Sensitivity Asymmetry (δ) for Each Adapting Field Condition Differenced from the δ_{control} Value.

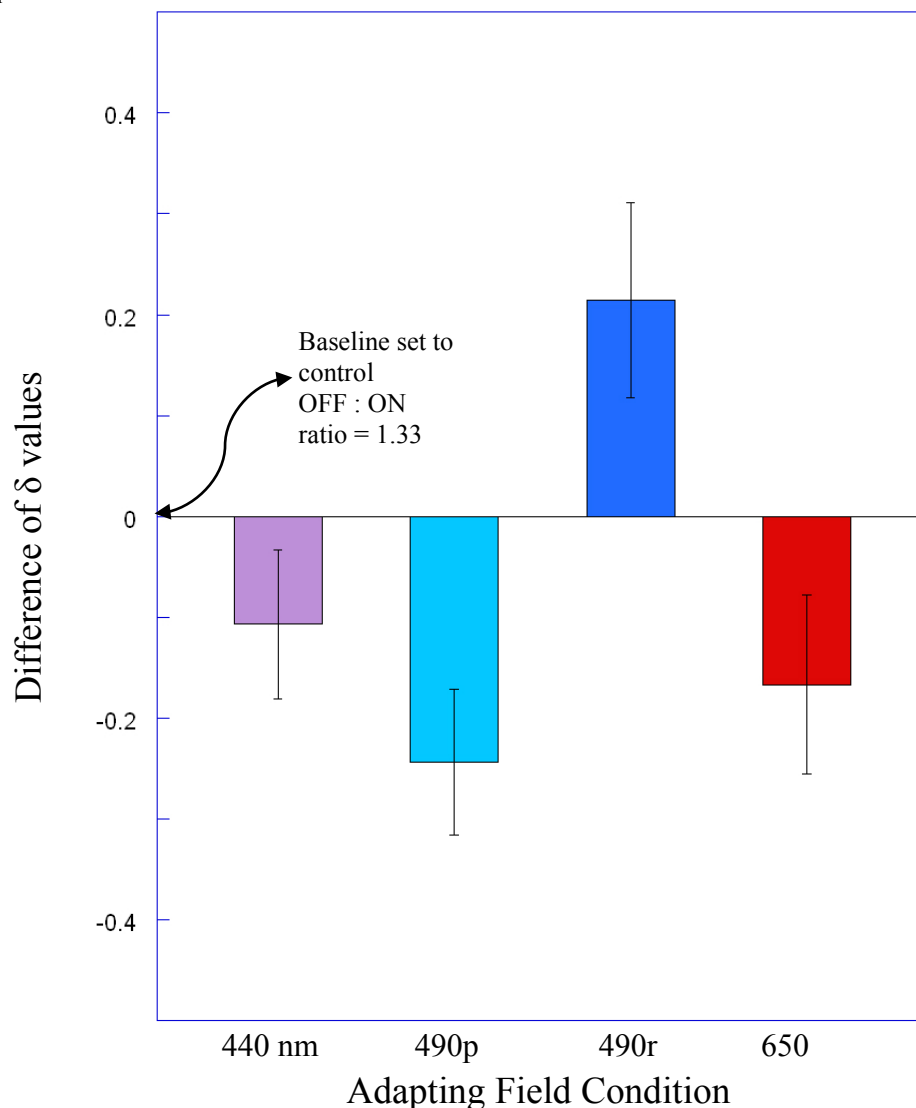


Figure 4. Mean sensitivity asymmetry (δ) for each adapting field condition differenced from the δ_{control} value. Baseline is set to the asymmetry ratio of the control condition. Negative bars indicate a relative advantage for S-ON stimuli compared to the control condition, and positive values indicate a relative advantage for S-OFF stimuli compared to the control condition. This figure illustrates the directional nature of the adapting fields' effects on the $\text{SWL}_S(\text{OFF}):\text{SWL}_S(\text{ON})$ sensitivity ratio. Of note is the relative advantage for $\text{SWL}_S(\text{OFF})$ sensitivity in the 490r condition, compared to the relative advantage for $\text{SWL}_S(\text{ON})$ sensitivity in all other conditions. This reversal tentatively supports the S-OFF cone receptive field properties of the M2 ipRGCs, since ipRGC would be most likely to respond to a “bright” 490 nm light over any other condition. Further, the lack of a monotonic relationship between the control, 490p and 490r conditions supports the conclusion that the asymmetry shifts are not simply based on the mean luminances of the stimuli. Error bars are \pm SEM.

Figure 5. Mean X ($\delta_{\text{adapting field}}/\delta_{\text{control}}$) Sensitivity Ratios for 440 nm, 490p and 490r Adapting Field Conditions.

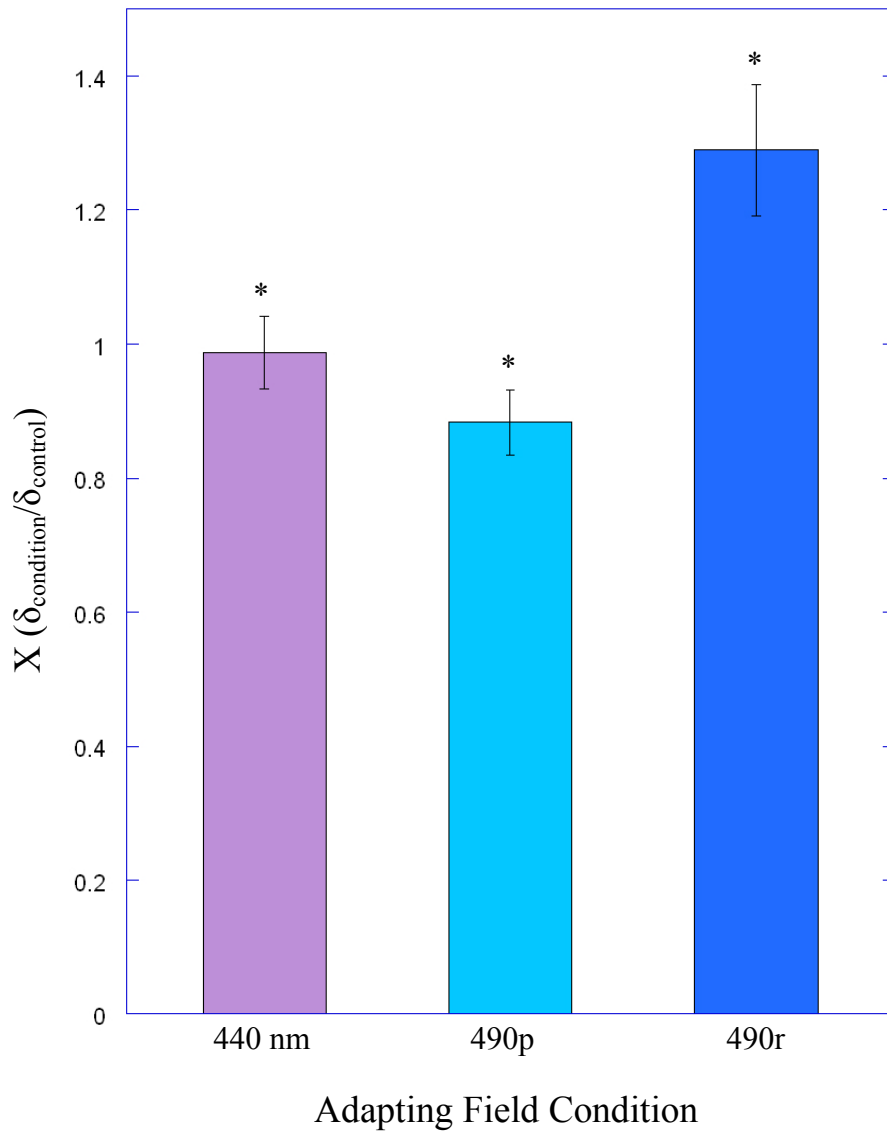


Figure 5. Mean X ($\delta_{\text{adapting field}}/\delta_{\text{control}}$) sensitivity ratios for 440 nm, 490p and 490r adapting field conditions. Significant differences were found between all three conditions, with the greatest sensitivity asymmetry found in the 490r condition. Error bars are \pm SEM. Asterisk (*) denote significant differences.

Figure 6. Log Contrast Sensitivity as a Function of Log Spatial Frequency Across All Adapting Field Conditions.

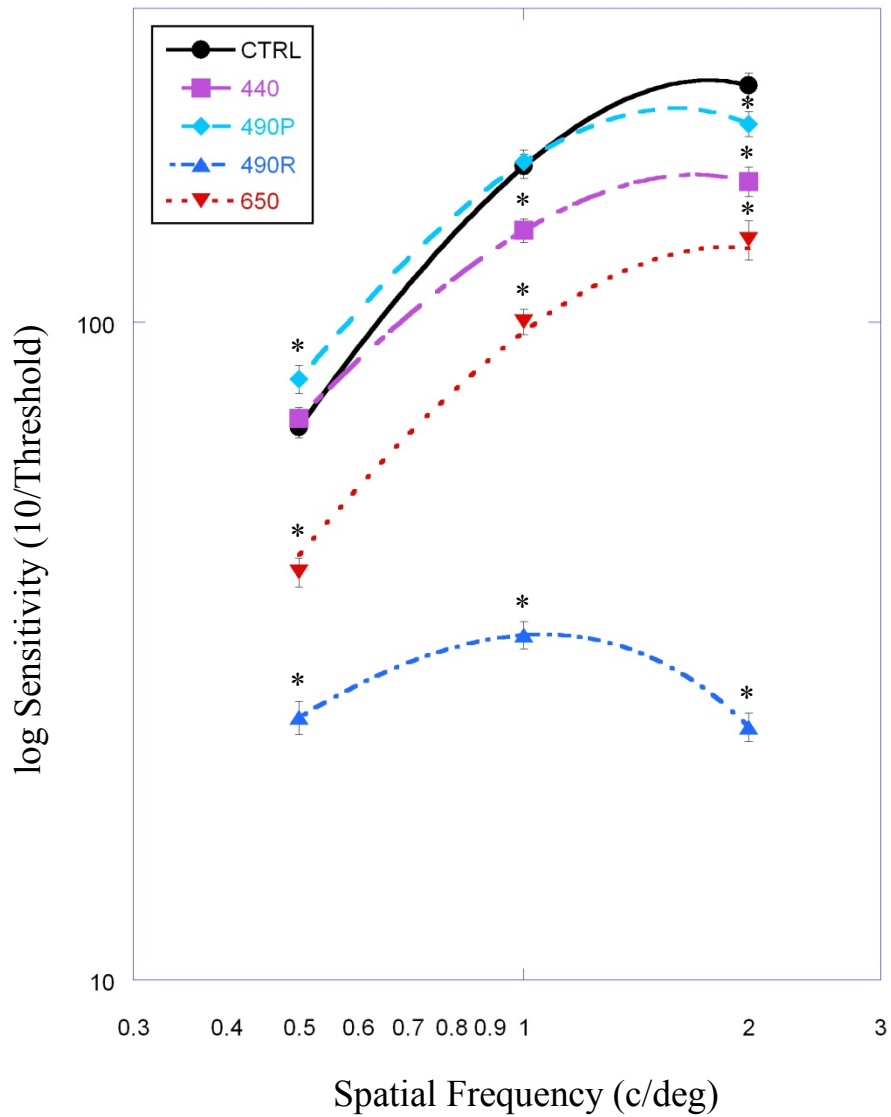


Figure 6. Log contrast sensitivity as a function of log spatial frequency across all adapting field conditions. For clarity, data were fit with a double exponential template (see text). Error bars are \pm SEM; where error bars are not visible, they are less than the width of the data markers. Asterisk (*) denote significant differences from control condition.

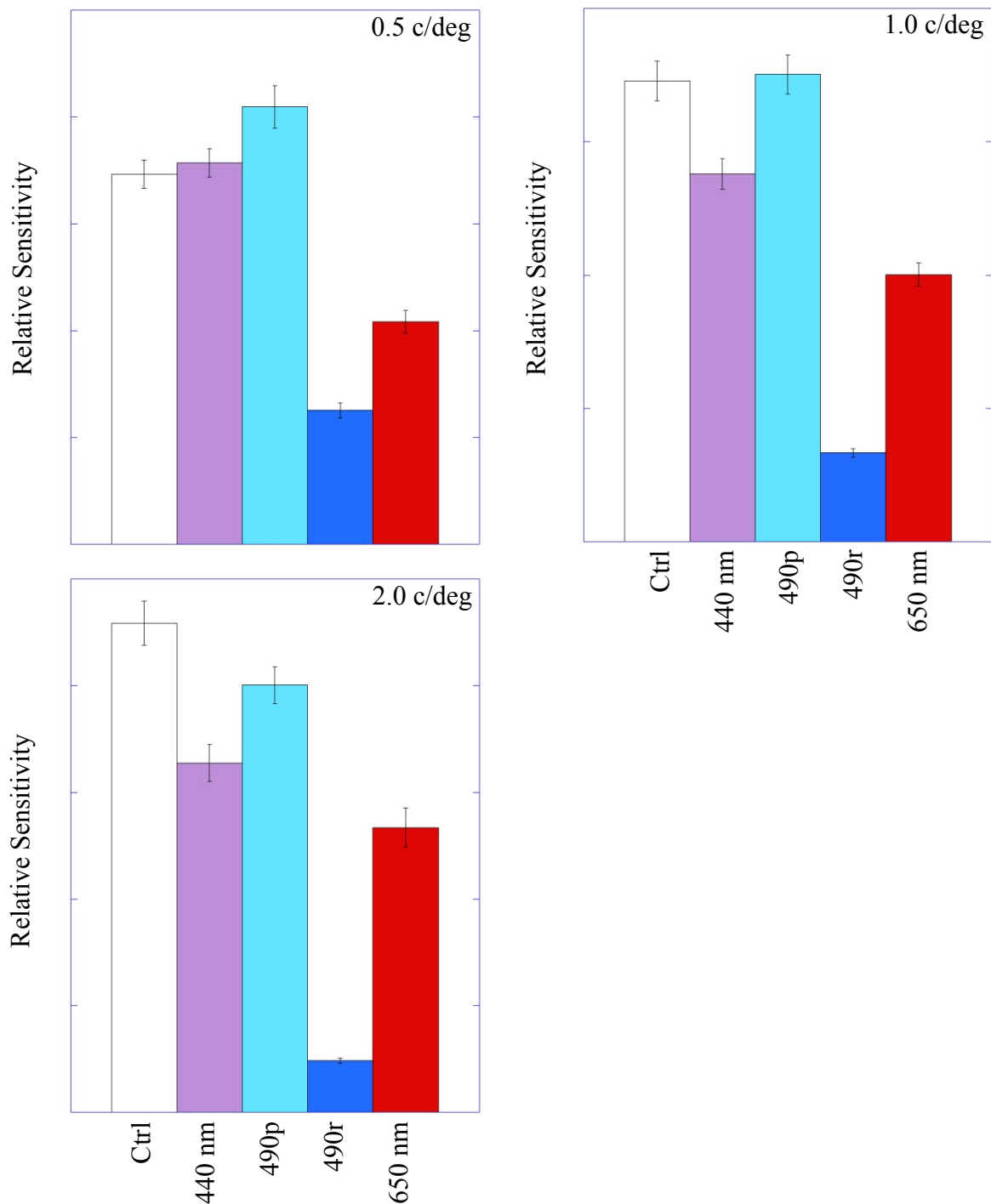
Figure 7. Relative Contrast Sensitivity by Adapting Field Condition.

Figure 7. Relative contrast sensitivity (10/threshold) by adapting field condition. Separate plots illustrate different degree visual angle conditions. All pairwise contrasts were significant except the following. In the 0.5 c/deg condition, there was no significant difference between the control and 440 nm conditions. In the 1.0 c/deg condition, there was no difference between the control and 490p conditions.

Appendix A

Consent Form

Lakehead
UNIVERSITY

CONSENT FORM

A psychophysical examination of contributions of intrinsically-photosensitive retinal ganglion cells to the image-forming visual system in humans

I, _____, the undersigned, hereby consent to participate as a subject in the research project entitled *a psychophysical examination of contributions of intrinsically-photosensitive retinal ganglion cells to the image-forming visual system in humans* conducted at Lakehead University under the direction of Stewart Madon and Dr. Michael Wesner. The procedures in this research project have been explained to me and are as follows:

1. This study is designed to ascertain whether a newly discovered type of ganglion cell contributes to traditional, image-forming vision.
2. The study will consist of one session lasting approximately 120-150 minutes. First, I will complete a questionnaire. Then my visual functioning will be assessed using a Freiberg Acuity Test, in which I will have to identify which of 8 positions on a ring contains a gap, a colour-blindness task in which I will arrange coloured chips in order of hue, and automated perimetry measurements, in which I will have to respond when I see a dot of light presented. Based on these preliminary assessments, I may then be asked to participate in the experiment. The experiment begins with me sitting in the dark for 7 minutes and then viewing a white computer display for 3 minutes. After that, I will be positioned in a head/chin rest in front of a computer screen and given one of two computer tasks (either viewing blue gratings or trying to detect light stimuli).
3. My consent is given of my own free choice without undue inducement or any element of force, fraud, deceit duress, or any form of constraint or coercion. I understand that I am free to withdraw my consent at any time without prejudice to me. Participating in one stage of the study does not oblige me to participate in later stages. I further understand that all results obtained from this research will be kept confidential and remain in secure storage at Dr. Wesner's lab at Lakehead University for 5 years. An impartial reference code will be used for all data files, figures and sign-up sheets. These codes also will be incorporated into any published works that come from this research effort. None of my responses in the computer tasks can be traced back to me. In return for my participation, I will be accorded 3 credits. If I wish to have a summary of the results, I can request a copy from the investigators.

Name of Participant (Please Print)

Signature

Date

Name of Witness (Please Print)

Signature

Date

I would like a copy of the research findings: Yes / No

Email Address: _____

Appendix B

Screening Questionnaire

1. Please enter your name in the name box and provide an email address and phone number where you can be reached
 - a. Name:
 - b. Email Address:
 - c. Phone Number:
2. Please enter your student number
3. Sex (defined by chromosome set, e.g., XX, XY):
 - a. Male (XY)
 - b. Female (XX)
 - c. Other (e.g., XXY, XYY, XXX, single-X, etc.)
4. Age (in years)
5. Handedness
 - a. Right
 - b. Left
 - c. Ambidextrous
6. Do you have normal/corrected-to-normal vision (e.g., 20/20)?
 - a. Yes
 - b. No
 - c. Not Sure (Please Specify)
7. Do you wear corrective lenses
 - a. Yes
 - b. No

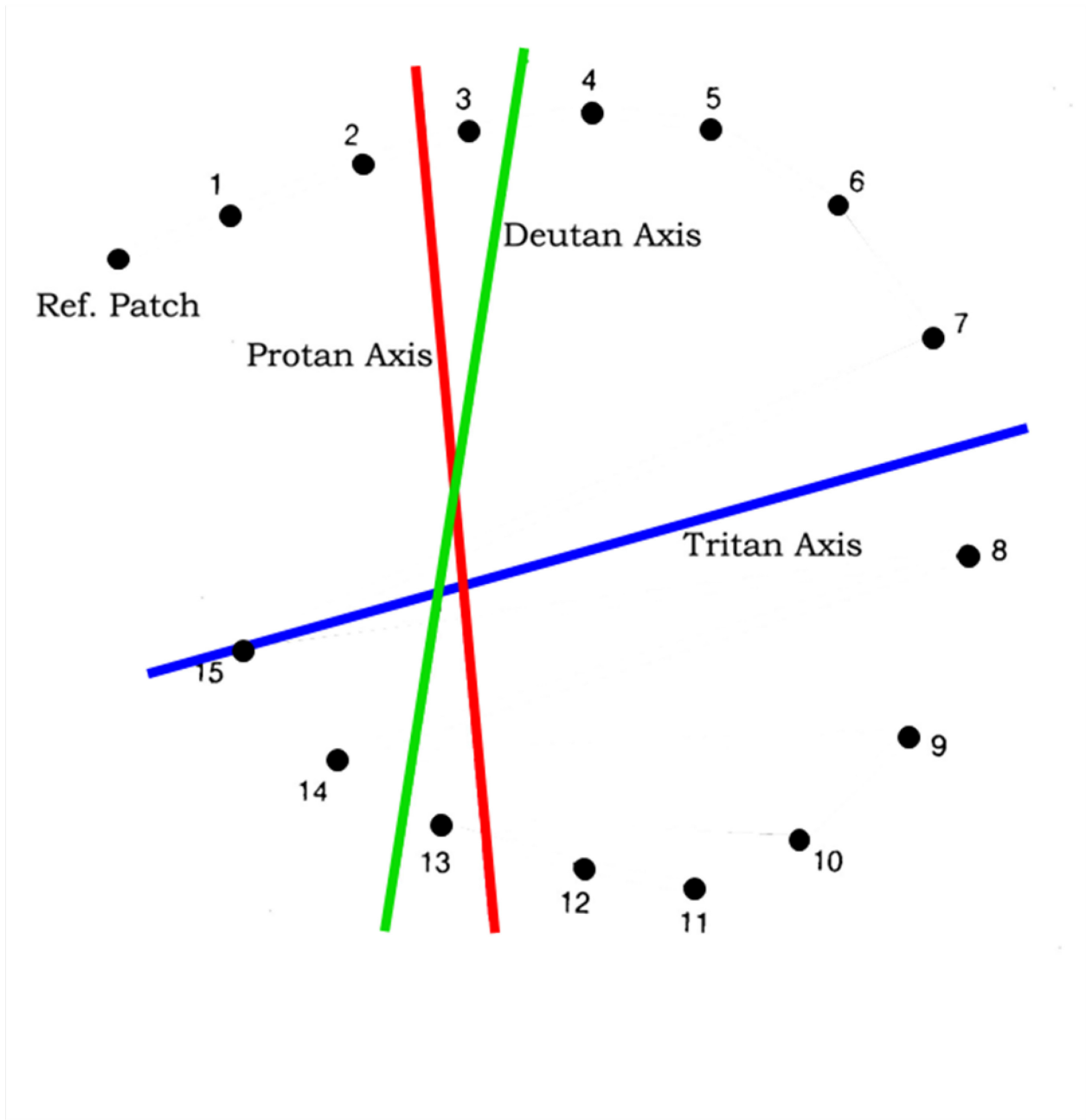
8. Have you recently had laser-eye surgery (lasik) or any other ocular surgeries?
 - a. Yes
 - b. No

9. Do any of the following medical conditions apply to you? (CHECK ALL THAT APPLY)
 - a. Depression
 - b. Seasonal Affective Disorder
 - c. Colour-Blindness
 - d. Parkinson's
 - e. Glaucoma
 - f. Migraines (diagnosed)
 - g. Premenstrual Dysphoric Disorder (PMDD) or Premenstrual Syndrome (PMS)

10. I consent to be contacted as a potential participant in the research project entitled a "psychophysical examination of contributions of intrinsically-photosensitive retinal ganglion cells to the image-forming visual system in humans" conducted at Lakehead University under the direction of Stewart Madon and Dr. Michael Wesner. My consent is given of my own free choice and I understand that I am free to withdraw my consent at any time without prejudice to me. I understand that filling out this questionnaire does not oblige me to participate in the study. I also understand that any information collected in this questionnaire will be kept secure as per Lakehead University Research Ethics guidelines.
 - a. Yes, I provide my consent
 - b. No, I do not provide my consent

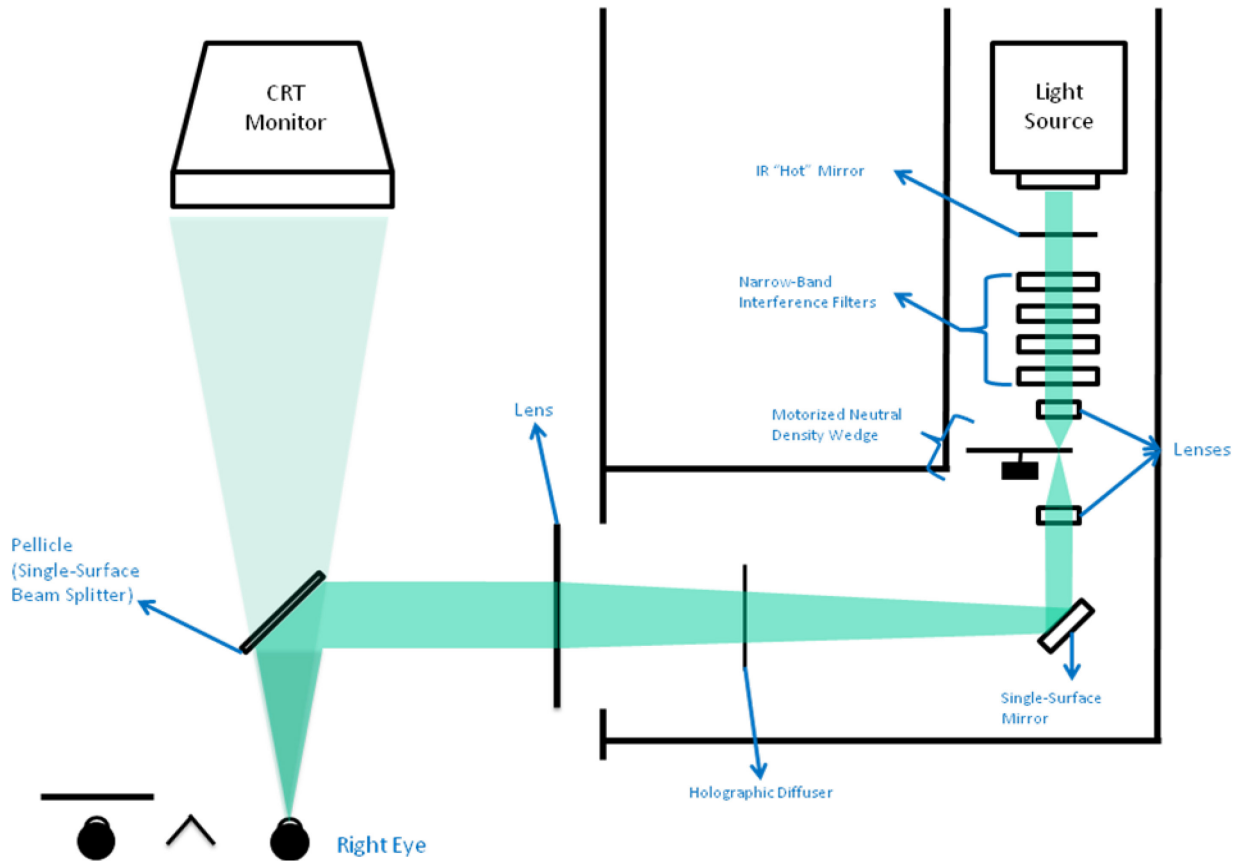
Appendix C

Farnsworth D-15 Scoring Template



Appendix D

Schematic of Hybrid Testing Apparatus



Appendix E

Optical Density Calibration Values (partially reproduced from Pokorny, Smith, & Lutze, 1987).

Wavelength (nm)	TL ₁	TL ₂
400	0.600	1.000
410	0.510	0.583
420	0.433	0.300
430	0.377	0.116
440	0.327	0.033
450	0.295	0.005
460	0.267	-
470	0.233	-
480	0.207	-
490	0.187	-
500	0.167	-
510	0.147	-
520	0.133	-
530	0.120	-
540	0.107	-
550	0.093	-
560	0.080	-
570	0.067	-
580	0.053	-
590	0.040	-
600	0.033	-
610	0.027	-
620	0.020	-
630	0.013	-
640	0.007	-
650	0.000	-

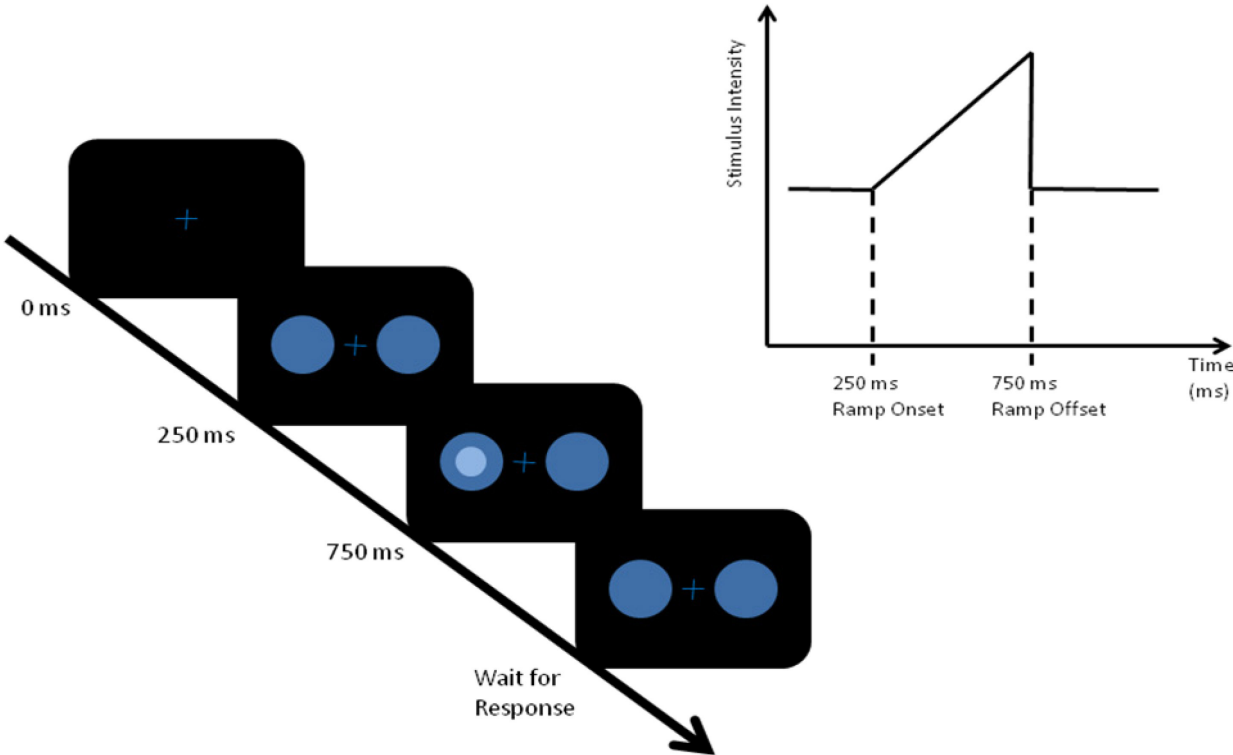
Note. This is a partial reproduction of the lookup table from Pokorny, Smith & Lutze (1986) study on the optical density of the lens and ocular medium. The values in the above table are used in their formula:

$$T_L = T_{L1} [1 + 0.02(A-32)] + T_{L2}$$

where T_L is the total optical density of the lens and ocular medium, T_{L1} is portion affected by aging after age 20 years, T_{L2} is the portion of stable after age 20 years, and A is the age of the participant in years.

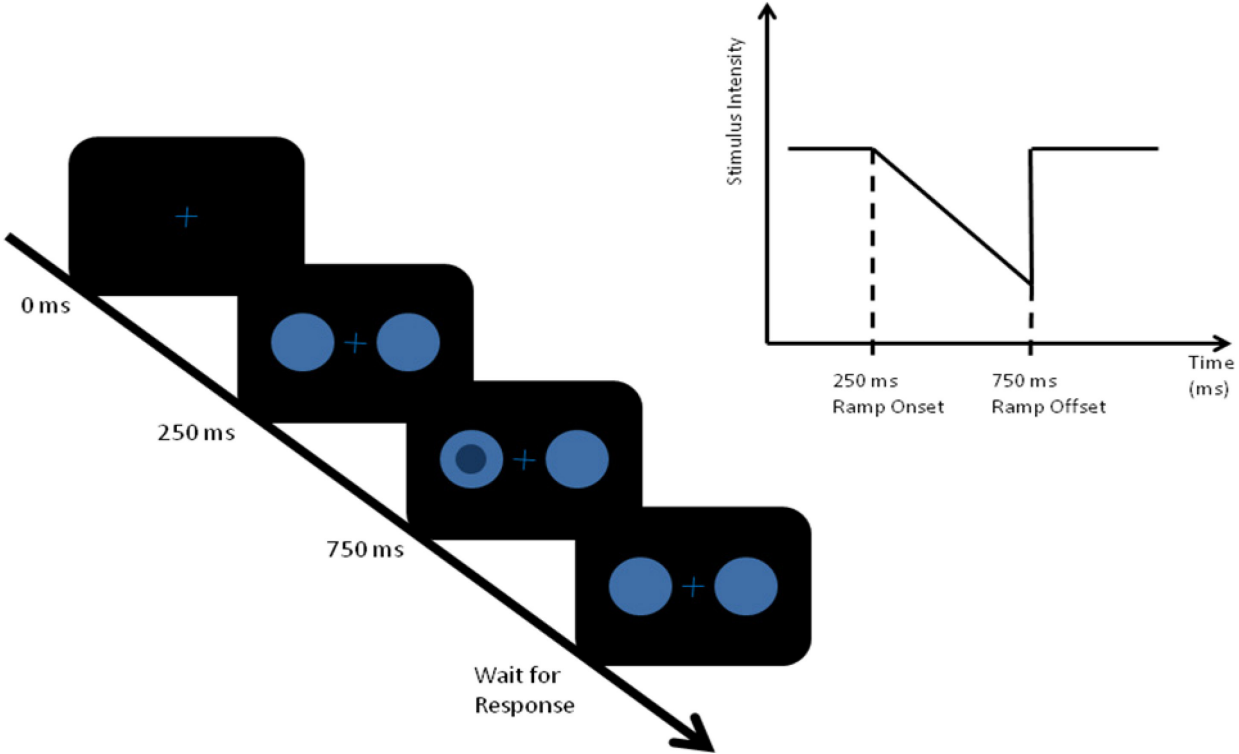
Appendix F

“Ramp-up” Stimulus Design



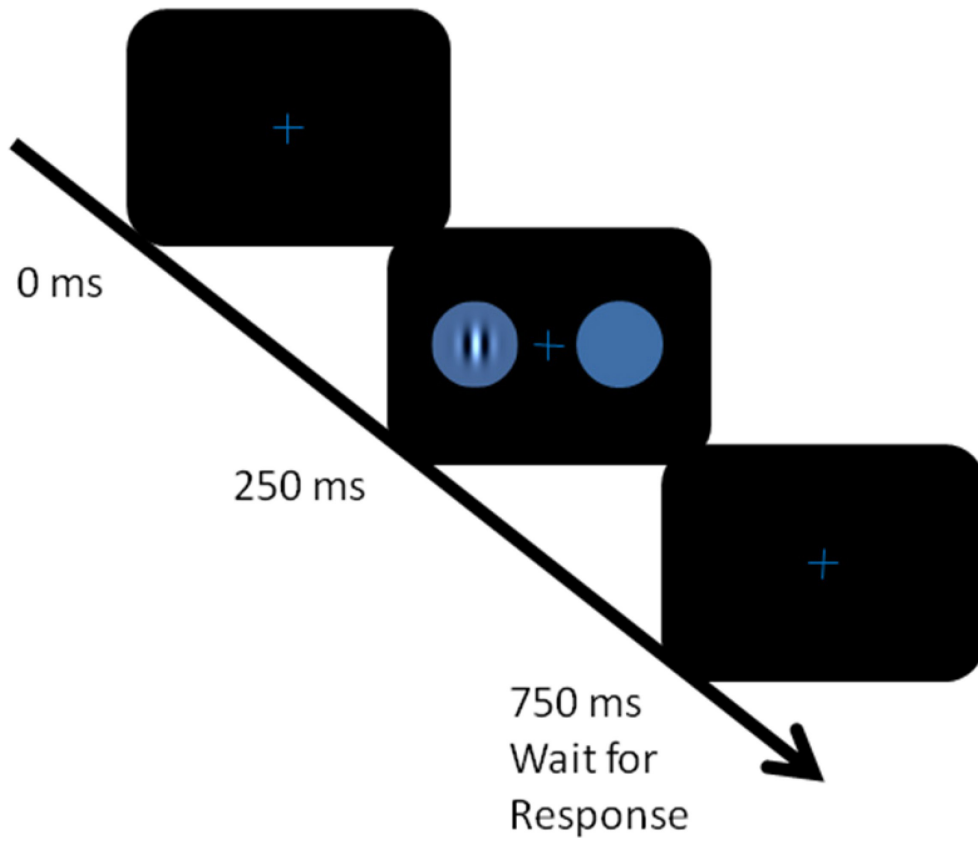
Appendix G

“Ramp-down” Stimulus Design



Appendix H

Stimulus Sequence for Contrast Sensitivity Task



Appendix I

Recruitment Letter

Dear Potential Participant,

We are currently recruiting participants for our project, entitled *A psychophysical examination of contributions of intrinsically-photosensitive retinal ganglion cells to the image-forming visual system in humans*. What follows is a series of screening questions designed to assess your eligibility to participate.

Our study proposes to use non-invasive psychophysical tasks to test the connection of a newly-discovered, intrinsically photosensitive retinal ganglion cell to cells normally associated with traditional, conscious vision. This experiment will take place over 1 session lasting approximately 2.5 hours. Participants will be asked to fill out a demographic questionnaire, and take part in a few computerized tests designed to assess different visual functions.

Participation in this experiment is strictly voluntary, and you may withdraw at any time without bias or penalty. If at any time you feel discomfort during the experiment, you will not be required to continue. The principle investigator or trained research assistants will be present at every stage of the experiment to ensure that you are not experiencing any adverse effects.

Information collected for this experiment will be held in strict confidentiality. At no point will any identifying information be released to individuals who are not part of the research team. All information will be securely stored in Dr. Wesner's laboratory at Lakehead University for a period of 5 years. Findings from the projects will be made available to participants upon completion of the project.

If you choose to participate in the study, you may be eligible for bonus marks, and all participants will be given a Tim Horton's Gift card as compensation.

If you have any questions or concerns regarding the experiment, please do not hesitate to contact me directly. I can be reached by phone (807) 343-8418 or through e-mail (smadon@lakeheadu.ca). You may also contact Lakehead University's Research Ethics Board at (807) 343-8283.

Thank you for your interest in our project,

Stewart Madon, M.A.
Ph.D. Clinical Psychology Candidate

Dr. Michael Wesner
Supervisor

If you are interested in participating, please go to:

<http://www.surveymonkey.com/s/S7QJ7PT>

to fill out the online screening questionnaire. Someone will contact you to set up an appointment.

Appendix J

Schematic of Short-Wavelength Automated Perimetry (SWAP) zones

